FACULTY OF HEALTH AND MEDICAL SCIENCES
UNIVERSITY OF COPENHAGEN

Tissue-engineering as an adjunct to pelvic reconstructive surgery

New potential concepts evaluated in animal studies

PhD thesis

Hanna Jangö

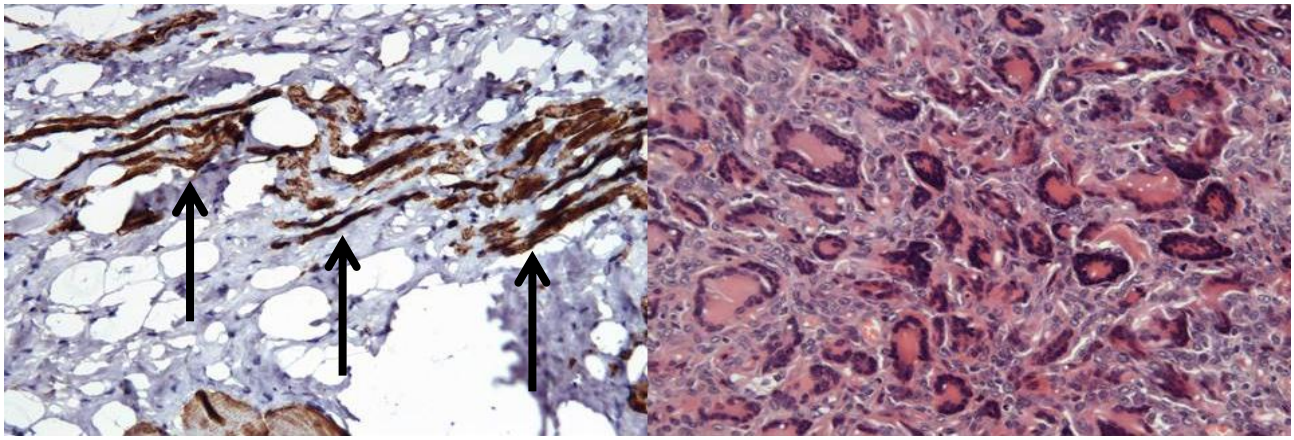

Section of Urogynecology, Department of Obstetrics and Gynecology, Herlev Hospital
Faculty of Health and Medical Sciences, University of Copenhagen

This thesis has been submitted to the Graduate School at the Faculty of Health and Medical Sciences, University of Copenhagen.

Herlev og Gentofte Hospital

SUBMITTED

March 16, 2016

THESIS DEFENCE

June 17, 2016

Herlev Hospital, Lille Auditorium

ACADEMIC SUPERVISORS

Professor Gunnar Lose, MD, DMSc

Department of Obstetrics and Gynecology, Herlev University Hospital, Denmark

Søren Gräs, MD

Department of Obstetrics and Gynecology, Herlev University Hospital, Denmark

Lise Christensen, MD, DMSc

Department of Pathology, Herlev University Hospital, Denmark

ASSESSMENT COMMITTEE

Chairman: Professor Claus Høgdall, MD, DMSc

Department of Obstetrics and Gynecology, Rigshospitalet, University of Copenhagen, Denmark

Associate Professor Susanne Axelsen, MD, PhD

Department of Obstetrics and Gynecology, Aarhus University Hospital, Denmark

Professor Anders Lindahl, MD, PhD

Department of Clinical Chemistry and Transfusion, Institute of Biomedicine, Sahlgrenska Academy,

University of Gothenburg, Sweden

This PhD study was supported by the Danish National Advanced Technology Foundation and by the Nordic Urogynecological Association.

Colplast A/S, Humlebæk, Denmark, provided the scaffolds used in the studies and provided laboratory facilities for histological and biomechanical testing.

Acknowledgements

I am indebted to Professor Gunnar Lose, my principal supervisor, for giving me the opportunity to discover this area of research. You have inspired me with your enthusiasm and commitment, your straight-forwardness and your extraordinary scientific and political robustness.

My deepest gratitude to my co-supervisors, Søren Gräs and Lise Christensen, for helping me throughout the project. Søren for helping me discover the big picture from the important details, and Lise for kindly guiding me through the surprisingly beautiful world of pathology.

I am also very thankful for the practical assistance and support provided from all of the members of the URITE group in the beginning of the PhD-project. Special thanks to the staff both at the Panum Institute and at the Frederiksberg Campus for helping me out with the animals.

The warmest thanks to the colleagues who have supported and encouraged me throughout the project. Especially, thanks to Mette Bing and Niels Klarskov for always helping me structuring my thoughts and to Karin Reenberg for always being helpful. Also, the deepest thanks to all my officemates through the years - you have been the best and I already miss sharing the small and big obstacles and victories with you.

To my wonderful family and friends – thank you for your continuous support and for bringing joy, music and laughter into my life.

My heartfelt gratitude to my husband Henrik and our children August, Sigrid and Esther. You keep reminding me of the truly important things in life and for that I could not be more grateful.

Virum, March 2016

Hanna Jangö

Contents

Studies included in the PhD thesis

The thesis is based on the following studies, which will be referred to by their number.

1. Jangö H, Gräs S, Christensen L, Lose G. Muscle fragments on a scaffold in rats: a potential regenerative strategy in urogynecology. Int Urogynecol J. 2015 Dec 24;26(12):1843–51.[1]
2. Jangö H, Gräs S, Christensen L, Lose G. Tissue engineering with muscle fiber fragments improves the strength of a weak abdominal wall in rats. (submitted)[2]
3. Jangö H, Gräs S, Christensen L, Lose G. Examinations of a new long-term degradable polycaprolactone scaffold in three abdominal wall models in rats. (manuscript)[3]
4. Jangö H, Gräs S, Christensen L, Lose G. Modification and evaluation of a transabdominal vaginal model – a pilot study in rabbits. (unpublished data)

Summary

This PhD-thesis is based on animal studies and comprises three original papers and unpublished data. The studies were conducted during my employment as a research fellow at the Department of Obstetrics and Gynecology, Herlev University Hospital, Denmark.

New strategies for surgical reconstruction of pelvic organ prolapse (POP) are warranted. Traditional native tissue repair may be associated with poor long-term outcome and augmentation with permanent polypropylene meshes is associated with frequent and severe adverse effects. Tissue-engineering is a regenerative strategy that aims at creating functional tissue using stem cells, scaffolds and trophic factors. The aim of this thesis was to investigate the potential adjunctive use of a tissue-engineering technique for pelvic reconstructive surgery using two synthetic biodegradable materials; methoxypolyethyleneglycol-poly(lactic-co-glycolic acid) (MPEG-PLGA) and electrospun polycaprolactone (PCL) - with or without seeded muscle stem cells in the form of autologous fresh muscle fiber fragments (MFFs). To simulate different POP repair scenarios different animal models were used.

In Study 1 and 2, MPEG-PLGA was evaluated in a native tissue repair model and a partial defect model of the rat abdominal wall. We found that the scaffold was fully degraded after eight weeks. Cells from added MFFs could be traced and had resulted in the formation of new striated muscle fibers. Also, biomechanical changes were found in the groups with added MFFs.

In Study 3, the long-term degradable electrospun PCL scaffold was evaluated in three rat abdominal wall models representing different loads on the scaffold. Surprisingly, cells from the MFFs did not survive. After eight weeks, a marked inflammatory foreign-body response was observed with numerous giant cells located between and around the PCL fibers which appeared not to be degraded. This response caused a considerable increase in the thickness of the mesh, resulting in a neo-tissue PCL construct with strength comparable to that of normal rat abdominal wall. The foreign-body inflammatory response did not differ between the groups in terms of cellularity, cell types or thickness, and no differences were found between groups when comparing biomechanical properties.

In study 4, we modified a new transabdominal rabbit vaginal model to avoid the erosions known to occur following vaginal mesh implantation. A partial defect was created on the anterior vaginal wall in the vesico-vaginal space and on the anterior vaginal wall close to the cervix. This was a feasibility study aimed at obtaining results comparable to those seen in the rat model. The model was easy to perform and no vaginal erosions were observed.

In conclusion:

- In two rat abdominal wall models, cells from autologous MFFs, seeded on the quickly degradable MPEG-PLGA scaffold, survived implantation and contributed to the regenerative process by forming extra striated muscle fibers and influencing the biomechanical properties of the regenerated tissue.
- Consequently, MFFs seeded on an MPEG-PLGA scaffold is a potentially advantageous cell-delivering strategy to regenerate tissue at pelvic reconstructive surgery.

- In three rat abdominal wall models, a long-term degradable PCL scaffold caused a marked foreign-body response and formed a neo-tissue PCL construct that provided biomechanical tissue reinforcement to the abdominal wall, even at maximal load.
- Consequently, the PCL scaffold might be beneficial in pelvic reconstructive surgery, providing initial biomechanical reinforcement, although long-term studies showing the tissue response at full degradation are required.
- Cells from the MFFs did not survive in or around the neo-tissue PCL construct, possibly because of the massive inflammatory response.
- Consequently, as a scaffold material, with the purpose of delivering cells to a specific anatomical site, the PCL scaffold seems poor.
- A transabdominal rabbit vaginal model was feasible and might be advantageous in the evaluation of meshes used for pelvic reconstructive surgery, especially when long-term studies are needed.

Dansk resumé

Denne ph.d.-afhandling er baseret på dyreforsøg og omfatter tre originale artikler samt upublicerede data. Studierne er udført under min ansættelse som klinisk assistent på Gynækologisk-Obstetrisk afdeling, Herlev Hospital, Danmark.

Nye strategier for rekonstruktiv kirurgisk behandling af genital prolaps (*pelvic organ prolapse*, POP) er efterspurgte. Konventionel prolaps-kirurgi med forstærkning af patientens eget væv (*native tissue repair*) har en dårlig lang-tids effekt, og forstærkning af vævet med permanent, syntetisk polypropylen net kan forårsage hyppige og alvorlige bivirkninger. Regenerativ medicin og herunder *tissue-engineering* har til formål at skabe nyt, funktionelt væv ved brug af stamceller, implantater (net) og trofiske faktorer. Formålet med denne afhandling var at undersøge et muligt supplement til urogynækologisk kirurgi i form af *tissue-engineering* med to forskellige syntetiske bionedbrydelige materialer, methoxypolyethyleneglycol-poly(lactic-co-glycolic acid) (MPEG-PLGA) og elektrospundet polycaprolactone (PCL). Begge materialer blev undersøgt med og uden muskelstamceller i form af autologe friske muskel fiber fragmenter (MFFs). For at simulere forskellige prolapskirurgi scenarier blev forskellige dyre-modeller anvendt.

I studie 1 og 2, undersøgte vi MPEG-PLGA i en *native tissue repai*r model og i en partiel muskeldefekt-model i abdominalvæggen hos rotter. Vi fandt, at nettet var fuldstændigt nedbrudt efter otte uger og at celler fra MFFs kunne spores, idet de havde dannet nye tværstribede muskelfibre. Vi fandt også ændringer i de biomekaniske egenskaber i de grupper, der havde fået MFFs.

I studie 3 vurderede vi det langtidsnedbrydelige elektrospundne PCL net i tre abdominale rotte-modeller, der hver repræsenterede forskellige belastninger, som nettet blev udsat for. Overraskende fandt vi, at cellerne fra MFFs ikke overlevede. Efter otte uger fandt vi et udtalt inflammatorisk fremmedlegeme respons med talrige kæmpeceller mellem og omkring PCL fibrene, som ikke var nedbrudt. Dette medvirkede til en betragtelig fortykkelse af nettet med dannelse af et *neo-tissue PCL construct* med en styrke, der modsvarede en normal abdominalvæg hos rotten. Fremmedlegemereaktionen var ensartet i alle grupper uden forskel i cellularitet, celletyper eller tykkelse, og der var ingen forskelle i de biomekaniske egenskaber mellem grupperne.

I studie 4 videreudviklede vi en ny vaginal kaninmodel med transabdominal adgang for at undgå de erosioner, som hyppigt opstår, når net indsættes transvaginalt i dyremodeller. En partiel defekt kunne udføres på den anteriore vaginalvæg i det vesico-vaginale rum og højere op mod cervix. Dette studie havde til formål at vurdere gennemførligheden for at kunne sammenligne resultater med dem fra rotte-modellerne. Modellen var enkel at udføre og forårsagede ikke vaginal erosion.

Det konkluderes at:

- I to abdominalvægsmodeller hos rotter, fandt vi at celler fra autologe MFFs, som var tilføjet det hurtigt nedbrydelige MPEG-PLGA-net, overlevede og deltog i den regenerative proces med dannelse af ekstra, tværstribede muskelfibre, hvilke påvirkede vævets biomekaniske egenskaber.
- Derfor kunne kombinationen af MFFs og et net af MPEG-PLGA udgøre en fordelagtig cellekilde for regenerering af vævet ved prolapskirurgi.

- I tre abdominalvægsmodeller hos rotter forårsagede det langsomt nedbrydelige net af PCL et massivt fremmedlegeme respons med dannelse af et *neo-tissue PCL construct* hvilket ydede mekanisk støtte af abdominalvæggen, selv i en model hvor nettet havde været udsat for maksimal belastning.
- I egenskab af at yde initial forstærkning af vævet, kan PCL-nettet muligvist være fordelagtigt ved rekonstruktiv urogynækologisk kirurgi. Langtidsstudier, der vurderer vævsreaktionerne når PCL er helt nedbrudt, er dog nødvendige.
- Celler fra MFFs overlevede ikke i eller omkring dette *neo-tissue PCL construct*, muligvis grundet det udtalte inflammatoriske respons.
- Derfor er PCL formentlig ikke et hensigtsmæssigt materiale, hvis formålet er at levere celler til et specifikt anatomisk område.
- En vaginal kaninmodel med transabdominal adgang var gennemførlig og kunne således være fordelagtig ved testning af implantater til prolapskirurgi; især hvor langtids studier er påkrævede.

Abbreviations

ANOVA	analysis of variance
ECM	extracellular matrix
MFFs	muscle fiber fragments
MPEG-PLGA	methoxypolyethyleneglycol-poly(lactic-co-glycolic acid)
MSCs	mesenchymal stem cells
PCL	polycaprolactone
POP	pelvic organ prolapse
SD	standard deviation

Introduction and background

Definition of pelvic organ prolapse

Pelvic organ prolapse (POP) is defined as descent of the anterior vaginal wall, the posterior vaginal wall, the uterus (cervix), or the apex of the vagina (vaginal vault or cuff scar after hysterectomy)[4]. The descent can involve one or more compartments and should be correlated with relevant POP symptoms[4]. Typical POP symptoms include seeing or feeling a bulge in the vaginal introitus, increased heaviness, and compartment-related symptoms such as urinary incontinence or voiding dysfunction (anterior compartment; cystocele), anal incontinence and defecation problems (posterior compartment, rectocele)[4]. Symptoms often occur when the descent reaches the level of the hymen or beyond, but are often not specific for the compartment involved[4].

Anatomic findings of POP can be found in more than 50% of women over 40 years of age[5], but most of these women are asymptomatic. POP related symptoms are reported by 8-12% of women[6,7] and the diagnosis is based on both subjective symptoms and objective findings[8]. In women with POP referred from general practitioners, 75% have affected quality of life[9] and women with advanced stage of POP have affected quality of life[10].

Conservative approaches for POP treatment consist primarily of pelvic floor muscle training[11] and the use of a pessary, a passive mechanical device that supports the vagina[12,13]. Surgical treatment of POP aims at restoring the normal vaginal anatomy and restoring or maintaining normal bladder, bowel and sexual function[14]. In Denmark, 80-year old women have a 18.7% lifetime risk of undergoing POP repair[15]. The corresponding risks in the UK and the US are 9.5%[16] and 12.6%[17], respectively.

Reconstructive surgery for pelvic organ prolapse

The most common surgical procedures for POP are anterior and posterior repair (colporrhaphy) for anterior and posterior POP, respectively[14]. In colporrhaphy, the native tissue is repaired by plication, i.e. folding and suturing of the fascia underneath the vaginal epithelium. Together, anterior and posterior compartment surgery account for more than 90% of reconstructive surgery of POP[18]. However, several other vaginal approaches exist along with different abdominal approaches[14].

Anatomical failure rate after POP surgery has previously been reported to vary between 29% and 70%[18,19]. The recognition of this initiated a time period with the introduction of biological and synthetic materials to reinforce the tissue at POP surgery[20], but according to more recent results the risk of repeated POP surgery is still 15.8%[16]. In contrast, a Danish study found that 2% had repeat surgery 1-5 years after conventional vaginal repair[21].

The use of degradable biological materials combined with native tissue repair has generally failed to improve clinical outcome compared to native tissue repair alone[22]. Synthetic permanent meshes, with polypropylene being the most common, have shown improved anatomical outcome and reduced recurrence rate compared to native tissue repair[14,23]. However, the studies comparing anterior colporrhaphy with and without mesh reinforcement failed to find any differences in symptoms and quality of life between groups[14]. Furthermore, POP in the other compartments was found to be more common after mesh surgery than after native tissue repair[14]. This supports the theory that POP is caused by failure of both local fascia tissue support and of ligament suspension[24]. Failure of local fascia tissue support, i.e. of the pubocervical and the rectovaginal fascia (midlevel vaginal support) causes prolapse of the anterior and posterior

compartment (cystocele and rectocele, respectively), while failure of the suspensory fibers of the paracolpium and parametrium (upper vaginal support) causes vaginal and uterine prolapse[25,26].

In 2008 the FDA (the US Food and Drug Administration) issued a public warning because of recognition of serious and potentially life-threatening adverse events related to the use of permanent synthetic meshes placed transvaginally during reconstructive surgery[27]. In 2011, the FDA launched an update, stating that these adverse events are not rare and that the use of mesh does not improve outcome[28]. In 2016, the FDA announced two orders sharpening the requirements for using transvaginal surgical mesh in POP repair[29]. The first order was a reclassification of mesh from class II to class III, which generally includes high-risk medical devices. The second order was a requirement for the manufacturers to submit rigorous premarket approval applications to prove safety and effectiveness of the mesh.

Correspondingly, in 2015 the SCENIHR (Scientific Committee on Emerging and Newly Identified Health Risks) published an opinion for the European Commission on the use of transvaginal meshes for POP surgery[30]. They concluded that these mesh types should only be considered in complex cases, in particular after failed primary repair surgery or when primary surgery was expected to fail. They also emphasized the need for further improvement in the composition and design of synthetic meshes for future progress in pelvic reconstructive surgery.

Regenerative medicine and tissue-engineering

Stem cells are generally defined by their ability to confer self-renewal, their ability to form clonal cell populations, and their ability to differentiate into a number of different cell-types[31]. During the

last two decades, intensified stem cell research has been employed with the purpose of developing new tissues or even new organs in different medical fields.

In regenerative medicine, the aim is to create a functional tissue for use in the repair or replacement of a tissue function that has been lost due to damage, disease or age. Tissue-engineering is often used as a synonym to regenerative medicine, but traditionally it refers to the use of a scaffold in combination with stem cells[32]. Most regenerative medicine strategies use ex vivo culturing of cells[33]. The use of trophic factors and other biologically active molecules can be used as alternatives or as adjuncts to cell-based therapies. Facilitated endogenous repair represents a branch of tissue-engineering, which uses biological stimuli and manufactured scaffolds while avoiding the culturing of cells[33].

Regenerative medicine in urogynecology

In urogynecology, the use of stem or progenitor cells has been most intensely studied in connection with injection treatments for stress urinary incontinence, where primarily muscle derived cells have been injected into the urethral sphincter with the objective to restore its function[34]. Numerous animal studies[35–37] and a growing number of clinical studies[36–40] have been carried out to evaluate the effect of these treatments, but although results from animal studies have provided promising proof of concept, results obtained from clinical studies have only shown moderate effect[34,37].

Similarly, several animal studies[37] and one clinical study[41] have been published and five ongoing clinical studies (www.clinicaltrials.gov) investigate the potential of treating anal incontinence with muscle derived stem cell injections to improve the function of the external anal sphincter.

In 2009, Ho et al. were the first to evaluate a tissue-engineering strategy for the treatment of POP in a rat vaginal model by seeding skeletal muscle-derived stem cells on scaffolds of porcine small intestine submucosa[42]. They demonstrated that muscle-derived stem cells differentiated into smooth muscle cells when implanted in the rat vagina, which could be beneficial in the treatment of POP[42]. However, transdifferentiation of muscle derived stem cells has not been demonstrated by others. A yet limited number of experimental studies have since examined different candidate cells and scaffolds for potential POP repair[43–50], but to date no clinical studies have been identified (www.clinicaltrials.gov and www.clinicaltrialsregister.eu).

Candidate scaffolds

Generally, three classes of scaffolds for tissue-engineering exist[51]:

- Naturally derived materials, e.g. silk or collagen
- Acellular tissue matrices, e.g. small intestine submucosa or dermis
- Synthetic polymers, e.g. polypropylene or MPEG-PLGA

Naturally derived materials and acellular tissue matrices might be advantageous due to biological recognition, but synthetic polymers can be produced in a large scale and allow for controlling and alteration of specific properties[51]. Mangera et al. evaluated seven different natural or synthetic candidate scaffolds with regard to cell attachment, the formation of extracellular matrix (ECM) and biomechanical properties resembling those of native tissue[52]. They seeded oral fibroblasts on the scaffolds and found that the synthetic electrospun poly(L)-lactic acid and the natural small intestine submucosa both showed superior cell attachment and increased collagen and elastin formation[52]. Poly(L)-lactic acid showed biomechanical properties that were closest to those of

native tissue[52] and it was concluded that this scaffold might be the preferable for tissue-engineering application in POP surgery[52,53]. However, several unanswered questions regarding the choice of scaffold still remain. Degradation time, biocompatibility and the modification of biomechanical properties, which is caused by in vivo implantation as well as the specific combination effect of added cells, must all be considered.

For the purpose of POP repair, a tissue-engineering concept should contribute to restoration of normal function by restoring native, healthy tissue properties and anatomy. Ideally, the scaffold should function as an anchor for the added stem cells, providing a three-dimensional structure for the cells to grow on, and at the same time provide tissue reinforcement. The added cells would grow on and into the scaffold and be integrated with the host tissue while the tissue is held in place by the scaffold. When the scaffold is fully degraded, the cells should have formed new functional tissue, capable of providing durable anatomical correction and thus, functional restoration.

Candidate cell sources

Embryonic stem cells are derived from totipotent cells of the early embryo and are capable of unlimited, undifferentiated division[54,55]. The culturing of these cells was first described from mouse embryos in 1981[54,55] whereas culturing of human embryonic stem cells was first described in 1998[56]. The embryonic stem cells can differentiate into all adult cell types and have a great therapeutic potential. However, the clinical use of these cells is limited by 1) the risk of tumorigenicity, 2) immunogenicity since the cells are allogenic, 3) ethical concerns, and 4) extensive regulatory demands[57,58].

Adult (somatic) stem cells are multipotent or unipotent cells that are capable of proliferating and differentiating into one or more phenotypic cells and tissues[59]. Bone-marrow derived mesenchymal stem cells (MSCs) were the first adult stem cells to be described[60] and can be obtained from almost all tissues of the body[61]. The use of adult stem cells is also subjected to strict regulatory demands, but is considered safe and without ethical concerns.

There are three groups of candidate cell sources for tissue-engineering application in POP reconstructive surgery[62]:

- Muscle-derived stem cells, harvested from skeletal muscle
- MSCs, e.g. adipose or bone marrow MSCs
- Fibroblasts

The specific combination of cell source, scaffold and biological stimuli is complex, and although several cells have shown promising results for POP repair[42–45,50,63] a superior cell source remains to be identified[64].

Muscle fiber fragments

The inclusion of in vitro cultured cells for clinical use is considered an 'advanced therapy' medicinal product by EMEA (European Medicines Agency) (European Union Regulation 1394/2007) and is thus limited by strict regulatory demands[36]. In addition, an increasing number of animal studies have demonstrated that the proliferative potential of muscle cells may be compromised by the culturing process[65,66].

In contrast, minced skeletal muscle has a remarkable regenerative ability, which was described already decades ago by Studitsky[67] and Carlson[68]. This technique has recently been reintroduced

by Corona et al. for potential use in tissue-engineering of volumetric loss of muscle tissue[69]. Skeletal muscle tissue contains muscle stem cells called satellite cells[70] that can undergo asymmetric division into new, quiescent satellite cells and proliferating myoblasts[71]. The preparation of autologous fresh muscle fiber fragments (MFFs) is easy, quick, inexpensive, and does not depend on advanced facilities or technologies[64]. The MFFs can be harvested, prepared and applied during the same surgical procedure, which makes the method clinically attractive. Moreover, the MFFs are exempted from the strict regulatory demands associated with the clinical use of cultured muscle cells[64].

Our research team has previously shown that MFFs formed striated muscle tissue when they were seeded on methoxypolyethyleneglycol-poly(lactic-co-glycolic acid) (MPEG-PLGA) scaffolds and implanted in the rat abdominal wall[44]. Our team has further performed a clinical study, injecting MFFs into the urethral sphincter of women with stress urinary incontinence[39]. This study showed a beneficial effect, which was comparable to that found by others using cultured stem cells[72–76].

Trophic factors

Tissue-engineering strategies for POP repair may benefit from the addition of bioactive substances to the cell scaffold complex[64], since the tissue metabolism of the vaginal wall is altered in women with POP[77].

Estrogen has an important role in the regulation of lower urinary tract function[78]; however, its importance for the development of POP is controversial[64]. Clinical data have indicated that systemic administration of estrogens in postmenopausal women with urinary incontinence would actually worsen the symptoms[79]. This may be caused by the fact that estrogen decreases the

production of vaginal smooth muscle cells and tropoelastin[80]. Yet, locally administered estrogen might still improve urinary incontinence[79] and symptoms of POP[81,82], although robust evidence is lacking. The mechanisms of estrogens in the treatment of POP needs to be further evaluated[78].

In patients with stress urinary incontinence, platelets have been added to the autologous cells injected to the urethral sphincter to improve the regenerative potential[83]. Platelet-rich plasma is known to release bioactive factors that affect the response in muscle regeneration[84], since it contains growth factors and bioactive proteins with fundamental effects on tissue repair[85].

Several studies have shown that only a small percentage of added MSCs for regenerative purposes are actually integrated into the host damaged tissue despite substantial tissue repair[86]. This indicates that the tissue repair is caused indirectly by a paracrine effect of the MSCs and not by the MSC engraftment[86]. The stem cell secretome is defined as a complex set of secreted molecules from stem cells that are essential for several biological functions, for example cell growth, differentiation, signaling, adhesion and angiogenesis[31]. Studies have shown that MSCs probably exert their regenerative function by the secretion of cytokines, growth factors and extracellular vesicles[31]. The secretome strategy circumvents the implantation of cells[86], which underlines the crucial role of the trophic factors in the regenerative process.

Candidate animal models

No consensus exists with regard to the optimal animal model for POP repair[87], and different animal models and species have been explored in basic urogynecology research. Currently, rodents are the most frequently used animals. They are inexpensive and easy to work with in large numbers[87], but vaginal implantation is difficult. Larger animals like rabbits and sheep allow the use

of vaginal implantation[87], but transvaginal implantation of POP meshes in these species generally results in high exposure rates[88]. This high risk of exposure may be caused by the contaminated environment and anatomical differences amongst species. In addition, the rabbit vagina is regionally different in terms of histology and function[89] and this may affect the outcome if the meshes are implanted at different sites. Non-human primates like squirrels or rhesus macaque monkeys are bipedal and can spontaneously develop POP after delivery. They allow testing in a model that largely mimics that of women with POP[90], but the use of these primates is subjected to strict ethical regulations and considerable costs[87,90].

Despite several feasible models, no consensus regarding the optimal animal model for POP repair exists[87,90,91]. The models are thus chosen according to the specific research question, since different models provide different aspects in terms of structural and biomechanical responses[87,91].

Aims

The overall aim of this thesis was to evaluate new tissue-engineering strategies that could serve as adjuncts to reconstructive pelvic surgery.

The specific aims of the thesis were:

- To confirm our previous results and to further evaluate the potential regenerative effect of MFFs seeded on an MPEG-PLGA scaffold in terms of histological and biomechanical properties in two rat abdominal wall models.
- To evaluate if a newly developed electrospun PCL scaffold would be able to 1) provide biomechanical tissue reinforcement and 2) act as a carrier for muscle stem cells in the form of MFFs in different rat abdominal wall models.
- To assess a new rabbit vaginal model for the evaluation of tissue-engineering concepts in POP repair.

Materials and Methods

Common methodology Study 1-3 – Rat studies

Animals

Animal housing and caretaking was provided by the Animal Facility at Panum Institute, University of Copenhagen, Denmark. The Danish Animal Experiments Inspectorate approved the study (permission no. 2012-15-2934-00242), and their guidelines for care and use of laboratory animals were followed. We used a total of 72 Sprague Dawley retired female breeders, weighing 245-315 grams (Taconic, Lille Skensved, Denmark).

Scaffolds

MPEG-PLGA

MPEG-PLGA is a quickly degradable, freeze-dried scaffold - spongy and porous - with multiple interconnected pores[92]. Compared to PLGA (Vicryl, polyglactin mesh), the MPEG-PLGA is more hydrophilic[92]. The MPEG-PLGA scaffold has been tested in animal models for cartilage repair where it was found to enable regeneration of the cartilage defects[93], and the MPEG-PLGA scaffold has been CE-marked for cartilage repair.

Our research team has previously demonstrated that the MPEG-PLGA was fully degraded eight weeks after subcutaneous implantation in rats[44,92], and that MFFs seeded on the scaffold had generated fragmented striated muscle tissue[44].

PCL

Since the MPEG-PLGA scaffold is fragile, with no inherent strength, we wanted to evaluate a stronger, degradable scaffold. PCL is an FDA approved polymer, which was used to form an electrospun scaffold comprising a thin layer of randomly spun fibers with a mean thickness of 1.58 µm (standard deviation (SD) ±0.96 µm) (Coloplast A/S, Humlebaek, Denmark). The electrospinning process allows engineering of scaffolds to mimic native ECM with high porosity and a nanoscale topography[94,95]. The estimated degradation time of PCL has been found to be approximately two to four years[96]. The electrospun PCL scaffold used in our studies has previously been tested in vitro and it was demonstrated that cultured human fibroblasts can successfully be seeded on the scaffold[97]. The PCL scaffold has not previously been tested in vivo.

Abdominal wall models

In total, we used four different rat abdominal wall models (Table 1). The more fragile MPEG-PLGA scaffold was tested in two models, and the PCL scaffold was tested in three models.

Table 1. Overview over scaffolds and models used in the different rat studies.

Study	Scaffold	Models used; with and without MFFs			
		Native tissue repair model	Partial defect model	Full thickness defect model	Subcutaneous model
Study 1	MPEG-PLGA	X			
Study 2	MPEG-PLGA		X		
Study 3	PCL		X	X	X

MPEG-PLGA models: Study 1 and 2The two different models for the MPEG-PLGA scaffold were:

- Native tissue repair model (Study 1): a small full-thickness sample of the abdominal wall was removed, the defect was sutured and the scaffold was placed on the repaired defect (Figure 1). The model was modified from Ozog et al.[98].
- Partial defect model (Study 2): The most superficial muscle layer was removed and replaced by the scaffold (Figure 2). The partial defect model was modified from Valentin et al.[99].

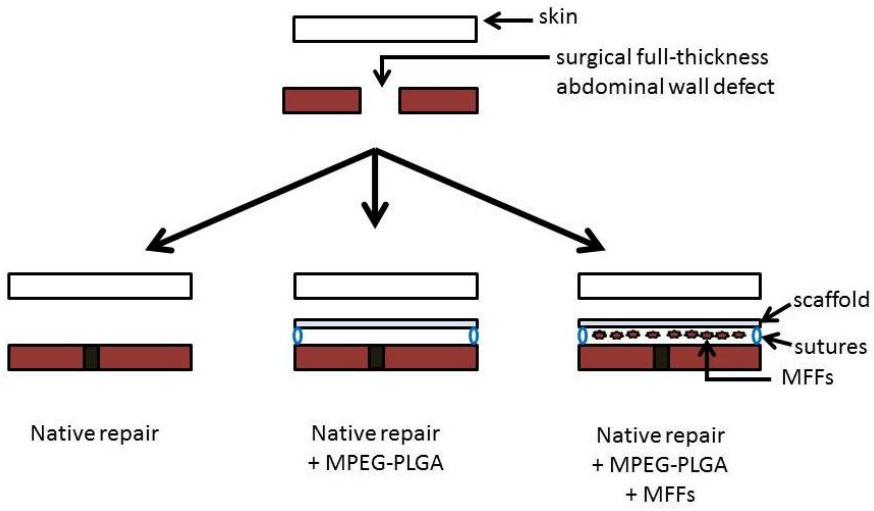

Figure 1. Native tissue repair model: overview of the three groups in Study 1. Adapted from[1].

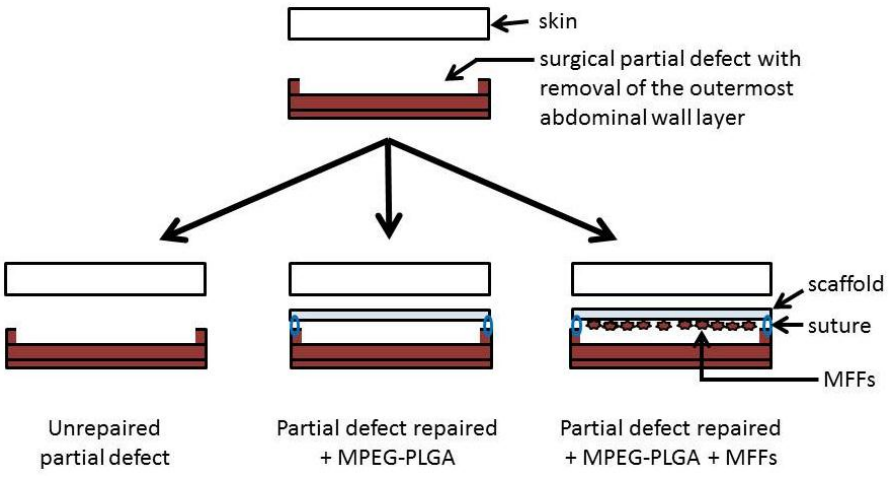

Figure 2. Partial defect model: overview of the three groups in Study 2. Adapted from[2].

Thus, both Study 1 and 2 consisted of 3 groups each, with six animals in each group.

Prior to Study 2, we performed an initial evaluation of the surgical feasibility and the biomechanical strength of the partial defect in euthanized rats. We compared the normal abdominal wall (n=9) with a partial defect, where 1) only the outermost layer was removed (n=3) and where 2) the two outermost layers were removed (n=3) (Figure 3). As removal of a single layer was easier to perform and the two partial defect models appeared to be comparable upon biomechanical testing the partial defect with removal of one muscle layer only was chosen for Study 2.

Figure 3. Two different partial defect models: overview of the three groups compared in the initial study for Study 2.

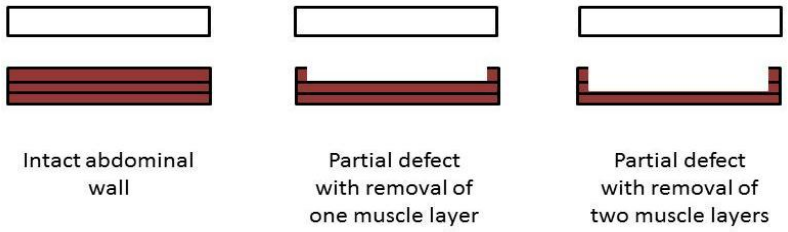

PCL models: Study 3

In study 3, we evaluated the tissue and the biomechanical responses to the PCL scaffold in three abdominal wall models with different loads (Figure 4):

1. Subcutaneous placement, corresponding to the model tested by Boennelycke et al.[44,92], in which the scaffold was placed on the intact abdominal muscle layers. There was no load on the scaffold.

2. Partial defect model, corresponding to the aforementioned model in Study 2 and modified from Valentin et al.[99], where the outermost muscle layer was removed. The scaffold was subjected to some load.
3. Full-thickness defect model, where all three muscle layers were removed[100] and replaced by the PCL scaffold. The scaffold was subjected to maximal load.

The full-thickness model was chosen to evaluate whether the PCL scaffold was capable of providing biomechanical tissue reinforcement even in case of considerable load.

Each of the three models had implanted PCL scaffolds with and without MMFs, thus leading to a total of six groups with six animals in each group:

Figure 4. Overview of the six groups in Study 3. Adapted from[3].

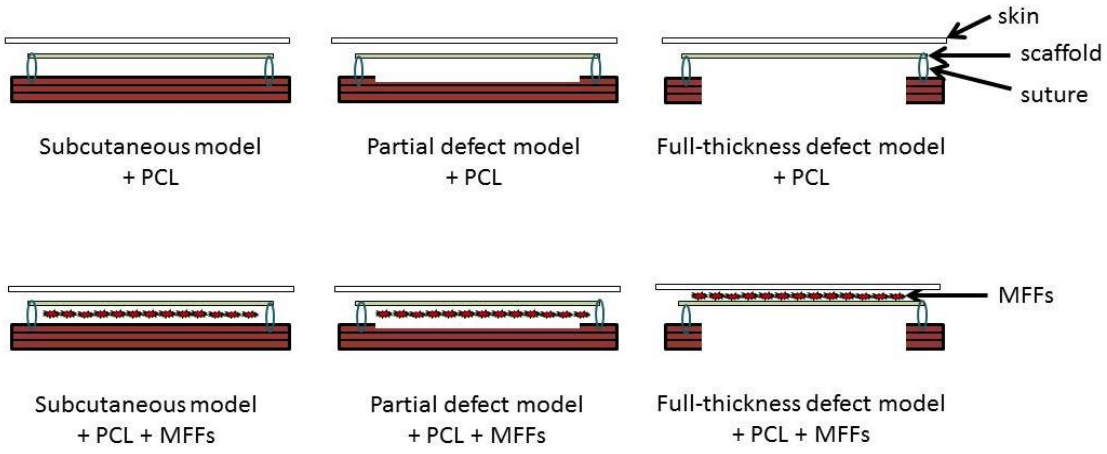

Implantation

The rats were anesthetized with Hypnorm/Midazolam 0.3 ml/100 g (Hypnorm, VetaPharma Ltd., Leeds, UK and Midazolam, Hameln Pharmaceuticals GmbH, Hameln, Germany). We performed a midline skin incision on the abdomen followed by subcutaneous blunt dissection.

Surgeries for the different models were performed as follows:

- In the native tissue repair model (Study 1), a longitudinal full-thickness portion of the abdominal wall measuring approximately 3.0×0.1 cm was resected. The defect was sutured continuously with Vicryl 4-0. For later identification and location, one non-absorbable Prolene 5-0 suture was placed in each end of the repaired defect.
- In the partial defect model (Study 2 and 3), a defect was created by removing the outermost muscle layer lateral to the rectus muscle, over an area measuring 3.0×1.5 cm.
- In the subcutaneous model (Study 3), the scaffold was placed on the intact abdominal wall layers.
- In the full-thickness model (Study 3), all three muscle layers were removed over an area measuring 3.0×1.5 cm, lateral to the rectus muscle.

For partial and full-thickness defect models, the defected areas were marked using a grid. In all cases of scaffold implantation, these were placed longitudinally to the midline covering the defect. All scaffolds measured 2.5×4.0 cm, thus, oversizing the defect with 0.5 cm on each border for the partial defect and the full-thickness defect. The implants were held in place by four non-degradable Prolene sutures, one stitch in each corner for later identification, followed by a continuous degradable Vicryl 4-0 suture along the borders. The skin was closed using staples (Reflex One, REF 3036, ConMed, Utica, NY, USA). Antibiotic prophylaxis and analgesia were administered according to veterinarian recommendations.

Preparation and labeling of the MFFs

In the native tissue repair model, the partial defect model and in the full-thickness defect model, the removed abdominal wall muscle was used for preparation of the MFFs. In the subcutaneous model, a muscle biopsy from the thigh was obtained, using a biopsy punch of 4 mm. The muscle tissue was placed in a sterile petri dish and cut into fine pieces using two scalpels (Figure 5). The resulting MFFs were labeled with the fluorescent dye PKH26 (Sigma-Aldrich, St. Louis, MO, USA). The PKH26 have long aliphatic tails that bind irreversibly to lipid regions of the cell membrane[101], and was chosen since it is traceable several weeks after in vivo implantation[42,102].

Figure 5. Preparation of MFFs. Adapted from[64].

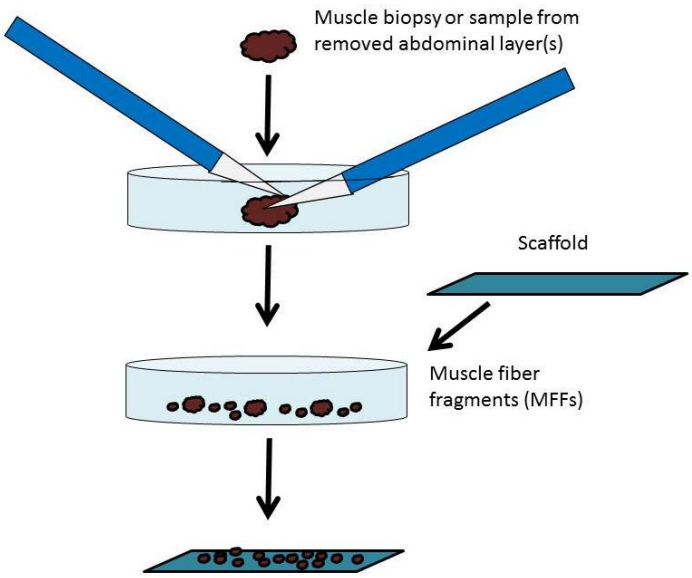

The labeled MFFs were then applied to the scaffold as a thin layer on the surface. The preparation and labeling of the MFFs were performed while the animal was anesthetized. At implantation, the scaffold was placed with the MFFs facing down, i.e. between the scaffold and the abdominal muscle layers, in all models except the full-thickness model, where the MFFs were located on the superior surface of the scaffold instead, i.e. between the scaffold and the skin (Figures 1-3).

Explantation

After eight weeks, the rats were euthanized by cervical dislocation. A midline skin incision was performed followed by subcutaneous blunt dissection to present the abdominal wall musculature with attached subcutaneous and fascia tissue. Sutures in the corners were located and 1.0 cm wide tissue strips were marked prior to removal (Figure 6). A full-thickness sample of all abdominal layers was removed en bloc, including the area of implantation and surrounding tissue. After removal, the tissue was cut into four strips (Figure 6), where strips A and D were used for histological testing and strips B and C for biomechanical testing.

Figure 6. Marking of tissue strips before removal. Adapted from[1–3].

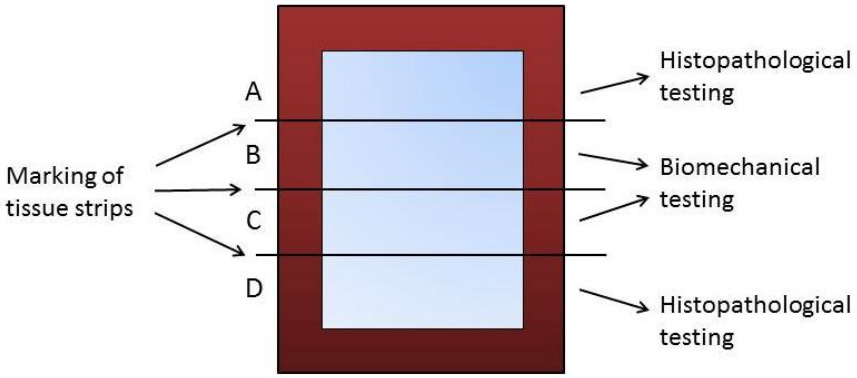

Histopathology and immunohistochemistry

Tissue samples were fixed in 10% buffered formalin, embedded in paraffin and cut in 5 µm sections. All samples were stained with hematoxylin and eosin (H&E). Samples from Study 1 and 2 were stained with van Gieson/alcian blue (van Gieson acid fuchsin solution, Sigma Aldrich, HT 254; alcian blue, Dako, pH 2.3, code no. AR 160) and samples from Study 3 were stained with Masson trichrome (Sigma-Aldrich, St. Louis, MO; USA). The neighboring sections were immuohisto-

chemically analyzed for desmin (Dako, Glostrup, Denmark), a cytoplasmic marker of smooth and skeletal muscle. The paraffin embedded sections were stained using the EnVision FLEX+ (Dako, Glostrup, Denmark) polymer peroxidase diaminobenzidine system, and a Trisethylenediaminetetraacetic acid (EDTA) solution pH9.0 (Dako) was used to perform heat-induced epitope retrieval. Anti-human desmin mouse monoclonal antibody (Dako IR 606 ready-to-use), which cross-reacts with both mouse and rat proteins, was applied for 20 min at ambient temperature in the Dako Autostainer Link 48.

In Study 3, the quantity of giant cells was calculated as a percentage of nuclei using H&E stained specimens. Also, in Study 3, we performed orcein staining (Orcein Stain Kit, Artisan, Dako, Denmark) to stain the elastin fibers.

The slides were viewed under an Olympus BX60 Microscope (Olympus, Center Valley, PA, USA). Images were analyzed using the Image-Pro Plus 7.0 software (Media Cybernetics, Inc., Rockville, MD, USA).

Bonar score

In Study 1 and 2, we evaluated histopathological characteristics of the connective tissue after full degradation of the MPEG-PLGA scaffold using the semi quantitative Bonar score. The Bonar score (range 0-20), which was recently published by Fearon et al.[103], provides a standardized evaluation of five distinct parameters of the regenerative process of connective tissue: cell morphology, collagen arrangement, cellularity, vascularity, and ground substance tissue response. The score uses a predefined number of fields that require evaluation at a predefined magnification[103].The score was originally established for the evaluation of tendon injuries[104,105] and a higher score

represents a more advanced stage of the regenerative repair process. We assessed collagen arrangement with the additional use of polarization filter imaging of the van Gieson-stained fibers. The ground substance was evaluated using the alcian blue staining for mucopolysaccharides; the other outcomes were assessed using the H&E stained specimens. Assessment of Bonar score was performed by senior pathologist L.C. who was blinded to group allocation.

The Bonar score was not used in evaluation of the PCL implants (Study 3) because the PCL was not degraded, and apart from a few collagen fibers and scattered blood vessels no measurable signs of de novo connective tissue production were found.

Fluorescence

To detect PKH26 fluorescence, frozen samples were cut into 16-µm sections and evaluated in a fluorescence microscope Olympus BX51 (Olympus, Center Valley, PA, USA). If no fluorescence was detected, the sample was re-cut and examined further to ensure the absence of fluorescence-positive cells in nearby foci.

Uniaxial biomechanical testing

Directly after removal, the tissue for biomechanical testing was placed in sterile petri dishes with sterile phosphate-buffered saline (PBS). Approximately 2-4 hours after removal, the samples were tested using a TA.XT plus Texture Analyser (Stable Micro Systems, Godalming, Surrey, UK) with a 5 kg load cell and TA 94 Pneumatic Grips (Thwing-Albert Instrument Company, West Berlin, NJ, USA), using a pressure of 3 bar. Testing was performed in a controlled environment with a constant temperature of 23°C and a relative humidity of 50%. To secure a tight grip without

squeezing the tissue, the clamps were modified with a grip paper (3M). A preload of 0.1 N was applied to the inserted tissue strips to remove slack and the grip-to-grip distance was measured and defined as elongation of zero. Two tissue samples, strips B and C, from each rat were tested (Figure 6). Strip B was inserted with a grip-to-grip separation of 1.0 cm, while strip C was inserted with a grip-to-grip separation of 3.0 cm. Only the part of the tissue placed between the grips was subjected to testing. Thus, strip B-testing only involved the area with scaffold and underlying tissue or defect, whereas strip C-testing also involved the surrounding normal tissue (Figure 7). For strip B, the clamps moved with a speed of 0.333 mm/second. For strip C, they moved with a speed of 1 mm/second. The difference in speed between the two grip-to-grip distances was chosen to ensure constant strain-rate.

Load (N) and elongation (mm) were recorded until failure. The biomechanical results were analyzed with Exponent Version 6,1,3,0 software (Stable Micro Systems, Surrey, UK). Load was plotted against elongation, forming bilinear curves with a low- and a high stiffness zone (Figure 8). Data were reported as stiffness in the low- and high-stiffness zones (N/mm), load at failure (N) and elongation at failure (mm).

Figure 7. Biomechanical testing of tissue strip B, only including the central part of the scaffold, and strip C, also including the surrounding tissue. Adapted from[3].

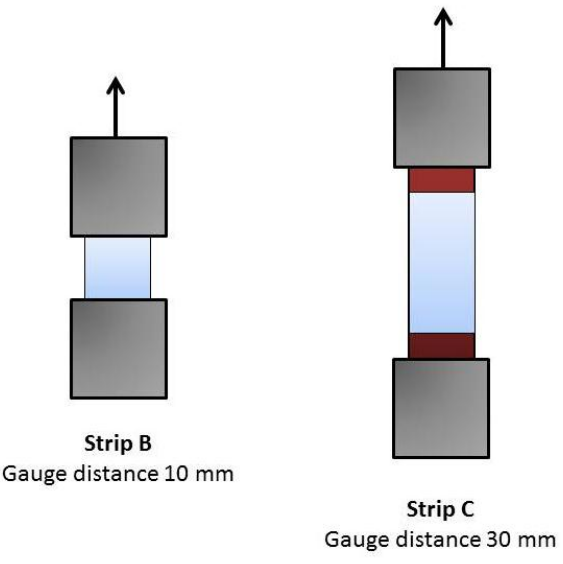

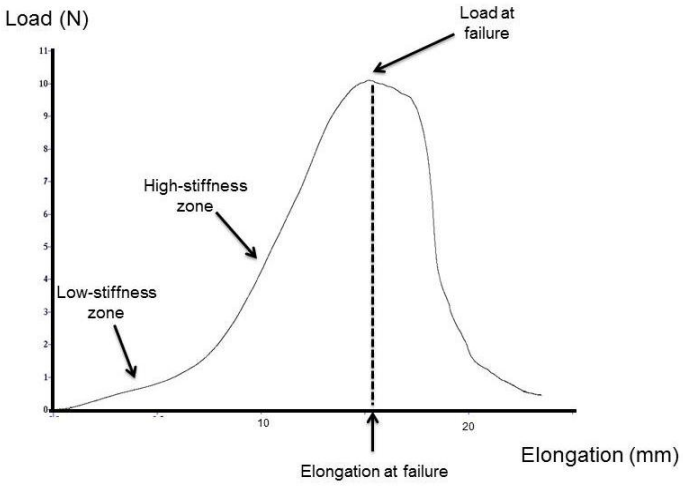

Figure 8. Load-elongation curve visualizing the low- and the high-stiffness zones, load at failure and elongation at failure. Adapted from[1].

Methodology Study 4 – Pilot study in rabbits

We performed a feasibility pilot study to evaluate a new vaginal model in rabbits. The study was approved by the Danish Animal Experiments Inspectorate (permission no. 2013-15-2934-00842/ACHOV) and guidelines for care and use of laboratory animals were followed. Animal husbandry was provided by the Department of Experimental Medicine, Frederiksberg Campus, University of Copenhagen, Denmark.

The vaginal model was based on a model previously presented by Zhang et al. who used an abdominal approach and placed polypropylene meshes in the vesico-vaginal space of the rabbit[106].

We used a total of four female New Zealand white rabbits, weighing 3.3-4.0 kg. The animals were anesthetized with an intramuscular injection of Ketamin 35 mg/kg and Xylazin 10 mg/kg, supplemented with inhalation of Isoflurane.

The experiments were performed in a conventional operating theatre; the abdomen was shaved, disinfected and draped in a sterile fashion. An intramuscular injection of antibiotics (Streptocillin 0.1 ml/kg) and a subcutaneous injection of analgesics (Rimadyl 4 mg/kg and Temgesic 0.1 ml/kg) were administered. A vertical midline incision through the skin, measuring approximately 5 cm,

was performed, the bicornuate duplex uterus was identified and lifted up through the skin incision to present the vaginal wall, and the peritoneum between the bladder and the vagina was cut open to access the anterior vaginal wall. We performed a partial vaginal wall defect by creating two superficial longitudinal incisions: one incision of 1.5-2.0 cm in length was performed on the anterior vaginal wall in the vesico-vaginal space and another incision measuring 1.0-1.5 cm in length was performed on the anterior vaginal wall close to the cervix. The distal ends of both incisions were marked by single Prolene 5-0 sutures for later identification of the area. In two rabbits, the incisions were left unsutured, and no scaffolds were inserted. In one of the other two rabbits, a scaffold measuring 1.0×2.0 cm was placed longitudinally covering the incision in the vesico-vaginal space, and another scaffold measuring 1.0×1.0 cm was placed covering the incision close to the cervix (Figure 9). In one of the two rabbits the scaffold material was MPEG-PLGA and in the other the scaffold was the electrospun PCL, both scaffolds are described earlier. In both animals with scaffolds, a muscle biopsy from the abdominal wall incision was harvested and used to produce MFFs labeled with PKH26 as described above. After having placed the MFFs between the scaffolds and the vaginal wall, the vagina and uterus were again placed in the abdomen, the fascia was closed using continuous Vicryl 4-0 suture, and the skin was closed using staples (Reflex One, REF 3036, ConMed, Utica, NY, USA). A total of 30 ml of physiological saline was injected subcutaneously at the different injection sites to ensure rehydration. Intramuscular injection of Antisedan (Zoetis, New Jersey, US) was given immediately postoperatively to reduce sedation time. The animals were given postoperative antibiotics and analgesia as recommended by veterinarians and were checked daily for the entire observation period. After eight weeks, the rabbits were euthanized by injection of pentobarbital with lidocaine into the ear veins, followed by cervical dislocation.

At autopsy, the vagina and bladder were identified and evaluated macroscopically, and defects and scaffolds were measured prior to their removal en bloc. The posterior vaginal wall and the bladder were cut open to evaluate erosions and/or signs of infection, and the tissue samples were harvested for histological, fluorescence and biomechanical testing (Figure 9). Biomechanical testing was performed as described for tissue strip B in Study 1-3. The parts of the anterior vaginal wall that were not used for histological or biomechanical testing served as controls for the biomechanical testing.

Figure 9. Overview of placement of scaffolds in the rabbit vaginal model and tissue samples used for histological and biomechanical testing.

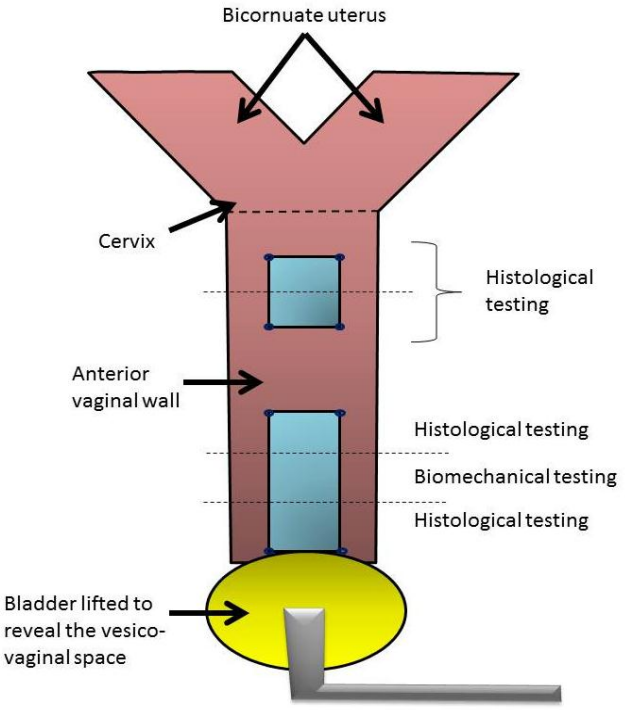

Statistical analyses

In Study 1 and 2, the Bonar score was evaluated and data were reported as median and range. Groups were compared using the non-parametric Kruskal-Wallis test of variance. Significant findings were further analyzed with post hoc Mann-Whitney test with inbuilt Bonferroni correction.

Biomechanical data were reported as mean ± SD since data were assumed to be normally distributed after evaluation of quantile-quantile plots. Differences between groups were evaluated with one-way Analysis of Variances (ANOVA). Levene's test was used to test variance of homogeneity between groups. For outcomes with significant difference in variance, one-way ANOVA with Welch correction was used. If significant differences between groups were found, using ANOVA, post hoc multiple comparisons analyses were performed with inbuilt Tukey's correction.

For Study 3, three different models were used with and without MFFs. If no significant differences between the six groups were found, the groups with or without MFFs in the same model were pooled to evaluate the possible differences between models. Discrete data regarding localized infection were presented as numbers (%) and groups were compared using Fisher's exact test.

For all statistical analyses, *P* values <0.05 were considered statistically significant. All statistical analyses were performed using the statistical software R[107].

Results

In all studies, surgery and the postoperative period were well tolerated, and no animals developed erosions or hernia. Both the MPEG-PLGA scaffold and the PCL scaffold were easy to handle, although the MPEG-PLGA scaffold was more fragile.

Results: Study 1

Histological findings

In the native tissue repair model, we found that the MPEG-PLGA scaffold was completely degraded after eight weeks in all animals. The Bonar score ranged from 5 to 7, and although there was a borderline significant difference between groups ($p=0.044$), a post hoc test comparing groups revealed no significant differences ($p=0.16$). In the animals with MPEG-PLGA seeded with MFFs, we found desmin-positive cells forming extra muscle fibers with striation (Figure 10a). PKH26 fluorescence-positive cells were visible in all six animals that had MFFs seeded on the MPEG-PLGA scaffold (Figure 10b), but not in those without MFFs that served as negative controls. The staining pattern of desmin- and PKH26-positive cells differed, but samples were prepared from different locations and not from neighboring sections.

Figure 10. Extra muscle fibers in the group with native tissue repair with MFFs. (a) Desmin immunostaining, with arrows pointing out the extra muscle tissue stained dark brown. Striated muscle tissue of the abdominal wall is marked M. (b) PKH26 fluorescence labeling with arrows pointing out examples of red fluorescence-positive cells. Original magnification ×200. Adapted from[1].

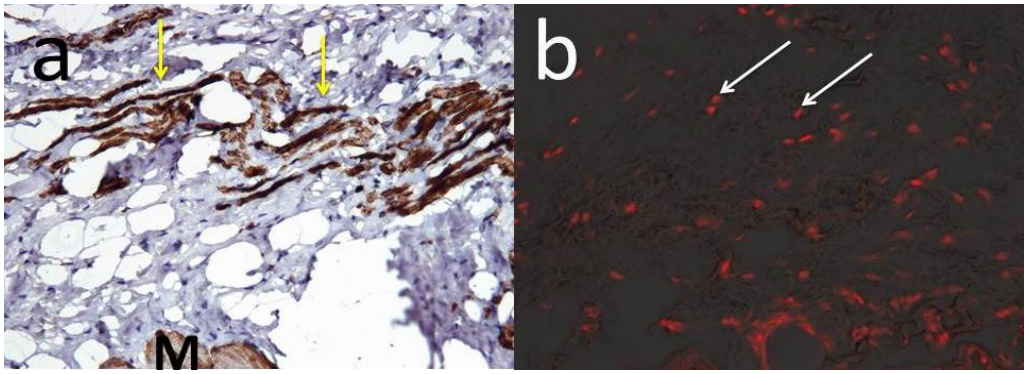

Biomechanical findings

Uniaxial biomechanical testing (see Table 2 in[1]) revealed that the group with MPEG-PLGA seeded with MFFs was significantly stiffer in the high-stiffness zone than the group with MPEG-PLGA alone when the smaller tissue strip B was tested ($p=0.032$). The group with MPEG-PLGA seeded with MFFs was also borderline significantly stiffer than the native tissue repair group ($p=0.054$) (Figure 11). Furthermore, we found a decreased elongation at failure for the group with MFFs seeded onto the scaffold compared to the native tissue repair group ($p=0.046$) (Figure 12). There were no significant differences in load at failure or stiffness in the low-stiffness zone for the smaller tissue strip B. No differences were found between groups when comparing the biomechanical properties of the larger tissue strip C that also included the surrounding normal tissue.

Figure 11. Boxplot of stiffness in the high-stiffness zone in the repair near tissue strip B.

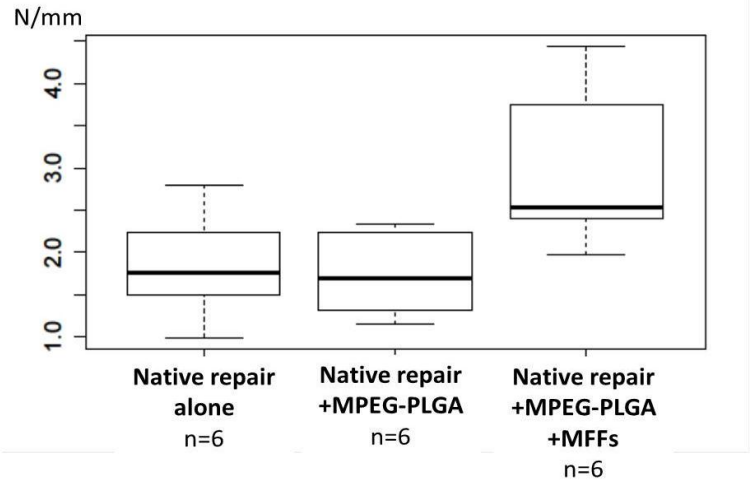

Figure 12. Boxplot of elongation at failure in the repair near tissue strip B.

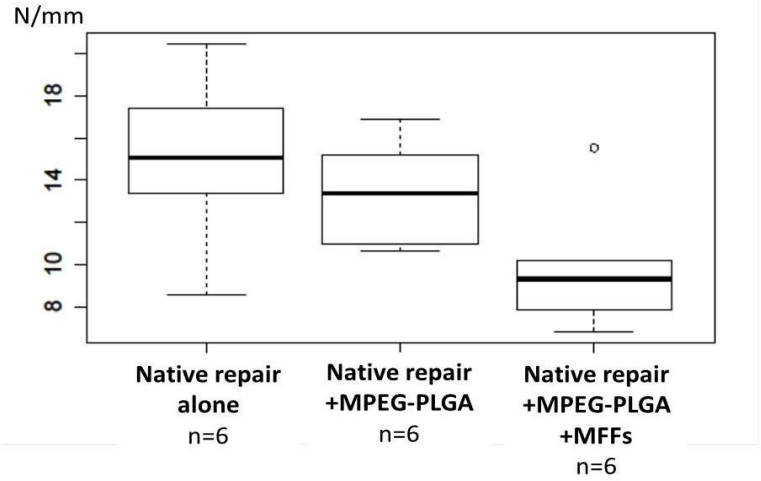

Results: Study 2

Histological findings

When evaluating the MPEG-PLGA scaffold with and without MFFs in the partial defect model, we found no remnants of the MPEG-PLGA scaffold after eight weeks. However, in some animals we

found remnants of Vicryl sutures used to secure the scaffold (Figure 13). No significant differences in Bonar score (ranging between 5 and 6) were found (p=0.35).

Irregular desmin-positive muscle cells were found adjacent to the more well-defined remaining muscle layers in all groups (Figure 14). In the partial defect model, the outermost muscle layer had been removed, leaving an uneven surface, and it was not possible to differentiate between the irregular superficial muscle layer and cells originating from the MFFs (Figures 13 and 14). PKH26 fluorescence-positive cells were only found in those animals that had had their scaffold seeded with MFFs (Figure 15).

Figure 13. Van Gieson/alcian blue staining. Black arrow points out remnants of Vicryl suture, yellow arrows point out fragments from the removed muscle layer or from the MFFs.
M marks the normal underlying muscle layers.
Original magnificantion ×40.

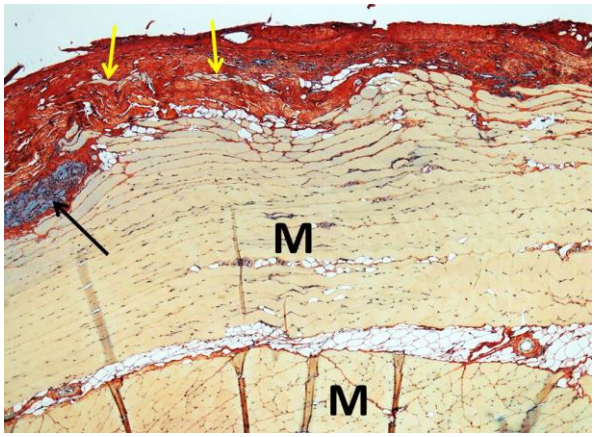

Figure 14. Desmin immunostaining of specimens in Study 2. Arrows point out examples of desmin-positive cells stained dark brown separated from the normal underlying muscle layers. Original magnification ×200. Adapted from[2].

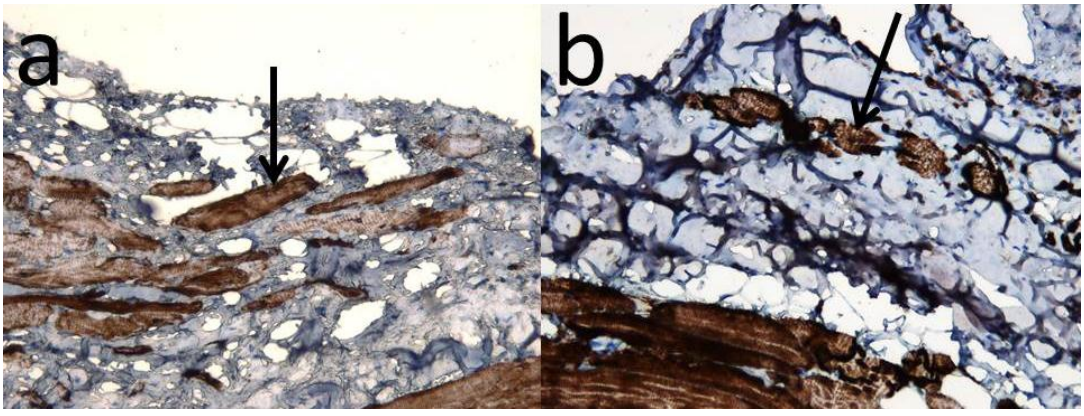

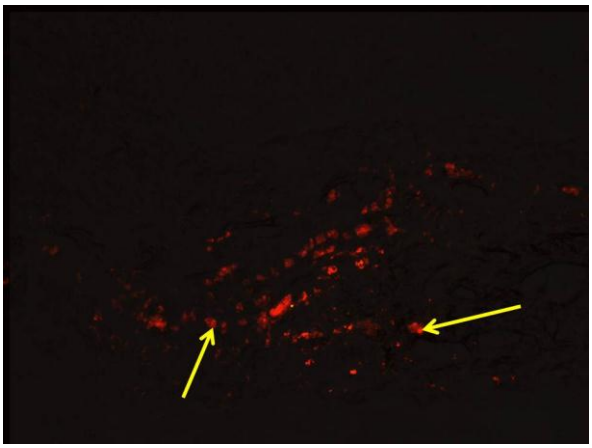

Figure 15. PKH26 fluorescence positive cells found in the group with MFFs in Study 2 are marked with yellow arrows. Original magnification ×200. Adapted from[2].

Biomechanical findings – initial study

In the initial study, we evaluated how removal of one and two muscle layers affected the biomechanical load at failure compared to the normal abdominal wall in rats (Table 2). There was a significant weakening of the abdominal wall when one layer was removed (p=0.006) and also when two layers were removed (p=0.001), but as no differences were found in the weakening between the two defect models (p=0.75), the partial defect model with removal of a single muscle layer was chosen for the final part of Study 2.

Table 2. Initial study prior to Study 2, evaluation of different partial defect models.

	Normal abdominal wall	**Partial defect, removal of one muscle layer**	**Partial defect, removal of two muscle layers**	**p-value** (ANOVA)
Number of rats	9	3	3	
Number of samples tested	51	10	11	
Load at failure (N) mean (SD)	10.1 (2.5)	4.4 (1.4)	3.2 (0.6)	<0.001

Biomechanical findings – final study

In the final study (see Table 3 in[2]), we found that the group with MPEG-PLGA seeded with MFFs had an increased load at failure compared with the group with MPEG-PLGA alone (p=0.034), for the smaller tissue strip B (Figure 16). This could not be found when comparing load at failure of the larger tissue strip C that also included the surrounding tissue (p=0.25). No significant differences between groups were found for the remaining biomechanical properties in strip B and strip C.

Figure 16. Boxplot of load at failure in tissue strip B that included the partial defect area only.

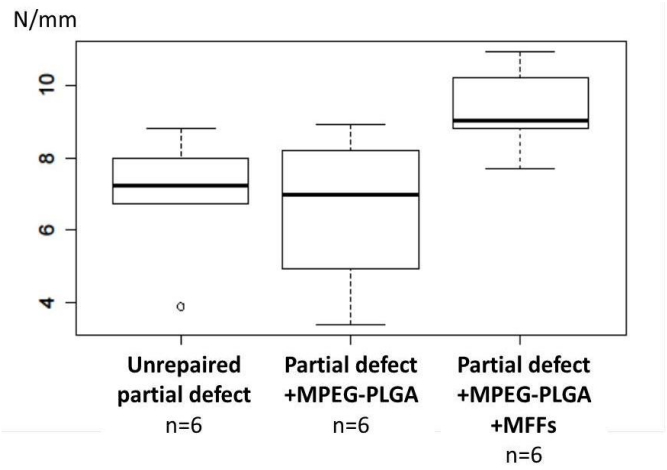

Results: Study 3

Macroscopic findings

In Study 3, we compared three models with different loads. Macroscopically, the PCL scaffold was intact and clearly not degraded after eight weeks (Figure 17). Six animals from different groups (Table 3) had signs of localized infection on the superficial surface of the scaffold (facing the skin). The thickness of the PCL scaffold was increased from approximately 50 µm to 1.6 mm with no differences between groups (p=0.70) (Table 3) or models (p=0.31). The mean shrinkage in the area

(measured as length × width before removal of the scaffold) was 11.1% with borderline non-significant differences between groups (p=0.05) (Table 3). When comparing the models, this difference became significant (p=0.014), revealing that scaffolds in the full-thickness model shrunk less than scaffolds in the subcutaneous model (p=0.011).

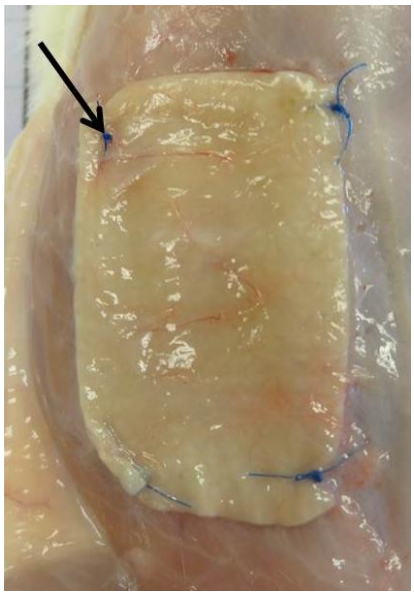

Figure 17. Macroscopic picture of intact scaffold. Arrow pointing out blue non-degraded corner suture. Adapted from[3].

Table 3. Study 3, comparing properties of neo-tissue PCL construct between the groups (adapted from[3]).

Variable of interest	**Subcutaneous model**		**Partial defect model**		**Full thickness defect model**		***p-value*** *(ANOVA)*
	without MFFs	**with MFFs**	**without MFFs**	**with MFFs**	**without MFFs**	**with MFFs**	
Thickness (mm)	1.42 (0.30)	1.50 (0.32)	1.63 (0.58)	1.76 (0.40)	1.47 (0.36)	1.58 (0.32)	*0.70*
Shrinkage (%)	15.7 (6.6)	16.2 (5.7)	10.6 (6.8)	12.7 (7.3)	9.6 (14.3)	1.7 (4.3)	*0.05*
Abscess present	2 (33%)	1 (17%)	0	1 (17%)	1 (17%)	1 (17%)	*0.98**
Nuclei (%)	2.4 (0.3)	2.5 (0.4)	2.5 (0.2)	2.6 (0.4)	2.7 (0.3)	2.7 (0.5)	*0.11*

Data are presented as means (SD) or numbers (%).
*Fisher's exact test.

Histological findings

Microscopically, we found a massive in-growth of inflammatory cells with large and numerous giant cells located around and between the PCL fibers (Figure 18a). When calculating the percentage of nuclei as a representative of the quantity of giant cells (Figure 19), we found no significant differences between groups (p=0.11) (Table 3) or models (p=0.33). There was some collagen formation (Figure 18b) and scattered vessels, which along with the many inflammatory cells formed a cellular "neo-tissue PCL construct" responsible for the increased thickness of the scaffold. The central middle "layer" of the PCL-tissue construct was acellular or partially acellular (Figure 20). The width of the acellular layer varied slightly, but there were no systematical differences between groups or models. No desmin or PKH26 fluorescence-positive cells were observed inside or around the construct.

In animals with macroscopic signs of infection, we found tissue with necrosis and hemosiderin-laden macrophages, plasma cells, lymphocytes and granulocytes corresponding to different stages of abscess formation (Figure 21).

Figure 18. Histological response eight weeks after implantation of the electrospun PCL scaffold (a) H&E staining showing numerous giant cells (orange arrows) located around and between the non-degraded PCL fibers (white arrows). (b) Some collagen formation (stained blue by Masson trichrome staining and marked by yellow arrow) was found between fibers and inflammatory cells. Original magnification ×200. Adapted from[3].

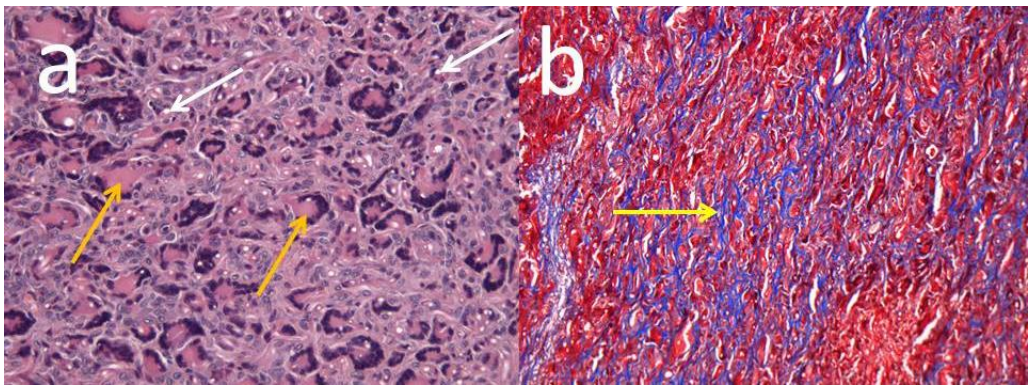

Figure 19. Calculation of percentage of nuclei as a measurement of number of giant cells inside the PCL scaffold. (a) H&E staining and the corresponding mask used for calculation of nuclear percentage (b). The percentage was calculated as the white area in (b) divided by the total area in (b). Original magnification ×400. Adapted from[3].

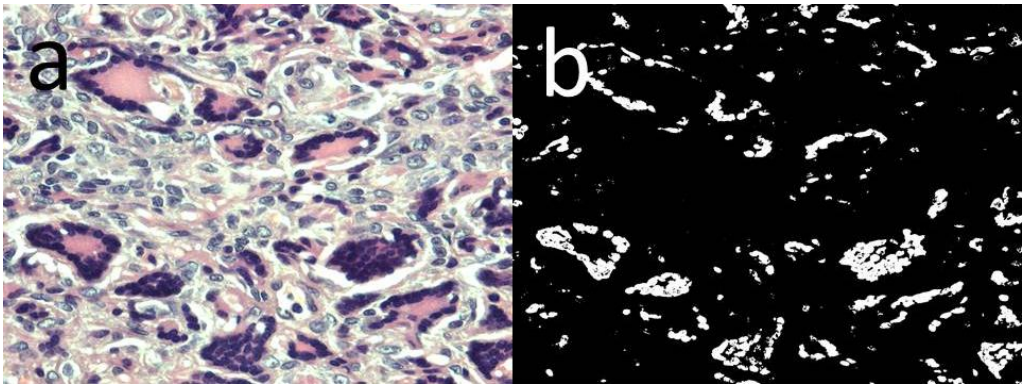

Figure 20. (a) Central acellular or partially acellular sample in Masson trichrome staining and (b)H&E staining, magnification ×40 and ×200, respectively. Adapted from[3].

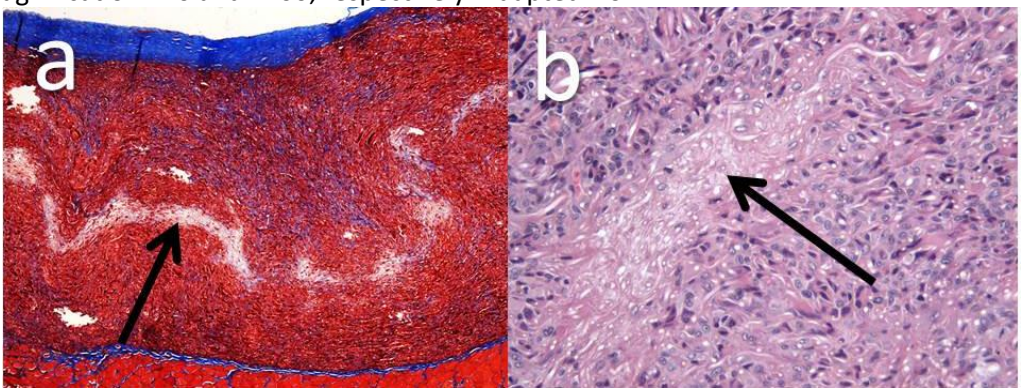

Figure 21. Abscess with necrosis and hemosiderin-laden macrophages, lymphocytes, plasma cells and granulocytes (H&E staining, magnification ×100 (a) and ×200 (b)). Adapted from[3].

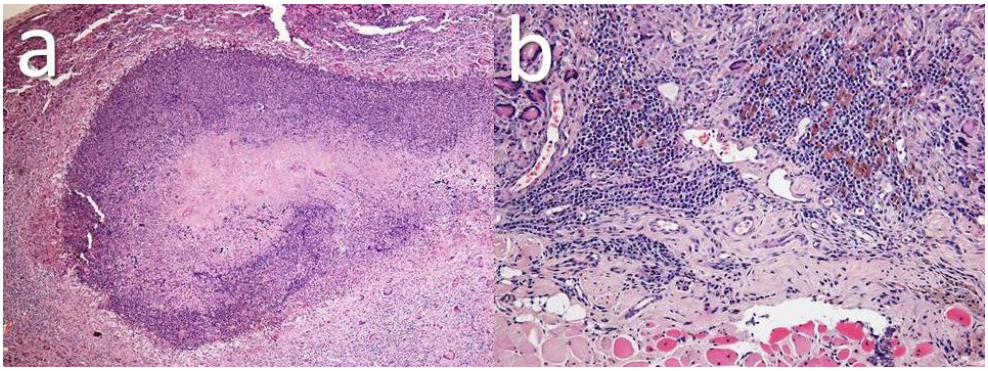

Biomechanical findings

We found no significant differences between groups for any of the biomechanical properties (see Table 2 in[3]), but there was a significant difference in elongation at failure between models (see Table 3 in[3]). For the smaller tissue strip B, the full-thickness model had reduced elongation at failure compared to the subcutaneous model (p=0.008) (Figure 22). For the larger tissue strip C, the full-thickness model had reduced elongation at failure compared with the partial defect model (p=0.002) (Figure 23).

Figure 22. Boxplot of elongation at failure, testing strip B (the defect/scaffold area).

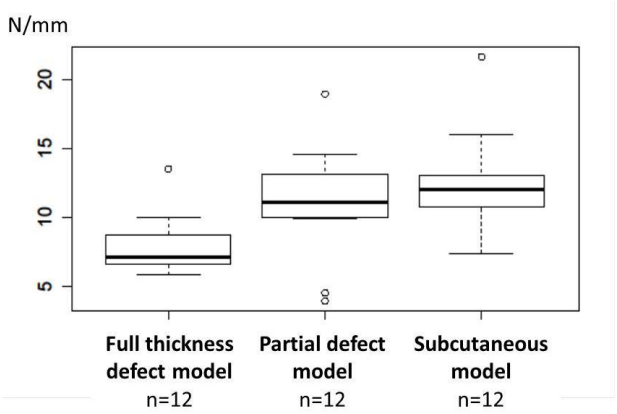

Figure 23. Boxplot of elongation at failure, testing strip C (the defect/scaffold area and the surrounding tissue).

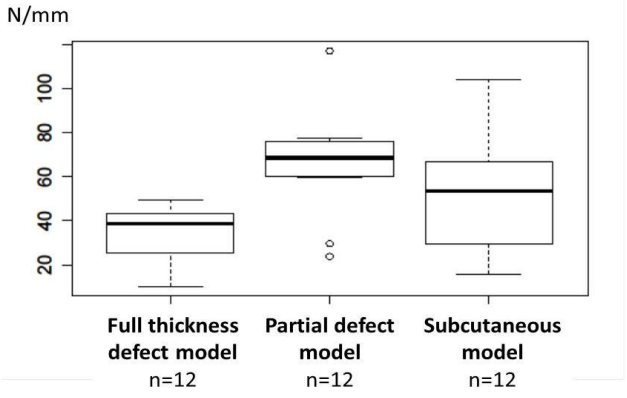

Results: Study 4

This feasibility study was carried out in four rabbits, where we performed a partial defect model and implanted scaffolds in the vesico-vaginal space and on the anterior vaginal wall close to the cervix (Figure 24). The surgical procedure was easy to perform and was well tolerated by all animals without causing erosions or infections. However, using rabbits rather than rats as laboratory animals required a more advanced setup, especially in terms of surveillance during and after anesthesia.

One rabbit had implantation of MFFs seeded on the MPEG-PLGA scaffold. These cells could be traced by fluorescence after eight weeks (Figure 25).

Figure 24. Placement of the two MPEG-PLGA scaffolds. Arrow marks the bladder.

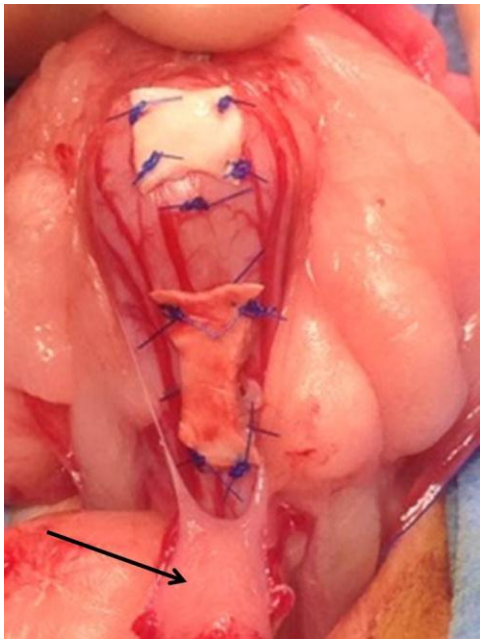

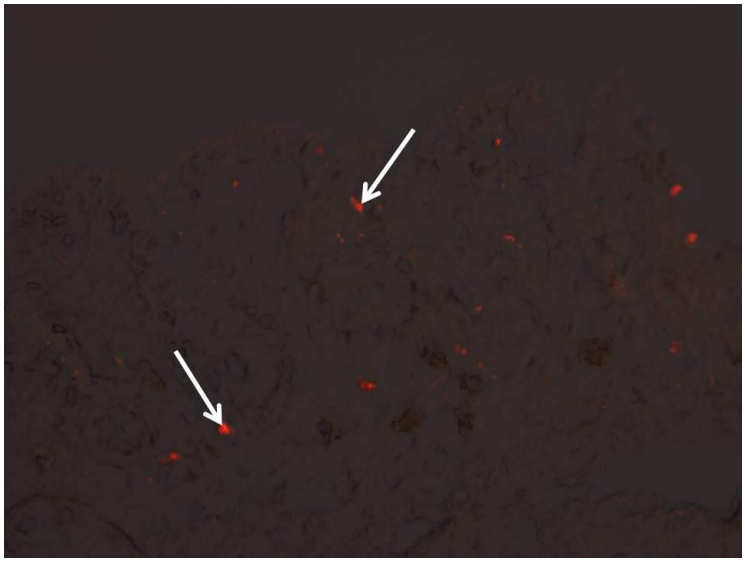

Figure 25. Fluorescence positive cells in the rabbit implanted with MFFs seeded on the MPEG-PLGA scaffold. Examples of these cells are marked with white arrows. Original magnification ×200.

The other rabbit had implantation of MFFs seeded on the PCL scaffold, which caused a marked inflammatory response with numerous and large giant cells located around and between the PCL fibers, lying both individually and in clusters (Figure 26). Fluorescence positive cells could not be identified. The biomechanical results are presented in Table 4.

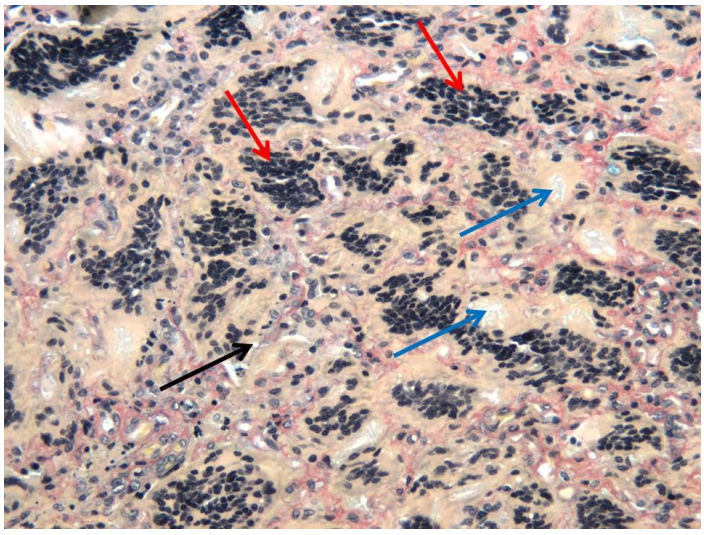

Figure 26. Van Gieson Alcian blue staining of tissue sample of rabbit vaginal wall implanted with MFFs seeded on the electrospun PCL scaffold. Red arrows mark giant cells, the black arrow marks a single PCL fiber and blue arrows mark bundles of PCL fibers. Original magnification ×200.

Table 4. Biomechanical properties of the vaginal tissue eight weeks after a partial defect was created with or without MFFs added to the scaffold in the vesico-vaginal space.

Model tested	Number of rabbits	Number of samples tested	Stiffness in the low-stiffness zone (N/mm)	Stiffness in the high-stiffness zone (N/mm)	Load at failure (N)	Elongation at failure (mm)
Normal vaginal wall*	4	7	1.49	11.24	2.36	47.06
Unrepaired partial defect*	2	2	1.24	6.64	1.60	45.23
MPEG-PLGA + MFFs	1	1	1.06	13.93	3.90	65.39
PCL + MFFs	1	1	3.29	13.42	2.56	32.72

* Data are presented as medians.

In one rabbit that had an unrepaired partial defect, the Prolene suture marking the caudal end of the defect in the vesico-vaginal space, had penetrated the bladder and caused formation of a bladder stone measuring 2×3×2 mm. The stone was adherent to the end of the Prolene suture.

Discussion

This thesis was carried out to evaluate new tissue-engineering strategies that could serve as adjuncts to pelvic reconstructive surgery. We evaluated scaffolds of MPEG-PLGA and PCL, with or without seeded MFFs and to simulate different POP repair scenarios different animal models were used.

In two rat abdominal wall models (Study 1 and 2), we confirmed previous findings that MFFs seeded on the short-term degradable MPEG-PLGA scaffold resulted in the formation of new tissue fibers or cells adjacent to the existing muscle layers. Also, we confirmed that this scaffold was completely degraded after eight weeks and did not appear to cause any connective tissue response when implanted alone[44,92]. Cells from the MFFs could be traced and the biomechanical properties were affected. These results suggest that MFFs seeded on a scaffold of MPEG-PLGA participate in the regenerative process and could provide a beneficial cell-delivering strategy for a potential new tissue-engineering approach to improve pelvic reconstructive surgery. However, the scaffold did not provide any initial tissue reinforcement. Moreover, a long-term animal study is needed to evaluate whether this combination of scaffold and cells has a durable regenerative effect before a clinical study can be initiated.

In contrast, cells from MFFs seeded on the long-term degradable PCL scaffold (Study 3) could not be traced by fluorescence or detected by immunohistochemistry, and did not affect the biomechanical properties. The PCL scaffold was clearly not degraded after eight weeks and a massive inflammatory foreign-body reaction inside the PCL scaffold resulted in the formation of a strong cellular neo-tissue PCL construct. This construct showed a remarkable ability to adapt and provided biomechanical tissue reinforcement, even in the model where the scaffold was subjected

to maximal load. Cultured human fibroblasts have proven capable of being seeded and cultured in vitro on an electrospun PCL scaffold similar to that used in our study[97]. Therefore, it is plausible, that the milieu within the construct was too unfavorable for the added MFFs to survive in vivo. Thus, a balanced inflammatory process seems essential for survival of added cells. Other studies using PCL have also found that cells can be seeded and cultured in vitro[108–110], and several studies have shown that cells can grow onto PCL in vivo[109,111]. In our study, the extent of the inflammatory foreign-body response was unexpectedly high, presumably causing a substantial release of tissue-degrading factors. Therefore, as a scaffold material, with the function of delivering cells to a specific anatomical site, the electrospun PCL scaffold used in Study 3 seems to be poor. Nevertheless, the neo-tissue PCL construct could replace the normal abdominal wall indicating a considerable potential for biomechanical tissue reinforcement. Although previous studies using degradable meshes at reconstructive POP surgery have failed to prove superior results compared with native tissue repair alone[14,22], the concept of using electrospun PCL might be an alternative to polypropylene meshes. Ideally, tissue-engineering strategies added to pelvic reconstructive surgery should restore tissue function by restoring anatomy. Thus, the scaffold should provide initial tissue reinforcement to enable both local fascia tissue support and ligament suspension. Our results indicate that the neo-tissue PCL construct could provide initial strength comparable to local tissue support, but it is plausible that the construct even could provide strength comparable to that required for ligament suspension, although testing at even higher load is required to verify this. Furthermore, a long-term animal study until full PCL degradation would be necessary to ensure formation of a functional tissue construct.

To evaluate a vaginal tissue-engineering model for POP repair, we modified a new trans-abdominal rabbit model, creating a partial defect in the vaginal wall (Study 4). This was a pilot

study with a low number of animals included and comparisons between histological and biomechanical properties of the implanted scaffolds were not meaningful. However, no erosions or exposure of the implanted scaffolds could be found. Cells from the MFFs seeded onto the MPEG-PLGA scaffold could be traced after eight weeks, and again, no trace of these cells was seen in the implanted PCL scaffolds. Similar to Study 3, the PCL scaffold caused a massive foreign-body response with numerous and large giant cells located around and between the PCL fibers. Obviously, larger studies are needed before the tissue response can be evaluated and compared using this model. However, it could be a promising alternative model for future tissue-engineering studies, especially those requiring long-term follow-up.

Eight weeks follow-up

Our results were limited to the follow-up time of eight weeks in all studies and represented just a snapshot of the ongoing regenerative process. In Study 1, we found increased stiffness in the group with MFFs, but it is uncertain whether this increase would have persisted at later time points. The degradation time of PCL is long and in Study 3, our results only reflected the initial tissue response. Long-term follow up to evaluate tissue response after full degradation of the PCL scaffold would require different animal models and species. With the gradual disappearance of the scaffold fibers, collagen formation may take over the load and eventually form scar tissue, but it is also possible that the foreign-body response to the PCL affects the collagen formation or the regenerative response. These questions can only be answered in studies with longer follow-up time.

Animal models

When designing studies to evaluate the potential of new meshes or scaffolds, preclinical studies in laboratory animals are ethically necessary to understand the host response and mechanisms of action[91]. A variety of different animal models have been used[91], but there is no consensus on the optimal animal model in the studying of reconstructive POP surgery per se[87,91]. Therefore, the choice must depend on the research question under consideration[87]. The vaginal tissue response of laboratory animals like rats, rabbits and sheep have shown to differ from that of humans and erosion rates ranging from 50 to 100% have been reported after transvaginal implantation of synthetic meshes in these animals[91]. It seems therefore reasonable that the hernia abdominal wall model should be considered a first line approach when new materials for POP repair are to be evaluated in vivo[91].

The MPEG-PLGA scaffold has previously been implanted subcutaneously in a rat abdominal wall model[44,92]. By using the native tissue repair model (Study 1) we wanted to evaluate whether performing and repairing a defect of the native tissue at the site of scaffold implantation would affect the regenerative response. In the partial defect model (Study 2), we induced a weakening of the abdominal wall to test the influence of MFFs added to the MPEG-PLGA scaffold on the biomechanical strength. In Study 1, the native tissue repair model itself was found to be strong, which was in accordance with a study using a small intestine submucosa-scaffold in a similar model[112]. Therefore, the use of the weakened abdominal wall model in Study 2 supplemented the results of Study 1; the MFFs were found to increase the load at failure when seeded on the MPEG-PLGA scaffold. Thus, the combination of MFFs and MPEG-PLGA could provide a cell-delivering approach, creating a functional tissue construct although the scaffold per se did not provide any initial tissue reinforcement. The electrospun PCL scaffold used in Study 3 had not previously been

tested in vivo. Therefore, we chose to evaluate the tissue response in three abdominal wall models, where increasing loads were applied to the scaffolds. The inherent strength of the PCL scaffold enabled testing of a full-thickness model, which would not have been possible with the MPEG-PLGA scaffold. Indeed, the PCL scaffold did provide biomechanical tissue reinforcement, even when exposed to the maximum load in the full-thickness model.

Using models with different loads allowed assessment for diverse possible clinical applications. We found that the properties of the resulting neo-tissue PCL construct were similar in all groups. If we had gradually increased the load to the mesh further the scaffold might have proven even stronger until eventual failure, resulting in herniation. Using a model with further load would have revealed whether the PCL scaffold could provide strength necessary for ligament suspension in POP surgery.

Although rodent abdominal wall models should be first-line studies when evaluating new reinforcement strategies for POP repair, the anatomy of the abdominal wall is clearly different from the elastic/collagenous, fibrous, smooth muscle and epithelial tissue of the vaginal wall. Therefore, we set out to develop a rabbit vaginal model. In order to avoid the high exposure rate previously found when meshes have been placed transvaginally[113–116], we chose a transabdominal approach. Placing the scaffold in the vesico-vaginal space has not been associated with vaginal erosion previously[106], and neither did our partial defect of the anterior vaginal wall with implanted scaffolds reveal any erosions, although this result must obviously be verified in a larger study.

Biomechanics and statistical considerations

To fully understand the pathogenesis of POP, in which a weakening of the supporting tissues are causing the vaginal tissue to prolapse, testing of the vaginal wall in women with and without POP is crucial. Knowing the area of the female pelvic floor and the pressure acting on it, one can estimate the load that applies to the vaginal tissues. The area of the pelvic floor is approximately 94 cm^2 in women without POP[117] . The peak load that applies to the pelvic floor is thus 129 N[118], whereas the loads that apply in quiet standing and in supine posture are considerably lower (37 N and 19 N, respectively)[118].

The substantial side effects shown in relation to vaginal reconstructive surgery using the non-degradable polypropylene mesh are probably caused by the mismatch between the strength of the native tissue and the mesh itself. Since the polypropylene mesh is strong and stiffer than the surrounding native tissue, the mesh bears the load that applies to the pelvic floor. Meanwhile, the native tissue becomes increasingly atrophic, eventually causing erosion and mesh protrusion through the vaginal wall. This phenomenon, known as “stress-shielding”[119], is also known from other medical fields, especially in orthopedics with casting of fractured extremities. Thus, the perfect material for prosthetic purpose in POP repair, with biomechanical properties similar to those required for both local fascia tissue support and of ligament suspension of the patient’s own tissue, is necessary in order to avoid potential severe adverse events.

We used uniaxial biomechanical testing in the studies, as we had access to this method. Multiaxial ball-burst test[120,121] or testing of active biomechanical properties[122] , to which we had no access, could probably have added further information that more realistically would imitate the biomechanical loads that apply to the vaginal wall in patients with POP. However, comparison to other materials used for POP repair is difficult since models, sample geometry and testing

techniques differ[123]. To evaluate differences between groups, we performed quantile-quantile plots to assess whether data on biomechanical properties were normally distributed. Normal distribution should be evaluated within groups and given the small numbers in each group, normality was difficult to evaluate. However, we assumed that data were normally distributed to allow parametric testing.

The low number of animals in each group increased the risk of type II error, i.e. failure to reject a false null hypothesis (page 169)[124]. This means that although there might have been a significant difference between groups, we could not find this difference due to the low number within each group. Parametric testing is superior to non-parametric testing in detecting even small differences (p. 189)[124]. Further, Tukey correction for multiple testing is more likely to find significant differences than the more robust Bonferroni correction[125].

A central challenge when aiming for a tissue-engineering strategy in POP repair is to decide which biomechanical forces we are up against. The local fascia tissue support provided by the midlevel vaginal support (pubocervical and rectovaginal fascia) is clearly weaker than the upper vaginal support by ligament suspension (suspensory fibers of paracolpium and parametrium). An ideal scaffold material should provide initial tissue reinforcement for both applications. Until such an ideal scaffold has been found, the biomechanical properties of a specific combination of scaffold and cells in vivo must be matched with a surgical procedure that allows regeneration of the native tissue.

Conclusions

We sought to develop a tissue-engineering adjunct to improve the outcome of pelvic reconstructive surgery and we evaluated potential concepts that need to be further developed before clinical studies can be initiated.

- We confirmed previous findings that MFFs seeded on the quickly degradable MPEG-PLGA scaffold survive and participate in the regenerative process to form extra striated muscle fibers in different rat abdominal wall models.
- Cells from MFFs seeded on MPEG-PLGA could be traced by fluorescence labeling and also affected some biomechanical properties.
- The long-term degradable PCL scaffold caused a marked foreign-body response, forming a neo-tissue construct that provided biomechanical tissue reinforcement even when subjected to substantial load.
- MFFs seeded on the PCL scaffold did not survive in the inflammatory milieu.

Taken together, MFFs seeded on MPEG-PLGA may provide a new cell-delivering strategy for pelvic reconstructive surgery in combination with native tissue repair, if a long-term study finds a durable regenerative effect. Furthermore, the electrospun PCL scaffold might be beneficial in POP or hernia repair to provide initial biomechanical reinforcement, but long-term animal studies showing the tissue response that follows the full degradation of PCL after 2-4 years are required. An optimal tissue-engineering strategy, that provides both initial biomechanical reinforcement and at the same time delivering cells to restore durable functional tissue, remains to be found.

Perspectives

The secretome

The potential clinical use of secretome introduces a new dimension of the therapeutic use of regenerative strategies[86]. Cell-free regenerative or tissue-engineering approaches have obvious benefits compared to cell-based strategies, and the use of the secretome may bypass issues related to tumorigenicity, immune compatibility and the risk of infection transmission associated with cell-based therapies[31]. Further, the biological variability can be minimized allowing more accurate dosing and thus, safer and more effective therapies[86]. The challenges with the culturing of cells could be avoided, and secretome therapies could be prepared in advance and be immediately available for treatment when desired, even in the treatment of acute conditions[31].
In the field of urogynecology, this secretome effect has been studied in a stress urinary incontinence rat model. It showed that proteins released by stem cells in conditioned media in vitro[126] gave results equivalent to those following systemic administration of MSCs when delivered locally as periurethral injections[127] and systemically by intraperitoneal injections[128]. Neither of these studies, however, identified the active cytokines of the secretome[127,128]. In POP, the metabolism of the vaginal wall is altered[77] and the regenerative potential of the pelvic structures may be compromised. A secretome strategy may therefore be superior, provided the altered tissue is still capable of undergoing regeneration upon stimulation.
Although the use of secretome mainly focuses on MSCs, similar mechanisms are evident for muscle stem cells that contain numerous signaling proteins that participate in the regenerative processes[129]. In relation to our studies using MFFs, the functions of the secretome were, at least

partially, responsible for the effects seen in the groups with added MFFs, but it should be noted that the MFFs also contained other cells and signaling molecules that may have affected the regenerative response.

Before secretome treatment can be considered for clinical studies, all the components of the secretome should be identified to increase our understanding of how it functions and how it can be used to obtain clinically optimal outcomes[86].

Genetics

Increasing evidence points to a genetic component in the etiology of POP. Pelvic tissue in women with a genetic predisposition for POP shows chronic abnormal ECM remodeling with increased proteolytic activity[130]. Also, aging, vaginal delivery and other factors known to modulate the tissue and alter the normal architecture with effect on biomechanical properties, may cause POP[130]. Studies on connective tissue properties in women with POP have indicated alterations in the remodeling and composition of collagen and elastin, but also in the up- and downregulation of matrix metalloproteinases[131–133]. Furthermore, differences in the gene expression between women with and without POP have been identified[131], and a recent systematic review also found that polymorphisms of the *COL1A1*-gene was associated with POP[134]. However, they concluded that testing for gene polymorphism could not be recommended based on the current evidence[134]. Extensive research would be needed before the pathogenesis of POP has been fully revealed[132]. The idea of being able to modify specific genes could be an interesting treatment option for POP in the future. Especially, in the field of tissue-engineering, the regenerative potential may benefit from local gene therapy in order to optimize the clinical outcome. Gene delivery by

electroporation is an increasing field of research, mainly focusing on cancer treatment options, but it has also been used for vaccination purposes and for the delivery of genes coding for other therapeutic molecules[135]. Electroporation was first described in 1982 by Neumann et al. and is a technique in which an electrical field is applied to cells or tissues to increase the permeability of the cell membrane, allowing DNA, chemicals or drugs to enter the cell[136].

Possible applications

There is an obvious need for new strategies to improve the outcome of POP surgery. Tissue-engineering could provide such an adjunct, ideally contributing to both initial biomechanical reinforcement while allowing the added cells or secretome to create a new, strong, elastic and functional regenerated tissue construct. Based on the results of this thesis, we have not found this new ideal concept. However, our results provide knowledge that enhances our understanding of how tissue-engineering can function. MPEG-PLGA does not per se provide biomechanical reinforcement, but the added cells were found to participate in a regenerative response. The PCL on the other hand provided initial biomechanical reinforcement, but here the seeded cells did not survive. Both strategies need to be evaluated with long-term follow up studies to assess whether the effects are durable. For MPEG-PLGA, a long-term study would probably require a six-month follow up, whereas a long-term PCL study would require 2-4 years of follow up due to the long degradation time. A recent study evaluated an electrospun composite consisting of poly(lactide-co-glycolide) blended with PCL[110]. This composite material could possibly combine the positive effects related to the two scaffolds used in our studies. Furthermore, another co-electrospun material of poly(L-lactide-co-caprolactone) and fibrinogen has been implanted in a canine

abdominal wall model and in a clinical setting, where it showed comparable results to implantation of polypropylene meshes, although long-term results were absent[111].

The combination of scaffold/mesh, cells and/or secretome, as well as the local microenvironment possibly modified by gene transfer generates a broad spectrum of strategies for potential future treatment options, which may be tailored to different surgical procedures for POP. Other fields of urogynecology may also benefit from these strategies. Clearly, stress urinary incontinence treatment share many resemblances with POP, both in terms of pathophysiology[130] and treatment options with the use of synthetic woven materials[137]. In contrast, defects of the levator ani muscle (avulsions) have just recently gained interest. No standard treatment options exist[138], but it is possible that MFFs may help in treating this condition, since they are capable of forming new striated muscle fibers.

The different tissue-engineering combinations for possible POP repair have an obvious overlap with hernia repair, and common strategies for both POP and hernia should be considered.

Currently, neither MPEG-PLGA nor PCL are available as commercial products for POP repair. To our knowledge, no other tissue-engineering products or ongoing clinical trials using stem cells or a secretome strategy for reconstructive POP surgery exist. Despite increasing interest in alternative reinforcement options for pelvic reconstructive surgery, the large gap between basic science and clinically expected outcome remains and awaits further exploration before tissue-engineering can be a realistic adjunct to restore functional tissue at POP surgery.

Future research

Tissue-engineering as an adjunct to improve pelvic reconstructive surgery while avoid complications related to permanent synthetic meshes seems promising. Future research is clearly warranted before tissue-engineering strategies can be implemented for treatment of POP in women:

- Long-term studies to evaluate whether MFFs seeded on MPEG-PLGA have a durable regenerative effect.
- Evaluation of survival and possible differentiation into smooth muscle tissue of the MFFs when implanted on MPEG-PLGA in a vaginal model.
- Short- and long-term studies to evaluate whether MFFs can be used alone, without scaffold, in order to assess whether they impose a regenerative effect on the tissue.
- Evaluation of the electrospun PCL scaffold in a long-term study with the purpose of uncovering properties of the regenerated tissue after full degradation of the PCL fibers have taken place.
- Evaluation of the electrospun PCL scaffold in a model with further increased load to evaluate the full biomechanical potential of the neo-tissue PCL construct.
- Development of new scaffolds that can provide both initial biomechanical reinforcement and at the same time function as stem cell carriers to provide an optimal tissue-engineering strategy to restore functional tissue.
- Studies of basic science to fully reveal the pathophysiological mechanisms of POP and the regenerative potential of the local supportive and suspensory tissues in women with POP.

References

1. Jangö H, Gräs S, Christensen L, Lose G. Muscle fragments on a scaffold in rats: a potential regenerative strategy in urogynecology. Int Urogynecol J. 2015 Dec 24;26(12):1843–51.
2. Jangö H, Gräs S, Christensen L, Lose G. Tissue engineering with muscle fiber fragments improves the strength of a weak abdominal wall in rats. Submitted.
3. Jangö H, Gräs S, Christensen L, Lose G. Examinations of a new long-term degradable polycaprolactone scaffold in three abdominal wall models in rats. Manuscript.
4. Haylen BT, Maher CF, Barber MD, Camargo S, Dandolu V, Digesu A, et al. An International Urogynecological Association (IUGA) / International Continence Society (ICS) joint report on the terminology for female pelvic organ prolapse (POP). Int Urogynecol J. 2016 Jan 11;n/a – n/a.
5. Swift SE. The distribution of pelvic organ support in a population of female subjects seen for routine gynecologic health care. Am J Obstet Gynecol. 2000 Aug;183(2):277–85.
6. Tegerstedt G, Maehle-Schmidt M, Nyrén O, Hammarström M. Prevalence of symptomatic pelvic organ prolapse in a Swedish population. Int Urogynecol J Pelvic Floor Dysfunct. 2005 Dec;16(6):497–503.
7. Slieker-ten Hove MCP, Pool-Goudzwaard AL, Eijkemans MJC, Steegers-Theunissen RPM, Burger CW, Vierhout ME. The prevalence of pelvic organ prolapse symptoms and signs and their relation with bladder and bowel disorders in a general female population. Int Urogynecol J Pelvic Floor Dysfunct. 2009 Sep;20(9):1037–45.
8. Haylen BT, de Ridder D, Freeman RM, Swift SE, Berghmans B, Lee J, et al. An International Urogynecological Association (IUGA)/International Continence Society (ICS) joint report on the terminology for female pelvic floor dysfunction. Int Urogynecol J. 2010 Jan;21(1):5–26.
9. Mouritsen L, Larsen JP. Symptoms, bother and POPQ in women referred with pelvic organ prolapse. Int Urogynecol J Pelvic Floor Dysfunct. 2003;14(2):122–7.
10. Jelovsek JE, Barber MD. Women seeking treatment for advanced pelvic organ prolapse have decreased body image and quality of life. Am J Obstet Gynecol. 2006;194(5):1455–61.
11. Li C, Gong Y, Wang B. The efficacy of pelvic floor muscle training for pelvic organ prolapse: a systematic review and meta-analysis. Int Urogynecol J. 2015;
12. Bugge C, Adams EJ, Gopinath D, Reid F. Pessaries (mechanical devices) for pelvic organ prolapse in women. In: Bugge C, editor. Cochrane Database of Systematic Reviews. Chichester, UK: John Wiley & Sons, Ltd; 2013.
13. Ding J, Chen C, Song X, Zhang L, Deng M, Zhu L. Changes in Prolapse and Urinary Symptoms After Successful Fitting of a Ring Pessary With Support in Women With Advanced Pelvic Organ Prolapse: A Prospective Study. Urology. Elsevier Inc.; 2015;1–6.
14. Maher C, Baessler K, Glazener CM a, Adams EJ, Hagen S. Surgical management of pelvic organ prolapse in women. Cochrane Database Syst Rev. 2013;(4):CD004014.

15. Løwenstein E, Ottesen B, Gimbel H. Incidence and lifetime risk of pelvic organ prolapse surgery in Denmark from 1977 to 2009. Int Urogynecol J. 2015 Jan 20;26(1):49–55.

16. Abdel-Fattah M, Familusi A, Fielding S, Ford J, Bhattacharya S. Primary and repeat surgical treatment for female pelvic organ prolapse and incontinence in parous women in the UK: a register linkage study. BMJ Open. 2011;1(2):e000206.

17. Wu JM, Matthews C a, Conover MM, Pate V, Jonsson Funk M. Lifetime risk of stress urinary incontinence or pelvic organ prolapse surgery. Obstet Gynecol. 2014;123(6):1201–6.

18. Olsen AL, Smith VJ, Bergstrom JO, Colling JC, Clark AL. Epidemiology of surgically managed pelvic organ prolapse and urinary incontinence. Obstet Gynecol. 1997 Apr;89(4):501–6.

19. Weber AM, Walters MD, Piedmonte MR, Ballard LA. Anterior colporrhaphy : A randomized trial of three surgical techniques. Am J Obs Gynecol. 2001;185(May 1999):1299–306.

20. Maher C, Baessler K, Barber M, Cheon C, Deitz V, DeTayrac R, et al. Pelvic organ prolapse surgery. In: 5th International Consultation on Incontinence Recommendations of the International Scientific Committee: Evaluation and Treatment of Urinary Incontinence, Pelvic Organ Prolapse, and Fecal Incontinence. 2013. p. 1377–442.

21. Mouritsen L, Kronschnabl M, Lose G. Long-term results of vaginal repairs with and without xenograft reinforcement. Int Urogynecol J. 2010 Apr 9;21(4):467–73.

22. Cox A, Herschorn S. Evaluation of current biologic meshes in pelvic organ prolapse repair. Curr Urol Rep. 2012;13(3):247–55.

23. Mettu JR, Colaco M, Badlani GH. Evidence-based outcomes for mesh-based surgery for pelvic organ prolapse. Curr Opin Urol. 2014;24(4):370–4.

24. Ashton-Miller JA, DeLancey JOL. Functional anatomy of the female pelvic floor. Ann N Y Acad Sci. 2007;1101:266–96.

25. DeLancey JO. The anatomy of the pelvic floor. Curr Opin Obstet Gynecol. 1994 Aug;6(4):313–6.

26. Koelbl H, Nitti V, Baessler K, SAlvatore S, Sultan A, Yamaguchi O. Comittee 4: Pathophysiology of urinary incontinence, faecal incontinence and pelvic organ prolapse. 5th Int Consult Incontinence Recomm Int Sci Comm Eval Treat Urin Incontinence, Pelvic Organ Prolapse, Fecal Incontinence. 2013;261–360.

27. Public Health Notifications (Medical Devices) > FDA Public Health Notification: Serious Complications Associated with Transvaginal Placement of Surgical Mesh in Repair of Pelvic Organ Prolapse and Stress Urinary Incontinence [Internet]. [cited 2012 Jul 6]. Available from: http://www.fda.gov/medicaldevices/safety/alertsandnotices/publichealthnotifications/ucm061976.htm

28. U.S. Food and Drug Administration. FDA safety communication: Update on serious complications associated with transvaginal placement of surgicalmesh for pelvic organ prolapse [Internet]. 2011 [cited 2014 Apr 6]. p. 1–6. Available from: http://www.fda.gov/MedicalDevices/Safety/AlertsandNotices/ucm262435.htm

29. Press Announcements - FDA strengthens requirements for surgical mesh for the transvaginal repair of pelvic organ prolapse to address safety risks.

30. SCENIHR. Opinion on The safety of surgical meshes used in urogynecological surgery. 2015.

31. Tran C, Damaser MS. Stem cells as drug delivery methods: Application of stem cell secretome for regeneration. Adv Drug Deliv Rev. Elsevier B.V.; 2015;82-83:1–11.

32. Bianco P, Robey PG. Stem cells in tissue engineering. Nature. 2001 Nov 1;414(6859):118–21.

33. Evans CH, Palmer GD, Pascher A, Porter R, Kwong FN, Gouze E, et al. Facilitated endogenous repair: making tissue engineering simple, practical, and economical. Tissue Eng. 2007;13(8):1987–93.

34. Wiafe B, Metcalfe PD, Adesida AB. Stem Cell Therapy : Current Applications and Potential for Urology. 2015;1–7.

35. Herrera-Imbroda B, Lara MF, Izeta A, Sievert K-D, Hart ML. Stress urinary incontinence animal models as a tool to study cell-based regenerative therapies targeting the urethral sphincter. Adv Drug Deliv Rev. Elsevier B.V.; 2015;82-83:106–16.

36. Gräs S, Lose G. The clinical relevance of cell-based therapy for the treatment of stress urinary incontinence. Acta Obstet Gynecol Scand. 2011 Aug;90(8):815–24.

37. Lane FL, Jacobs S. Stem cells in gynecology. Am J Obstet Gynecol. Elsevier Inc.; 2012;207(3):149–56.

38. Peters KM, Dmochowski RR, Carr LK, Robert M, Kaufman MR, Sirls LT, et al. Autologous muscle derived cells for treatment of stress urinary incontinence in women. J Urol. Elsevier Ltd; 2014;192(2):469–76.

39. Gräs S, Klarskov N, Lose G. Intraurethral Injection of Autologous Minced Skeletal Muscle: A Simple Surgical Treatment for Stress Urinary Incontinence. J Urol. 2014 Sep;192(3):850–5.

40. Kuismanen K, Sartoneva R, Haimi S, Mannerstrom B, Tomas E, Miettinen S, et al. Autologous Adipose Stem Cells in Treatment of Female Stress Urinary Incontinence: Results of a Pilot Study. Stem Cells Transl Med. 2014 Aug 1;3(8):936–41.

41. Frudinger A, Kölle D, Schwaiger W, Pfeifer J, Paede J, Halligan S. Muscle-derived cell injection to treat anal incontinence due to obstetric trauma: pilot study with 1 year follow-up. Gut. 2010 Jan;59(1):55–61.

42. Ho MH, Heydarkhan S, Vernet D, Kovanecz I, Ferrini MG, Bhatia NN, et al. Stimulating vaginal repair in rats through skeletal muscle-derived stem cells seeded on small intestinal submucosal scaffolds. Obstet Gynecol. 2009 Aug;114(2 Pt 1):300–9.

43. Hung M-J, Wen M-C, Hung C-N, Ho ES-C, Chen G-D, Yang VC. Tissue-engineered fascia from vaginal fibroblasts for patients needing reconstructive pelvic surgery. Int Urogynecol J. 2010 Sep;21(9):1085–93.

44. Boennelycke M, Christensen L, Nielsen LF, Gräs S, Lose G. Fresh muscle fiber fragments on a scaffold in rats-a new concept in urogynecology? Am J Obstet Gynecol. 2011 Sep;205(3):235.e10–4.

45. Hung M-J, Wen M-C, Huang Y-T, Chen G-D, Chou M-M, Yang VC. Fascia tissue engineering with human adipose-derived stem cells in a murine model: Implications for pelvic floor reconstruction. J Formos Med Assoc. Elsevier Taiwan LLC; 2014 Oct;113(10):704–15.

46. Wu Q, Dai M, Xu P, Hou M, Teng Y, Feng J. In vivo effects of human adipose-derived stem cells reseeding on acellular bovine pericardium in nude mice. Exp Biol Med. 2015;1–9.

47. Ulrich D, Edwards SL, Su K, Tan KS, White JF, Ramshaw JAM, et al. Human endometrial mesenchymal stem cells modulate the tissue response and mechanical behavior of polyamide mesh implants for pelvic organ prolapse repair. Tissue Eng Part A. 2014 Feb 21;20(3-4):785–98.

48. Roman Regueros S, Albersen M, Manodoro S, Zia S, Osman NI, Bullock AJ, et al. Acute In Vivo Response to an Alternative Implant for Urogynecology. Biomed Res Int. Hindawi Publishing Corporation; 2014;2014:1–10.

49. Edwards SL, Ulrich D, White JF, Su K, Rosamilia a., Ramshaw J a. M, et al. Temporal changes in the biomechanical properties of endometrial mesenchymal stem cell seeded scaffolds in a rat model. Acta Biomater. 2015;13:286–94.

50. Su K, Edwards SL, Tan KS, White JF, Kandel S, Ramshaw J a M, et al. Induction of endometrial mesenchymal stem cells into tissue-forming cells suitable for fascial repair. Acta Biomater. Acta Materialia Inc.; 2014;10(12):5012–20.

51. Olson JL, Atala A, Yoo JJ. Tissue engineering: current strategies and future directions. Chonnam Med J. 2011 Apr;47(1):1–13.

52. Mangera A, Bullock AJ, Roman S, Chapple CR, MacNeil S. Comparison of candidate scaffolds for tissue engineering for stress urinary incontinence and pelvic organ prolapse repair. BJU Int. 2013 Sep;112(5):674–85.

53. Chapple CR, Osman NI, Mangera A, Hillary C, Roman S, Bullock A, et al. Application of Tissue Engineering to Pelvic Organ Prolapse and Stress Urinary Incontinence. Low Urin Tract Symptoms. 2015 May;7(2):63–70.

54. Evans MJ, Kaufman MH. Establishment in culture of pluripotential cells from mouse embryos. Nature. 1981. p. 154–6.

55. Martin GR. Isolation of a pluripotent cell line from early mouse embryos cultured in medium conditioned by teratocarcinoma stem cells. Proc Natl Acad Sci U S A. 1981;78(12):7634–8.

56. Thomson JA, Itskovitz-Eldor J, Shapiro SS, Waknitz MA, Swiergiel JJ, Marshall VS, et al. Embryonic stem cell lines derived from human blastocysts. Science. 1998 Nov 6;282(5391):1145–7.

57. Tran C, Damaser MS. The potential role of stem cells in the treatment of urinary incontinence. Ther Adv Urol. 2015;7(1):22–40.

58. Kim JH, Lee S-R, Song YS, Lee HJ. Stem cell therapy in bladder dysfunction: where are we? And where do we have to go? Biomed Res Int. 2013;2013:930713.

59. Goldman HB, Sievert K-D, Damaser MS. Will we ever use stem cells for the treatment of

SUI?: ICI-RS 2011. Neurourol Urodyn. 2012 Mar;31(3):386–9.

60. Chamberlain G, Fox J, Ashton B, Middleton J. Concise Review: Mesenchymal Stem Cells: Their Phenotype, Differentiation Capacity, Immunological Features, and Potential for Homing. Stem Cells. 2007;25(11):2739–49.

61. Vaegler M, Lenis AT, Daum L, Amend B, Stenzl A, Toomey P, et al. Stem cell therapy for voiding and erectile dysfunction. Nat Rev Urol. Nature Publishing Group; 2012;9(8):435–47.

62. Chen B, Dave B. Challenges and Future Prospects for Tissue Engineering in Female Pelvic Medicine and Reconstructive Surgery. Curr Urol Rep. 2014 Aug 5;15(8):425.

63. Roman S, Mangera A, Osman NI, Bullock AJ, Chapple CR, MacNeil S. Developing a tissue engineered repair material for treatment of stress urinary incontinence and pelvic organ prolapse-which cell source? Neurourol Urodyn. 2014 Jun;33(5):531–7.

64. Boennelycke M, Gras S, Lose G. Tissue engineering as a potential alternative or adjunct to surgical reconstruction in treating pelvic organ prolapse. Int Urogynecol J. 2013 May 1;24(5):741–7.

65. Montarras D, Morgan J, Collins C, Relaix F, Zaffran S, Cumano A, et al. Direct isolation of satellite cells for skeletal muscle regeneration. Science. 2005 Sep;309(5743):2064–7.

66. Sacco A, Doyonnas R, Kraft P, Vitorovic S, Blau HM. Self-renewal and expansion of single transplanted muscle stem cells. Nature. 2008 Nov;456(7221):502–6.

67. Studitsky AN. Free auto- and homografts of muscle tissue in experiments on animals. Ann N Y Acad Sci. 2006 Dec 16;120(1):789–801.

68. Carlson BM. The regeneration of minced muscles. Monogr Dev Biol. 1972;4:1–128.

69. Corona BT, Garg K, Ward CL, McDaniel JS, Walters TJ, Rathbone CR. Autologous minced muscle grafts: a tissue engineering therapy for the volumetric loss of skeletal muscle. AJP Cell Physiol. 2013 Oct 1;305(7):C761–75.

70. Mauro A. Satellite cell of skeletal muscle fibers. J Biophys Biochem Cytol. 1961 Feb;9:493–5.

71. Tedesco FS, Dellavalle A, Diaz-Manera J, Messina G, Cossu G. Repairing skeletal muscle: regenerative potential of skeletal muscle stem cells. J Clin Invest. 2010 Jan;120(1):11–9.

72. Gräs S, Lose G. The clinical relevance of cell-based therapy for the treatment of stress urinary incontinence. Acta Obstet Gynecol Scand. 2011 Aug;90(8):815–24.

73. Stangel-Wojcikiewicz K, Jarocha D, Piwowar M, Jach R, Uhl T, Basta A, et al. Autologous muscle-derived cells for the treatment of female stress urinary incontinence: a 2-year follow-up of a Polish investigation. Neurourol Urodyn. 2014 Mar;33(3):324–30.

74. Carr LK, Robert M, Kultgen PL, Herschorn S, Birch C, Murphy M, et al. Autologous muscle derived cell therapy for stress urinary incontinence: a prospective, dose ranging study. J Urol. 2013 Feb;189(2):595–601.

75. Cornu J-N, Lizée D, Pinset C, Haab F. Long-term follow-up after regenerative therapy of the urethral sphincter for female stress urinary incontinence. Eur Urol. 2014 Jan;65(1):256–8.

76. Blaganje M, Lukanović A. Ultrasound-guided autologous myoblast injections into the extrinsic urethral sphincter: tissue engineering for the treatment of stress urinary incontinence. Int Urogynecol J. 2013 Apr;24(4):533–5.

77. Budatha M, Roshanravan S, Zheng Q, Weislander C, Chapman SL, Davis EC, et al. Extracellular matrix proteases contribute to progression of pelvic organ prolapse in mice and humans. J Clin Invest. 2011;121(5):2048–59.

78. Hanna-Mitchell AT, Robinson D, Cardozo L, Everaert K, Petkov G V. Do we need to know more about the effects of hormones on lower urinary tract dysfunction? ICI-RS 2014. Neurourol Urodyn. 2016 Feb;35(2):299–303.

79. Cody JD, Jacobs ML, Richardson K, Moehrer B, Hextall A. Oestrogen therapy for urinary incontinence in post-menopausal women. In: Cody JD, editor. Cochrane Database of Systematic Reviews. Chichester, UK: John Wiley & Sons, Ltd; 2012. p. 458–9.

80. Chakhtoura N, Zhang Y, Candiotti K, Medina CA, Takacs P. Estrogen inhibits vaginal tropoelastin and TGF-β1 production. Int Urogynecol J. 2012 Dec;23(12):1791–5.

81. Rahn DD, Ward RM, Sanses T V., Carberry C, Mamik MM, Meriwether K V., et al. Vaginal estrogen use in postmenopausal women with pelvic floor disorders: systematic review and practice guidelines. Int Urogynecol J. 2015;26(1):3–13.

82. Weber MA, Kleijn MH, Langendam M, Limpens J, Heineman MJ, Roovers JP. Local oestrogen for pelvic floor disorders: A systematic review. PLoS One. 2015;10(9).

83. Shirvan MK, Alamdari DH, Mahboub MD, Ghanadi A, Rahimi HR, Seifalian AM. A novel cell therapy for stress urinary incontinence, short-term outcome. Neurourol Urodyn. 2013 Apr;32(4):377–82.

84. Borrione P, Gianfrancesco A Di, Pereira MT, Pigozzi F. Platelet-rich plasma in muscle healing. Am J Phys Med Rehabil. 2010 Oct;89(10):854–61.

85. Foster TE, Puskas BL, Mandelbaum BR, Gerhardt MB, Rodeo SA. Platelet-rich plasma: from basic science to clinical applications. Am J Sports Med. 2009 Nov;37(11):2259–72.

86. Flower TR, Pulsipher V, Moreno A. A New Tool in Regenerative Medicine : Mesenchymal Stem Cell Secretome. J Stem Cell Res Ther. 2015;1(1):10–2.

87. Abramowitch SD, Feola A, Jallah Z, Moalli P a. Tissue mechanics, animal models, and pelvic organ prolapse: A review. Eur J Obstet Gynecol Reprod Biol. 2009;144(SUPPL 1):146–58.

88. Slack M, Ostergard D, Cervigni M, Deprest J. A standardized description of graft-containing meshes and recommended steps before the introduction of medical devices for prolapse surgery. Int Urogynecol J. 2012 Apr 7;23(S1):15–26.

89. Oh S-J, Hong SK, Kim SW, Paick J-S. Histological and functional aspects of different regions of the rabbit vagina. Int J Impot Res. 2003 Apr;15(2):142–50.

90. Couri B, Lenis A, Borazjani A. Animal models of female pelvic organ prolapse: lessons learned. Expert Rev Obs Gynecol. 2012;7(3):249–60.

91. Slack M, Ostergard D, Cervigni M, Deprest J. A standardized description of graft-containing

meshes and recommended steps before the introduction of medical devices for prolapse surgery. Consensus of the 2nd IUGA Grafts Roundtable: optimizing safety and appropriateness of graft use in transvaginal pe. Int Urogynecol J. 2012 Apr;23 Suppl 1:S15–26.

92. Boennelycke M, Christensen L, Nielsen LF, Everland H, Lose G. Tissue response to a new type of biomaterial implanted subcutaneously in rats. Int Urogynecol J. 2011 Feb 14;22(2):191–6.

93. Lind M, Larsen A, Clausen C, Osther K, Everland H. Cartilage repair with chondrocytes in fibrin hydrogel and MPEG polylactide scaffold: an in vivo study in goats. Knee Surgery, Sport Traumatol Arthrosc. 2008 Jul 17;16(7):690–8.

94. Sill TJ, von Recum HA. Electrospinning: Applications in drug delivery and tissue engineering. Biomaterials. 2008;29(13):1989–2006.

95. Ingavle GC, Leach JK. Advancements in electrospinning of polymeric nanofibrous scaffolds for tissue engineering. Tissue Eng Part B Rev. 2014;20(4):277–93.

96. Woodruff MA, Hutmacher DW. The return of a forgotten polymer—Polycaprolactone in the 21st century. Prog Polym Sci. 2010 Oct;35(10):1217–56.

97. Løvdal A, Vange J, Nielsen LF, Almdal K. Mechanical properties of electrospun PCL scaffold under in vitro and accelerated degradation conditions. Biomed Eng Appl Basis Commun. 2014 Jun;26(03):1450043:1–13.

98. Ozog Y, Konstantinovic ML, Verschueren S, Spelzini F, De Ridder D, Deprest J. Experimental comparison of abdominal wall repair using different methods of enhancement by small intestinal submucosa graft. Int Urogynecol J Pelvic Floor Dysfunct. 2009 Apr;20(4):435–41.

99. Valentin JE, Turner NJ, Gilbert TW, Badylak SF. Functional skeletal muscle formation with a biologic scaffold. Biomaterials. 2010 Oct;31(29):7475–84.

100. Konstantinovic ML, Lagae P, Zheng F, Verbeken EK, De Ridder D, Deprest JA. Comparison of host response to polypropylene and non-cross-linked porcine small intestine serosal-derived collagen implants in a rat model. BJOG an Int J Obstet Gynaecol. 2005 Nov;112(11):1554–60.

101. Wallace PK, Tario JD, Fisher JL, Wallace SS, Ernstoff MS, Muirhead K a. Tracking antigen-driven responses by flow cytometry: Monitoring proliferation by dye dilution. Cytom Part A. 2008;73(11):1019–34.

102. Corcos J, Loutochin O, Campeau L, Eliopoulos N, Bouchentouf M, Blok B, et al. Bone marrow mesenchymal stromal cell therapy for external urethral sphincter restoration in a rat model of stress urinary incontinence. Neurourol Urodyn. 2011 Mar;30(3):447–55.

103. Fearon A, Dahlstrom JE, Twin J, Cook J, Scott A. The Bonar score revisited: Region of evaluation significantly influences the standardized assessment of tendon degeneration. J Sci Med Sport. Sports Medicine Australia; 2014 Jul;17(4):346–50.

104. Cook JL, Feller J a., Bonar SF, Khan KM. Abnormal tenocyte morphology is more prevalent than collagen disruption in asymptomatic athletes' patellar tendons. J Orthop Res.

2004;22(2):334–8.

105. Maffulli N, Barrass V, Ewen SW. Light microscopic histology of achilles tendon ruptures. A comparison with unruptured tendons. Am J Sports Med. 2000;28(6):857–63.

106. Zhang K, Han J, Yao Y, Yang J, Qiao J. Local reaction to the different meshes at the vesicovaginal space in rabbit model. Int Urogynecol J. 2012 May 3;23(5):605–11.

107. R: The R Project for Statistical Computing [Internet]. [cited 2016 Jan 4]. Available from: https://www.r-project.org/

108. Choi JS, Lee SJ, Christ GJ, Atala A, Yoo JJ. The influence of electrospun aligned poly(ε-caprolactone)/collagen nanofiber meshes on the formation of self-aligned skeletal muscle myotubes. Biomaterials. 2008;29(19):2899–906.

109. Woodruff MA, Hutmacher DW. The return of a forgotten polymer—Polycaprolactone in the 21st century. Prog Polym Sci. 2010;35(10):1217–56.

110. Vashaghian M, Ruiz-Zapata AM, Kerkhof MH, Zandieh-Doulabi B, Werner A, Roovers JP, et al. Toward a new generation of pelvic floor implants with electrospun nanofibrous matrices: A feasibility study. Neurourol Urodyn. 2016 Feb;34(3):n/a – n/a.

111. Wu X, Wang Y, Zhu C, Tong X, Yang M, Yang L, et al. Preclinical animal study and human clinical trial data of co-electrospun poly(L-lactide-co-caprolactone) and fibrinogen mesh for anterior pelvic floor reconstruction. Int J Nanomedicine. 2016 Feb;389.

112. Ozog Y, Konstantinovic ML, Verschueren S, Spelzini F, De Ridder D, Deprest J. Experimental comparison of abdominal wall repair using different methods of enhancement by small intestinal submucosa graft. Int Urogynecol J Pelvic Floor Dysfunct. 2009 Apr;20(4):435–41.

113. Fan X, Wang Y, Wang Y, Xu H. Comparison of polypropylene mesh and porcine-derived, cross-linked urinary bladder matrix materials implanted in the rabbit vagina and abdomen. Int Urogynecol J. 2014 May;25(5):683–9.

114. Krause H, Goh J. Sheep and rabbit genital tracts and abdominal wall as an implantation model for the study of surgical mesh. J Obstet Gynaecol Res. 2009;35(2):219–24.

115. Pierce LM, Rao A, Baumann SS, Glassberg JE, Kuehl TJ, Muir TW. Long-term histologic response to synthetic and biologic graft materials implanted in the vagina and abdomen of a rabbit model. Am J Obstet Gynecol. Mosby, Inc.; 2009 May;200(5):546.e1–546.e8.

116. Higgins EW, Rao A, Baumann SS, James RL, Kuehl TJ, Muir TW, et al. Effect of estrogen replacement on the histologic response to polypropylene mesh implanted in the rabbit vagina model. Am J Obstet Gynecol. Elsevier Inc.; 2009 Nov;201(5):505.e1–505.e9.

117. Baragi R V., DeLancey JOL, Caspari R, Howard DH, Ashton-Miller JA. Differences in pelvic floor area between African American and European American women. Am J Obstet Gynecol. 2002;187(1):111–5.

118. Ashton-Miller JA, DeLancey JOL. On the Biomechanics of Vaginal Birth and Common Sequelae. Annu Rev Biomed Eng. 2009;11(1):163–76.

119. Feola A, Abramowitch S, Jallah Z, Stein S, Barone W, Palcsey S, et al. Deterioration in

biomechanical properties of the vagina following implantation of a high-stiffness prolapse mesh. BJOG an Int J Obstet Gynaecol. 2013 Jan;120(2):224–32.

120. Feola A, Barone W, Moalli P, Abramowitch S. Characterizing the ex vivo textile and structural properties of synthetic prolapse mesh products. Int Urogynecol J Pelvic Floor Dysfunct. 2013;24(4):559–64.

121. Mangera A, Bullock AJ, Chapple CR, MacNeil S. Are biomechanical properties predictive of the success of prostheses used in stress urinary incontinence and pelvic organ prolapse? A systematic review. Neurourol Urodyn. 2012 Jan;31(1):13–21.

122. Feola A, Pal S, Moalli P, Maiti S, Abramowitch S. Varying degrees of nonlinear mechanical behavior arising from geometric differences of urogynecological meshes. J Biomech. Elsevier; 2014;47(11):2584–9.

123. Todros S, Pavan PG, Natali AN. Biomechanical properties of synthetic surgical meshes for pelvic prolapse repair. J Mech Behav Biomed Mater. Elsevier; 2016;55:271–85.

124. Altman DG. Practical statistics for medical research. First edit. Chapman & Hall/CRC; 1991.

125. Ludbrook J. Multiple comparison procedures updated. Clin Exp Pharmacol Physiol. 1998 Dec;25(12):1032–7.

126. Stastna M, Van Eyk JE. Investigating the Secretome: Lessons About the Cells That Comprise the Heart. Circ Cardiovasc Genet. 2012 Feb 1;5(1):o8–18.

127. Dissaranan C, Cruz MA, Kiedrowski MJ, Balog BM, Gill BC, Penn MS, et al. Rat mesenchymal stem cell secretome promotes elastogenesis and facilitates recovery from simulated childbirth injury. Cell Transplant. 2014;23(11):1395–406.

128. Deng K, Lin DL, Hanzlicek B, Balog B, Penn MS, Kiedrowski MJ, et al. Mesenchymal stem cells and their secretome partially restore nerve and urethral function in a dual muscle and nerve injury stress urinary incontinence model. Am J Physiol Renal Physiol. 2015 Jan 15;308(2):F92–100.

129. Le Bihan MC, Bigot A, Jensen SS, Dennis JL, Rogowska-Wrzesinska A, Lainé J, et al. In-depth analysis of the secretome identifies three major independent secretory pathways in differentiating human myoblasts. J Proteomics. Elsevier B.V.; 2012;77:344–56.

130. Chen B, Yeh J. Alterations in connective tissue metabolism in stress incontinence and prolapse. J Urol. 2011 Nov;186(5):1768–72.

131. Campeau L, Gorbachinsky I, Badlani GH, Andersson KE. Pelvic floor disorders: Linking genetic risk factors to biochemical changes. BJU Int. 2011;108(8):1240–7.

132. Alperin M, Moalli PA. Remodeling of vaginal connective tissue in patients with prolapse. Curr Opin Obstet Gynecol. 2006 Oct;18(5):544–50.

133. Word RA, Pathi S, Schaffer JI. Pathophysiology of pelvic organ prolapse. Obstet Gynecol Clin North Am. 2009 Sep;36(3):521–39.

134. Cartwright R, Kirby AC, Tikkinen K a. O, Mangera A, Thiagamoorthy G, Rajan P, et al. Systematic review and metaanalysis of genetic association studies of urinary symptoms and

prolapse in women. Am J Obstet Gynecol. Elsevier; 2015;212(2):199.e1–199.e24.

135. Gehl J. Gene Electrotransfer in Clinical Trials. In 2014. p. 241–6.

136. Neumann E, Schaefer-Ridder M, Wang Y, Hofschneider PH. Gene transfer into mouse lyoma cells by electroporation in high electric fields. EMBO J. 1982;1(7):841–5.

137. Aboushwareb T, McKenzie P, Wezel F, Southgate J, Badlani G. Is tissue engineering and biomaterials the future for lower urinary tract dysfunction (LUTD)/pelvic organ prolapse (POP)? Neurourol Urodyn. 2011 Jun;30(5):775–82.

138. Schwertner-Tiepelmann N, Thakar R, Sultan AH, Tunn R. Obstetric levator ani muscle injuries: current status. Ultrasound Obstet Gynecol. 2012;39(4):372–83.

Int Urogynecol J (2015) 26:1843–1851
DOI 10.1007/s00192-015-2782-x

ORIGINAL ARTICLE

Muscle fragments on a scaffold in rats: a potential regenerative strategy in urogynecology

Hanna Jangö [1] · Søren Gräs [1] · Lise Christensen [2] · Gunnar Lose [1]

Received: 6 March 2015 / Accepted: 23 June 2015 / Published online: 24 July 2015

Abstract
Introduction and hypothesis The use of permanent synthetic meshes to improve the outcome of pelvic organ prolapse (POP) repair causes frequent and serious complications. The use of the synthetic, biodegradable scaffold methoxypolyethyleneglycol-polylactic-co-glycolic acid (MPEG-PLGA) seeded with autologous muscle fiber fragments (MFF), as an adjunct to native tissue POP repair, is a potential new alternative.
Methods A rat abdominal wall model of native repair was used with six animals in each of three groups: native repair, native repair + MPEG-PLGA, and native repair + MPEG-PLGA + MFF. MFF were labeled with PKH26-fluorescence dye. After 8 weeks labeled cells were identified in tissue samples and histopathological and immunohistochemical analyses of connective tissue organization and desmin reactivity of muscle cells were performed. Fresh tissue samples were subjected to uniaxial biomechanical testing. Statistical analyses were performed using one-way analysis of variance (ANOVA).
Results MPEG-PLGA was fully degraded after 8 weeks. Desmin-immunopositive (6/6) and PKH26-positive cells (6/6) were found only after native repair + MPEG-PLGA + MFF, indicating survival, proliferation, and integration of cells originating from the MFF. This group also showed significantly increased stiffness in the high stiffness zone compared with native repair + MPEG-PLGA ($p=0.032$) and borderline significantly higher stiffness compared to native repair ($p=0.054$).
Conclusions In this pilot study, MPEG-PLGA scaffolds seeded with autologous MFF affected some histological and biomechanical properties of native tissue repair in an abdominal wall defect model in rats. The method thus appears to be a simple tissue engineering concept with potential relevance for native tissue repair of POP.

Keywords Autologous muscle fiber fragments · Biodegradable scaffold · Rats · Regenerative medicine · Tissue engineering

Abbreviations

MPEG-PLGA	Methoxypolyethyleneglycol-polylactic-co-glycolic acid
MFF	Muscle fiber fragments
POP	Pelvic organ prolapse

Introduction

Synthetic, permanent meshes have been introduced for pelvic organ prolapse (POP) surgery to improve long-term outcome of conventional tissue repair. The use of permanent meshes is, however, controversial and the US Food and Drug Administration has issued public warnings caused by recognition of frequent and potentially serious and life-altering complications [1].

Regenerative medicine provides an attractive alternative to permanent meshes. It is a new medical field that aims at creating functional tissue by regenerating, repairing, or replacing nonfunctional tissue using stem cells. Tissue engineering is often used synonymously with regenerative medicine, but

✉ Hanna Jangö
hanna@jango.se

[1] Department of Obstetrics and Gynecology, Copenhagen University Hospital Herlev, Herlev Ringvej 75, 2730 Herlev, Denmark

[2] Department of Pathology, Copenhagen University Hospital Herlev, Herlev, Denmark

usually also involves the use of biodegradable scaffolds to anchor and support the cells.

A tissue engineering strategy with a scaffold and stem cells could be used either alone or as an adjunct to conventional surgery in the treatment of POP. The scaffold would secure the position of the cells and potentially provide initial support to the weakened vaginal and pelvic floor supportive tissues. As the scaffold gradually disappeared, the stem cells would proliferate and differentiate to provide more permanent support [2].

For tissue engineering of POP, autologous stem cells isolated from normal vaginal tissue would be optimal but potentially difficult to achieve. Skeletal muscle stem cells are easily achievable alternative candidates [2]. They are called "satellite cells" [3] and represent 2.5–6 % of all nuclei in a given muscle fiber [4]. Following activation, satellite cells can undergo asymmetric division into new, quiescent satellite cells or proliferating myoblasts [4]. In traditional tissue engineering strategies, in vitro expanded myoblasts are used, but several studies suggest that in vitro culturing of satellite cells is unnecessary and may even adversely affect the regenerative potential [5–7]. Furthermore, the use of in vitro cultured stem cells is time consuming, expensive, and subject to strict and increasing regulatory demands [8], which limits the clinical relevance.

In previous studies, we have demonstrated that autologous fresh muscle fiber fragments (MFF) with their associated satellite cells may be used instead of cultured myoblasts [9, 10]. This technique is simple and inexpensive and MFF can be harvested and implanted during the same surgical procedure making the method clinically feasible and attractive.

Methoxypolyethyleneglycol-polylactic-co-glycolic acid (MPEG-PLGA) is a synthetic, biodegradable scaffold with high biocompatibility [11], which has been used successfully as a carrier for MFF [9].

We hypothesize that the stem cells in MFF are able to improve the regenerative response of native tissue repair. The aim of the present study was to confirm our previous results and to investigate this potential further in a rat abdominal native repair model.

Materials and methods

Animals

Animal experiments were conducted at the Animal Facility at the Panum Institute, Copenhagen, Denmark. The Danish Animal Experiments Inspectorate approved the study (permission no. 2012-15-2934-00242) and their guidelines for care and use of laboratory animals were followed. We used a total of 18 Sprague Dawley retired female breeder rats, weighing 245–315 g (Taconic, Lille Skensved, Denmark).

Scaffolds

Scaffolds were made of MPEG-PLGA (Coloplast A/S, Humlebæk, Denmark). The MPEG-PLGA scaffold is a freeze-dried combination of glycolic acid and lactic acid, which makes the structure porous and spongy as previously described [11].

Surgery

The rats were anesthetized with Hypnorm/Midazolam 0.3 ml/100 g (Hypnorm, VetaPharma Ltd., Leeds, UK, and Midazolam, Hameln Pharmaceuticals GmbH, Hameln, Germany). To create a full-thickness defect which could be sutured without creating undue harm to the animals and which could provide MFF, we made a midline incision on the abdomen followed by subcutaneous blunt dissection and used a native repair model, modified from Ozog et al. [12]. The defect was made longitudinally, lateral to the rectus muscle. A full-thickness portion of the abdominal wall measuring approximately 3.0 × 0.1–0.2 cm was resected and the defect was sutured continuously with Vicryl 4–0 and with one nonabsorbable Prolene 5–0 suture in each end of the repaired defect for later identification. A scaffold measuring 2.5 × 4.0 cm was placed directly above, completely covering the sutured defect and the surrounding tissue. The scaffold was held in place by four Prolene 5–0 sutures, one stitch in each corner, followed by a continuous Vicryl 4–0 suture along the borders of the scaffold. The skin was closed using staples (Reflex® One, REF 3036, ConMed®, Utica, NY, USA). Antibiotic prophylaxis and analgesia were administered according to veterinarian recommendations.

Muscle fiber fragments

The removed tissue of the abdominal wall was used for preparation of MFF. The removed muscle sample was prepared in a sterile Petri dish with two scalpels, cutting the tissue into a fine mash with one drop of physiological saline. MFF were labeled with PKH26 (Sigma-Aldrich®, St. Louis, MO, USA), a fluorescent dye with long aliphatic tails that binds irreversibly to lipid regions of the cell membrane. The labeling was performed according to the manufacturer's instructions. The labeled MFF were then applied to the scaffold, creating a thin layer on the surface. Preparation of the MFF was performed while the defect in the abdomen of the rats was sutured. Thereafter, the scaffold was placed above the sutured defect with the MFF between the muscle layers and the scaffold (Fig. 1).

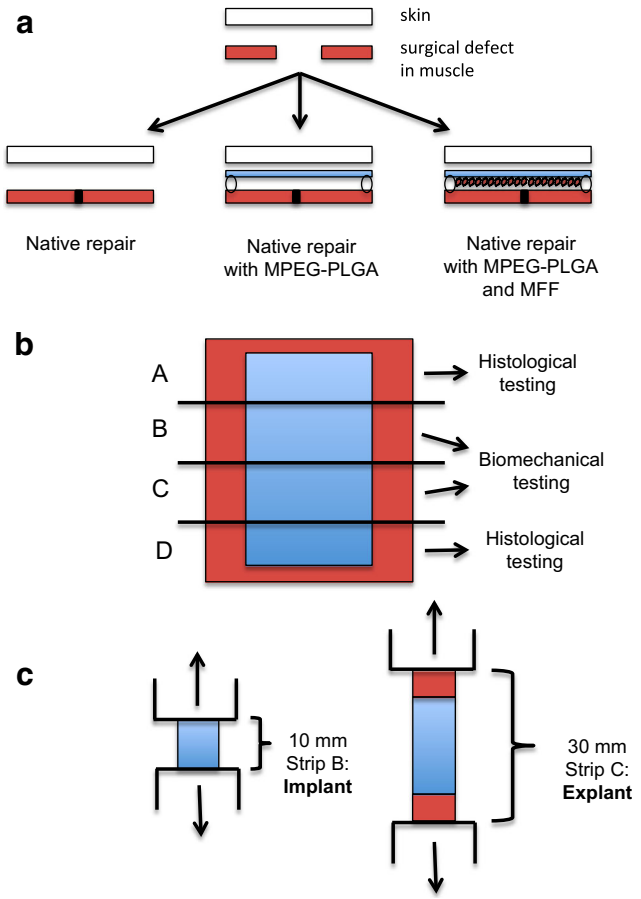

Fig. 1 Overview of groups, preparation, and testing of tissue samples. **a** Overview of the three groups: native repair, native repair + MPEG-PLGA, and native repair + MPEG-PLGA + MFF. **b** Removed tissue was cut into four strips (*A–D*). **c** Visualization of uniaxial biomechanical testing of repair-near strips (strip *B*) and larger strips (strip *C*)

Design

The animals were randomized into three groups with six animals in each as recommended by Slack et al. [13]. The groups were: native repair alone (control group), native repair + MPEG-PLGA, and native repair + MPEG-PLGA + MFF.

Explantation of tissue

The rats were euthanized by cervical dislocation 8 weeks after surgery. We performed a midline incision in the abdominal skin followed by subcutaneous blunt dissection to present the abdominal wall musculature with attached subcutaneous and fascial tissue. A full-thickness sample of the abdominal wall including the area of implantation and surrounding abdominal wall was removed en bloc. Before removal, 1.0-cm wide tissue strips were marked (Fig. 1). After removal, the tissue was cut into four strips (Fig. 1), where strips A and D were used for histological testing and strips B and C were used for biomechanical testing.

Histopathology and immunohistochemistry

Samples for histological examination were fixed in 10 % buffered formalin, embedded in paraffin, cut in 5-μm sections, and stained with hematoxylin and eosin (H&E) and van Gieson/alcian blue. Neighboring sections were immunohistochemically stained for desmin, which stains the cytoplasm of skeletal and smooth muscle cells, using the EnVision FLEX+ (Dako, Glostrup, Denmark) polymer peroxidase diaminobenzidine system. Heat-induced epitope retrieval was performed with a Tris-ethylenediaminetetraacetic acid (EDTA) solution pH 9.0 (Dako). Anti-human desmin mouse monoclonal antibody (Dako IR 606 ready-to-use), which cross-reacts with both mouse and rat proteins was applied for 20 min at ambient temperature in the Dako Autostainer Link 48. The slides were viewed under an Olympus BX60 Microscope (Olympus, Center Valley, PA, USA). The Image-Pro Plus 7.0 (Media Cybernetics, Inc., Rockville, MD, USA) software was used to analyze the images.

Connective tissue organization was scored using the Bonar score, recently published by Fearon et al. [14] The score (range 0–20) evaluates cell morphology, collagen arrangement, cellularity, vascularity, and ground substance tissue response in connective tissues. The Bonar score was originally developed for the evaluation of tendon injuries, where a high score stands for a more advanced stage of regenerative repair. Collagen arrangement was assessed through polarization of the van Gieson-stained fibers, and the nature of ground substance was evaluated using alcian blue staining for mucopolysaccharides; the other parameters were assessed using H&E staining. The assessment was performed in cooperation with senior pathologist L.C. blinded to the type of experimental model.

Fluorescence

Tissue samples for detection of PKH26 were evaluated in a fluorescence microscope on 16-μm frozen sections. If no fluorescence was detected, the sample was recut and examined further.

Uniaxial biomechanical properties

We used a TA.XT plus Texture Analyser (Stable Micro Systems, Godalming, Surrey, UK) tensiometer with a load cell of 5 kg. TA 94 Pneumatic Grips (Thwing-Albert Instrument Company, West Berlin, NJ, USA) were modified by using a grip paper (3 M) to secure a tight grip of the tissue strips without squeezing it. The tissue strips were inserted between the grips, using a pressure of 3 bar. A preload of 0.1 N was applied to all tissue strips to remove slack and the grip-to-grip distance was measured and

defined as elongation of zero. Two different tissue samples were examined: strips B and C (Fig. 1). The smaller and repair-near tissue strip B was inserted at a grip-to-grip separation of 1.0 cm, thereby only testing the tissue with the repaired native tissue defect between the grips, moving with a speed of 0.333 mm/s. The larger tissue strip C was inserted at a grip-to-grip separation of 3.0 cm, thereby including both the repair-near area and the surrounding tissue between the grips, moving with a speed of 1 mm/s. The speed was adjusted to the length of the tested tissue to ensure constant strain rate in order to make the speed of material deformation comparable between samples. Load and elongation were recorded throughout the testing period until the point of failure of the tissue. Biomechanical properties were analyzed with Exponent Version 6.1.30 software (Stable Micro Systems, Godalming, Surrey, UK).

Relative elongation was calculated as the change in elongation relative to the initial length. As previously described [15], load was plotted against relative elongation resulting in bilinear curves (Fig. 2) with a low- and a high-stiffness zone. Data were reported as stiffness (the slopes of the linear segments) (N/mm) in the low- and high-stiffness zones, load at failure of the tissue (N), and relative elongation at failure of the tissue.

Statistics

Bonar score results were analyzed using the Kruskal-Wallis test, with post hoc Mann–Whitney test (Bonferroni correction). Biomechanical data are presented as mean and standard deviation and analyzed using one-way analysis of variance (ANOVA). If there was a significant difference between groups using the one-way ANOVA, a multiple *t* test was performed (with inbuilt Bonferroni correction). Because of the limited number of animals, the results were also validated by the nonparametric Kruskal-Wallis analysis of variance test, which gave the same results. A p value <0.05 was considered statistically significant. All statistical analyses were performed using the statistical software R (version 3.1.1).

Results

All animals had an uneventful postoperative recovery. None of the rats had hernias, erosions, or signs of infection in the surgical area. There were no macroscopic signs of remnants of the implant after 8 weeks.

Histopathology

Histological evaluation (Fig. 3) showed that MPEG-PLGA alone or with MFF was fully degraded after 8 weeks. We found a significant difference in Bonar score (Table 1) using the Kruskal-Wallis test. However, post hoc analysis revealed no significant differences between groups (p=0.16). Desmin immunostaining demonstrated the presence of extra muscle tissue in all six animals from the native repair + MPEG-PLGA + MFF group (Fig. 4).

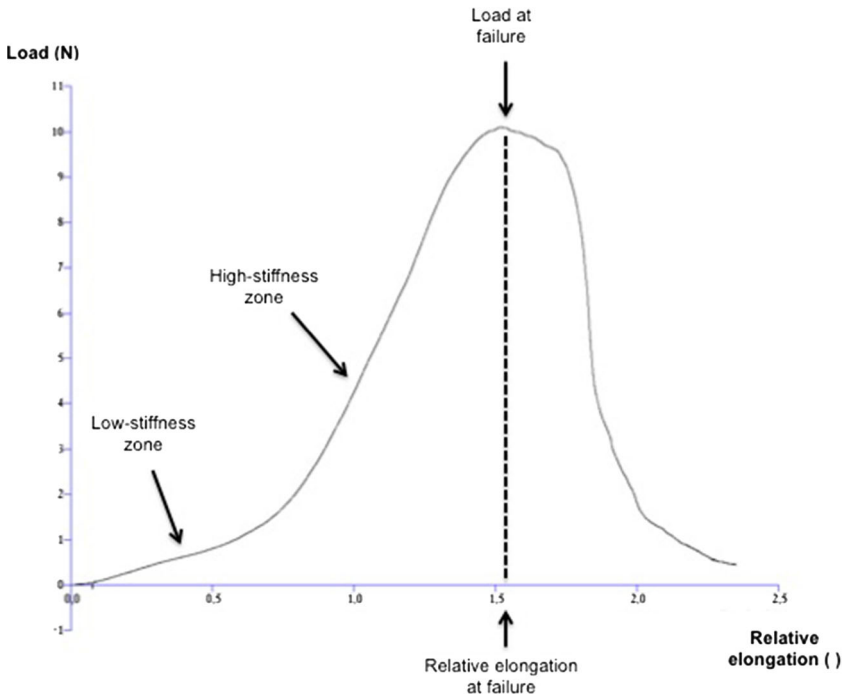

Fig. 2 Load-relative elongation curve with visualization of high- and low-stiffness zones, load at failure, and relative elongation at failure

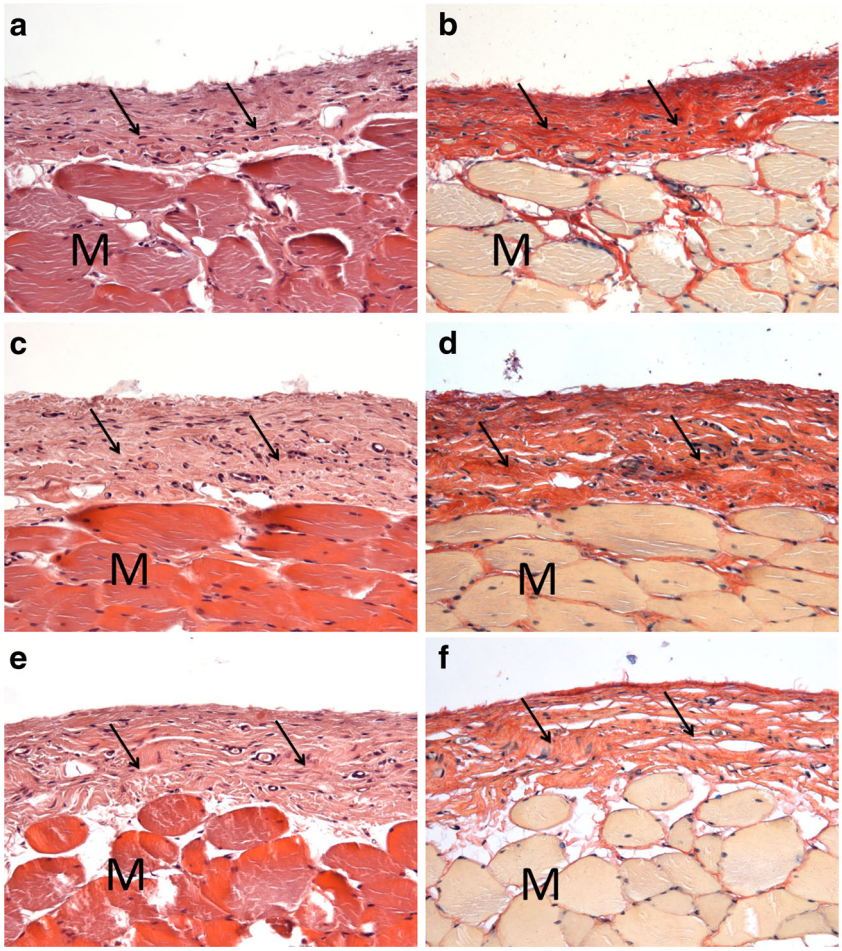

Fig. 3 Histological samples from area with native repair alone (**a**, **b**), native repair + MPEG-PLGA (**c**, **d**), and native repair + MPEG-PLGA + MFF (**e**, **f**) (striated muscle marked with *M*). No remnant MPEG-PLGA or tissue augmentation was identified by 8 weeks (marked with *arrows*). H&E (**a**, **c**, **e**) and van Gieson/alcian blue (**b**, **d**, **f**). Original magnification×200

Fluorescence

PKH26 fluorescence-positive cells were visible only in the six animals with native repair + MPEG-PLGA + MFF. The pattern of PKH26-positive cells differed from that seen with the desmin immunostaining (Fig. 4), but the samples were prepared from different locations of the removed sample tissue.

Biomechanical properties

Uniaxial biomechanical results for strips B and C were compared between the three groups (Table 2, Fig. 5). In the high-stiffness zone of the repair-near tissue strip B, native repair + MPEG-PLGA + MFF was slightly but significantly stiffer than the native repair + MPEG-PLGA group (p=0.032) and borderline significant compared with the

Table 1 Bonar score

	Native repair n=6	Native repair + MPEG-PLGA n=6	Native repair + MPEG-PLGA + MFF n=6	p value Kruskal-Wallis
Median (range)	6 (5–6)	6.5 (6–7)[a]	6 (5–6)	0.044

Semiquantitative evaluation of the connective tissue using the Bonar score, in which a higher Bonar score represents a recent immunological foreign body reaction

[a] Post hoc Mann–Whitney test with Bonferroni correction revealed no difference between native repair + MPEG-PLGA and native repair (p=0.16) or between native repair + MPEG-PLGA and native repair + MPEG-PLGA + MFF (p=0.16)

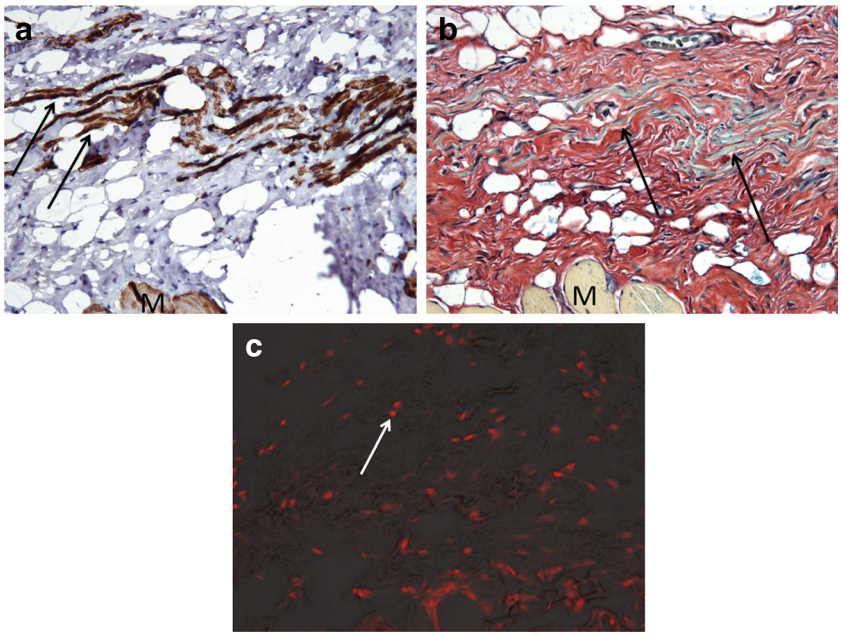

Fig. 4 Extra muscle tissue. Sites implanted with the MPEG-PLGA scaffold and MFF. **a** Desmin immunostaining. *Arrows* point out extra muscle tissue, stained *dark brown*. Striated muscle tissue of the abdominal wall marked *M*. **b** van Gieson/alcian blue. *Arrows* point out extra muscle tissue, stained *yellow*. Striated muscle tissue of the abdominal wall marked *M*. Note the bluish tinge of the muscle fibers, suggesting regeneration and immaturity. **c** PKH26 fluorescence labeling. *Arrow* points out red fluorescence-positive cell. Original magnification ×200

Table 2 Biomechanical properties

Biomechanical properties	Native repair $n=6$	Native repair + MPEG-PLGA $n=6$	Native repair + MPEG-PLGA + MFF $n=6$	p value ANOVA
Repair-near tissue strip B				
Stiffness in the low-stiffness zone (N/mm)				
Mean (SD)	0.15 (0.16)	0.15 (0.12)	0.27 (0.16)	0.19
Stiffness in the high-stiffness zone (N/mm)				
Mean (SD)	1.8 (0.6)	1.7 (0.5)	2.9 (0.9)[a]	0.024
Load at failure (N)				
Mean (SD)	12.8 (1.3)	11.7 (2.4)	13.2 (4.1)	0.82
Relative elongation at failure				
Mean (SD)	1.5 (0.4)	1.3 (0.2)	1.0 (0.3)[b]	0.013
Larger tissue strip C				
Stiffness in the low-stiffness zone (N/mm)				
Mean (SD)	0.12 (0.06)	0.11 (0.07)	0.06 (0.02)	0.08
Stiffness in the high-stiffness zone (N/mm)				
Mean (SD)	0.9 (0.1)	1.0 (0.3)	1.1 (0.3)	0.22
Load at failure (N)				
Mean (SD)	9.4 (1.5)	9.6 (1.4)	9.0 (1.9)	0.68
Relative elongation at failure				
Mean (SD)	0.7 (0.1)	0.6 (0.1)	0.6 (0.1)	0.09

Uniaxial biomechanical properties of the repair-near tissue strip B and of the larger tissue strip C

Post hoc analyses using a multiple t test with built-in Bonferroni correction

[a] The stiffness of native repair + MPEG-PLGA + MFF was significantly increased compared to native repair + MPEG-PLGA ($p=0.032$) and borderline significantly increased compared to native repair ($p=0.054$)

[b] The relative elongation of native repair + MPEG-PLGA + MFF was significantly decreased compared to native repair ($p=0.046$)

native repair group (p=0.054). Correspondingly, the relative elongation at failure in strip B was significantly lower for the native repair + MPEG-PLGA + MFF compared with the native repair group (p=0.046). We found no significant differences between groups regarding stiffness in the low-stiffness zone or load at failure, nor did we find significant differences between groups when testing the larger strip C that included the surrounding tissue.

Discussion

For development of a new potential POP repair strategy, we investigated a simple tissue engineering concept where the quickly biodegradable MPEG-PLGA scaffold seeded with autologous MFF was used as an adjunct to native tissue repair. By using an abdominal wall defect model in rats, we confirmed our previous findings [11] that the MPEG-PLGA scaffold is very biocompatible and disappears completely in 8 weeks. Desmin-positive muscle cells that were separated from the ordinary muscle layers of the abdominal wall were observed, and fluorescence-positive cells could be traced after 8 weeks, indicating survival and proliferation of cells originating from the MFF. We also found an increased stiffness in the high-stiffness zone and lower relative elongation at failure in the repair-near tissue. Taken together, our findings suggest that cells originating from the MFF participate in a regenerative process, which influences both histological and some biomechanical properties of the native tissue.

Minced skeletal muscle grafts have a remarkable capacity for muscle repair, which was discovered and described in detail decades ago [16, 17] and recently reintroduced as a potential tissue engineering therapy for volumetric loss of muscle tissue [18]. The muscle cells of the minced fibers die, but some of the satellite cells survive, are activated by the inflammatory process, and divide into proliferating myoblasts that ultimately fuse to form new muscle fibers. The MFF also contain other stem cells and extracellular components of importance for formation of new connective

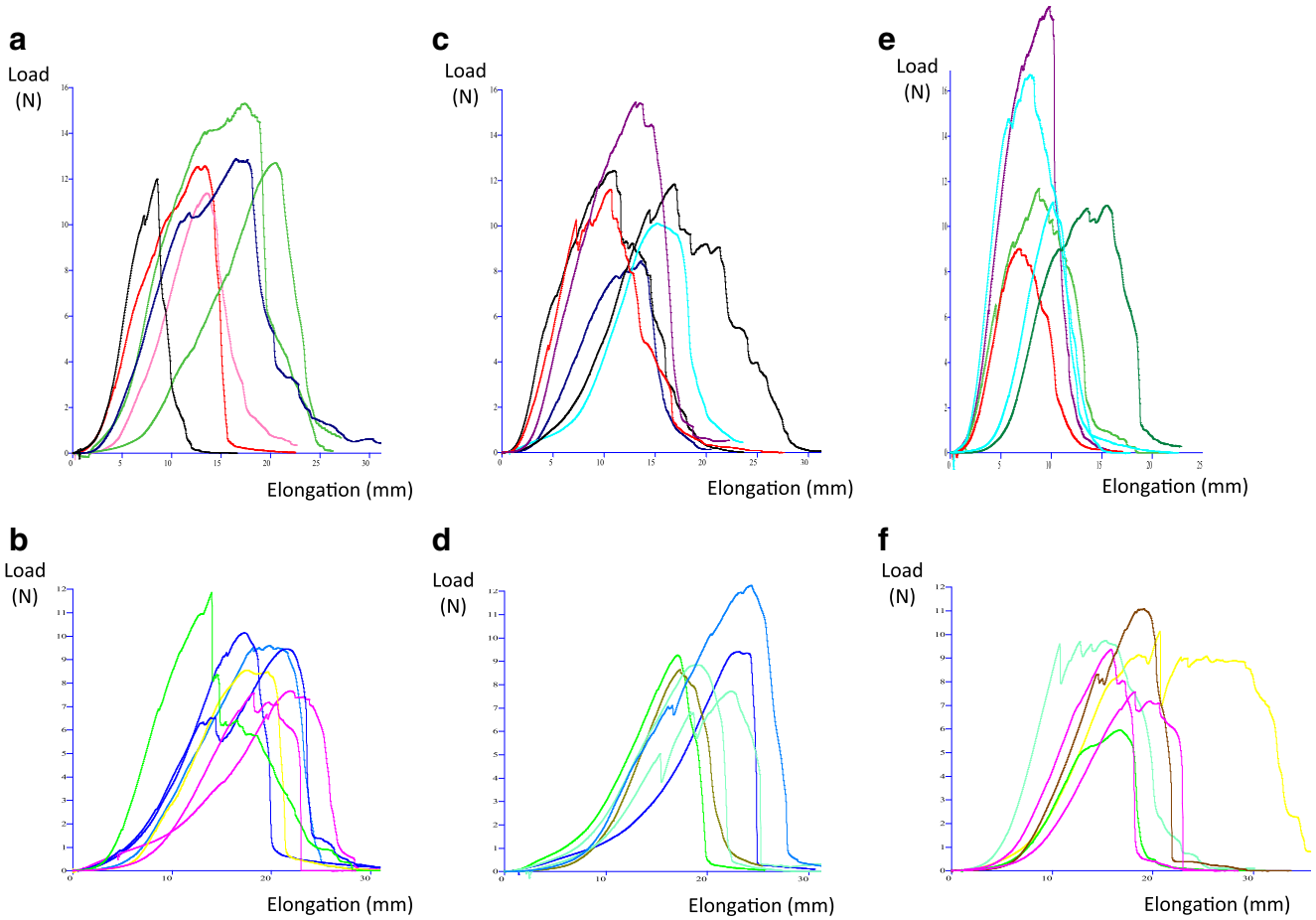

Fig. 5 Biomechanical results. Load-elongation curves representing native repair (**a**, **b**), native repair + MPEG-PLGA (**c**, **d**), and native repair + MPEG-PLGA + MFF (**e**, **f**). Results from the smaller, repair-near tissue strip B are visualized in **a**, **c**, and **e**, while results from the larger tissue strip C that also included surrounding tissue are presented in **b**, **d**, and **f**

tissue, vessels, and nervous supply [19], which could be beneficial in native tissue POP repair.

Desmin-positive cells and PKH26 fluorescence-positive cells were observed only at the implantation site in the MFF group, indicating integration of surviving cells or progeny cells from the MFF into a new tissue structure. The general distribution of desmin- and PKH26-positive cells differed; however, samples were harvested from different locations of the explanted tissue and the processing of specimens did not allow double staining or examination of consecutively cut specimens. This is a limitation in the study design, but our findings could indicate that both myogenic cells and other cells originating from the MFF are involved in the regenerating process. Identification of these cells would be of interest in future studies, which might also include histopathological and immunohistochemical comparisons of extracellular matrix components such as collagen types and elastin.

In support of the histopathological findings, we found significant biomechanical changes in the MFF group only. Near the repair site, the tissue was significantly stiffer and had a lower relative elongation at failure. From a clinical point of view, increased stiffness is not ideal, but it was only found in the high-stiffness zone, i.e., at loads that are not considered physiologically relevant [20]. We did not find a similar increase when we tested the larger strips that also included the surrounding normal tissue. Thus, the larger tissue strips are more representative of the abdominal wall as a whole. We assume that the increased stiffness in the repair-near strips is directly related to the regenerative process and consequently may change over time.

No optimal animal model for POP repair exists and repair of different abdominal wall defects in rats or rabbits are normally used as substitutes [21]. The abdominal wall native repair model we used mimics native repair in POP surgery, but unlike the vaginal walls of women with POP, the repaired abdominal tissue in rats is normal and has a remarkable regenerative capacity. Consequently, native repair in itself was very effective as previously observed by others [12]. In future studies, repair of weakened abdominal wall tissue as in the partial abdominal wall defect previously described [22] might be a more clinically relevant model. Furthermore, multiaxial biomechanical testing would mimic the actual loads experienced by the vaginal walls in women more closely.

By 8 weeks, no remnants of the MPEG-PLGA scaffold was observed and quickly degradable scaffolds are attractive from a safety point of view because of diminished risk of infection or chronic inflammation compared with long-term degradable scaffolds. However, our results only provide a snapshot of the ongoing regenerative process, and long-term animal studies would be needed to investigate whether autologous MFF seeded on MPEG-PLGA scaffolds have a lasting regenerative effect.

In conclusion, we found that MPEG-PLGA scaffolds seeded with autologous MFF significantly affect some biomechanical properties of the rat abdominal wall following native tissue repair. We also found that cells from MFF survive and integrate into the repaired tissue and taken together, these findings suggest that MFF influenced the regenerative response. Although this is a pilot study and the rat abdominal model is not optimal, the method appears to be a simple tissue engineering concept, which could potentially enhance the clinical outcome of conventional native tissue repair of degenerative disorders like POP or hernias.

Financial disclaimers The Danish National Advanced Technology Foundation and the Nordic Urogynecological Association have supported this study. Coloplast A/S provided scaffolds and facilities for biomechanical and histological testing.

Conflicts of interest G. Lose has received compensation as a consultant for Astellas. H. Jangö, S. Gräs, and L. Christensen have no conflicts of interest.

References

1. Safety Communications>FDA Safety Communication: UPDATE on Serious Complications Associated with Transvaginal Placement of Surgical Mesh for Pelvic Organ Prolapse (Internet). Available via http://www.fda.gov/MedicalDevices/Safety/AlertsandNotices/ucm262435.htm. Accessed 6 Apr 2014
2. Boennelycke M, Gras S, Lose G (2013) Tissue engineering as a potential alternative or adjunct to surgical reconstruction in treating pelvic organ prolapse. Int Urogynecol J 24(5):741–747
3. Mauro A (1961) Satellite cell of skeletal muscle fibers. J Biophys Biochem Cytol 9:493–495
4. Tedesco FS, Dellavalle A, Diaz-Manera J, Messina G, Cossu G (2010) Repairing skeletal muscle: regenerative potential of skeletal muscle stem cells. J Clin Invest 120(1):11–19
5. Collins CA, Olsen I, Zammit PS, Heslop L, Petrie A, Partridge TA et al (2005) Stem cell function, self-renewal, and behavioral heterogeneity of cells from the adult muscle satellite cell niche. Cell 122(2):289–301
6. Montarras D, Morgan J, Collins C, Relaix F, Zaffran S, Cumano A et al (2005) Direct isolation of satellite cells for skeletal muscle regeneration. Science 309(5743):2064–2067
7. Sacco A, Doyonnas R, Kraft P, Vitorovic S, Blau HM (2008) Self-renewal and expansion of single transplanted muscle stem cells. Nature 456(7221):502–506
8. Gräs S, Lose G (2011) The clinical relevance of cell-based therapy for the treatment of stress urinary incontinence. Acta Obstet Gynecol Scand 90(8):815–824
9. Boennelycke M, Christensen L, Nielsen LF, Gräs S, Lose G (2011) Fresh muscle fiber fragments on a scaffold in rats-a new concept in urogynecology? Am J Obstet Gynecol 205(3):235.e10–235.e14
10. Gräs S, Klarskov N, Lose G (2014) Intraurethral injection of autologous minced skeletal muscle: a simple surgical treatment for stress urinary incontinence. J Urol 192(3):850–855
11. Boennelycke M, Christensen L, Nielsen LF, Everland H, Lose G (2011) Tissue response to a new type of biomaterial implanted subcutaneously in rats. Int Urogynecol J 22(2):191–196

12. Ozog Y, Konstantinovic ML, Verschueren S, Spelzini F, De Ridder D, Deprest J (2009) Experimental comparison of abdominal wall repair using different methods of enhancement by small intestinal submucosa graft. Int Urogynecol J Pelvic Floor Dysfunct 20(4): 435–441
13. Slack M, Ostergard D, Cervigni M, Deprest J (2012) A standardized description of graft-containing meshes and recommended steps before the introduction of medical devices for prolapse surgery. Consensus of the 2nd IUGA Grafts Roundtable: optimizing safety and appropriateness of graft use in transvaginal pelvic reconstructive surgery. Int Urogynecol J 23(Suppl 1):S15–S26
14. Fearon A, Dahlstrom JE, Twin J, Cook J, Scott A (2014) The Bonar score revisited: region of evaluation significantly influences the standardized assessment of tendon degeneration. J Sci Med Sport 17:346–350
15. Shepherd JP, Feola AJ, Abramowitch SD, Moalli PA (2012) Uniaxial biomechanical properties of seven different vaginally implanted meshes for pelvic organ prolapse. Int Urogynecol J 23(5): 613–620
16. Studitsky AN (1964) Free auto- and homografts of muscle tissue in experiments on animals. Ann N Y Acad Sci 120:789–801
17. Carlson BM (1972) The regeneration of minced muscles. Monogr Dev Biol 4:1–128
18. Corona BT, Garg K, Ward CL, McDaniel JS, Walters TJ, Rathbone CR (2013) Autologous minced muscle grafts: a tissue engineering therapy for the volumetric loss of skeletal muscle. Am J Physiol Cell Physiol 305(7):C761–C775
19. Yin H, Price F, Rudnicki MA (2013) Satellite cells and the muscle stem cell niche. Physiol Rev 93(1):23–67
20. Jones KA, Feola A, Meyn L, Abramowitch SD, Moalli PA (2009) Tensile properties of commonly used prolapse meshes. Int Urogynecol J Pelvic Floor Dysfunct 20(7):847–853
21. Abramowitch SD, Feola A, Jallah Z, Moalli PA (2009) Tissue mechanics, animal models, and pelvic organ prolapse: a review. Eur J Obstet Gynecol Reprod Biol 144(Suppl 1):S146–S158
22. Valentin JE, Turner NJ, Gilbert TW, Badylak SF (2010) Functional skeletal muscle formation with a biologic scaffold. Biomaterials 31(29):7475–7484

Tissue engineering with muscle fiber fragments improves the strength of a weak abdominal wall in rats

Hanna JANGÖ, MD[1]; Søren GRÄS, MD[1]; Lise CHRISTENSEN, MD, DMSc[2]; Gunnar LOSE, MD, DMSc[1]

[1] Department of Obstetrics and Gynecology, Copenhagen University Hospital Herlev, Denmark
[2] Department of Pathology, Copenhagen University Hospital Herlev, Denmark

Correspondence: Hanna Jangö, Department of Obstetrics and Gynecology and Copenhagen University Hospital Herlev, Herlev Ringvej 75, DK-2730 Herlev
E-mail: hanna.jango@regionh.dk

Financial Disclaimers: The Danish National Advanced Technology Foundation and the Nordic Urogynecological Association have supported this study. Coloplast A/S provided scaffolds and facilities for biomechanical and histological testing.
Conflicts of Interest: G Lose has received compensation as a consultant for Astellas and Contura.
H Jangö, S Gräs and L Christensen have no conflicts of interest.

Introduction and hypothesis: *Alternative approaches to reinforce the native tissue in patients with pelvic organ prolapse (POP) are needed to improve surgical outcome. We wanted to 1) develop a weakened abdominal wall model in rats to mimic the weakened vaginal wall in women with POP and 2) evaluate the regenerative potential of a quickly biodegradable synthetic scaffold, methoxy-polyethyleneglycol-polylactic-co-glycolic acid (MPEG-PLGA) seeded with autologous muscle fiber fragments (MFFs) using this model.*
Methods: *In an initial pilot study with 15 animals, significant weakening of the abdominal wall and a feasible technique was established by creating a partial defect with removal of one abdominal muscle layer. Subsequently, 18 rats were evenly divided into three groups: 1) unrepaired partial defect; 2) partial defect repaired with MPEG-PLGA; and 3) partial defect repaired with MPEG-PLGA and MFFs labeled with PKH26-fluorescence dye. After eight weeks we performed histopathological and immunohistochemical testing, fluorescence analysis and uniaxial biomechanical testing.*
Results: *Both macroscopically and microscopically the MPEG-PLGA scaffold was found to be fully degraded with no signs of an inflammatory or foreign body response. PKH26-positive cells were found in all the animals from the group with added MFFs. Analysis of variance (ANOVA) showed a significant difference between groups with respect to load at failure (p=0.028), and post hoc testing revealed that the group with MPEG-PLGA and MFFs showed a significantly higher strength than the group with MPEG-PLGA alone (p=0.034).*
Conclusion: *Tissue engineering with MFFs seeded on a scaffold of biodegradable MPEG-PLGA might be an interesting adjunct to future POP-repair.*

ABBREVIATIONS

POP	pelvic organ prolapse
MFFs	muscle fiber fragments
MPEG-PLGA	methoxypolyethyleneglycol-polylactic-co-glycolic acid
SD	Standard deviation

INTRODUCTION

Alternatives to conventional pelvic organ prolapse (POP) reconstructive surgery with or without the use of meshes to support a weakened native tissue are of increasing interest. Regenerative therapy in the form of tissue engineering offers such potential. The classic tissue engineering approach relies on the use of tissue specific stem cells in combination with a biodegradable scaffold [1]. It is hypothesized that the scaffold will serve as breeding ground for the regenerative cells and provide temporary support to the vaginal wall until a permanent support from the regenerative cells has been generated [2,3].
Several cell sources for regenerative POP repair have been proposed, one being culture-expanded myoblasts [3–6]. Another is fresh autologous muscle fiber fragments (MFFs) with their associated muscle stem cells called satellite cells [7–10]. The use of MFFs is simple, inexpensive and allows harvesting, seeding and surgical implantation during the same procedure making the method clinically attractive [3]. We have previously shown in two different rat abdominal wall models that cells originating from MFFs seeded on a synthetic, biodegradable scaffold of methoxy-polyethyleneglycol-polylactic-co-glycolic acid (MPEG-PLGA) survive and participate in the regenerative process following implantation [8,10]. However, the models used were not eligible for testing differences in tissue strength, as the abdominal wall was intact in both models [8,10].
The vaginal wall of patients with POP is weakened with altered tissue metabolism and altered biomechanical properties [11,12]. The aim of this study was 1) to develop an animal model with weakened abdominal wall in rats and 2) to evaluate the effect of a tissue engineering strategy using this weakened tissue model.

MATERIALS AND METHODS

Methods have previously been described thoroughly [10]. A brief summarization of methods and a description of the model used in the present paper are presented below.

The Danish Animal Experiments Inspectorate approved the study (permission no. 2012-15-2934-00242) and their guidelines for care and use of laboratory animals were followed. Experiments were conducted at the Animal Facility at the Panum Institute, Copenhagen, Denmark. We used Sprague Dawley retired female breeder rats, weighing 245-303 g (Taconic, Denmark).

Methods to evaluate model – initial pilot study

Abdominal wall models, modified from Valentin et al. [13] were used. In a preliminary pilot study we evaluated a partial defect model with removal of a single muscle layer (n=3) and a partial defect model with removal of two muscle layers (n=3). These defects were compared with intact abdominal wall (n=9). The partial defects measured 3.0 x 1.5 cm and were performed lateral to the rectus muscle. We evaluated feasibility and biomechanical load at failure (N) to decide the model for the final study. Biomechanical testing was performed as described for tissue strip B below. Surgery was performed in dead animals and biomechanical testing was performed 1-2 hours after performing the defect. Since removal of one layer only was easier to perform and no differences in biomechanical results could be found we chose to use a partial defect model with removal of just one muscle layer in the main study.

Methods of model used in the main study

Animals were randomly assigned to three groups; 1) unrepaired partial defect (n=6), 2) partial defect with scaffold (n=6) and 3) partial defect with scaffold and MFFs (n=6) (Figure 1). The partial defect was performed as mentioned above. We used an MPEG-PLGA scaffold (Coloplast, Humlebaek, Denmark) measuring 2.5 x 4.0 cm and thus overlapping the defective area with 0.5 cm on all borders. The MFFs were prepared by cutting the removed outermost abdominal muscle into small fragments, which were labeled with PKH26 (Sigma-Aldrich®, St. Louis, MO, USA). The MFFs were applied to the MPEG-PLGA scaffold and positioned between the defect and the scaffold (Figure 1). The scaffold was held in place by four Prolene 5-0 sutures, one stich in each corner, and a continuous Vicryl 4-0 suture all around all four borders. The skin was closed using staples (Reflex® One, REF 3036, ConMed®, Utica, NY, USA). Antibiotic prophylaxis and analgesia were administered according to veterinarian recommendations.

Eight weeks after surgery the rats were euthanized by cervical dislocation. The abdominal skin was removed and for subsequent testing four tissue strips were marked on the abdominal wall prior to en bloc removal of the full-thickness tissue specimen (Figure 1). After removal, the tissue was cut into the marked four strips (Figure 1); strip A and D were used for histological testing and strip B and C were used for biomechanical testing.

Histopathology, immunohistochemistry and fluorescence

Samples used for histopathology and immunohistochemistry were fixed in 10% buffered formalin, embedded in paraffin, cut in 5 µm sections and stained with hematoxylin-eosin (H&E) and van Gieson/alcian blue. Neighboring sections were immuo-histochemically processed for desmin (Dako, Glostrup, Denmark), a cytoplasmic marker of skeletal and smooth muscle cells. The slides were viewed under an Olympus BX60 Microscope (Olympus, Center Valley, PA, USA) and Image-Pro Plus 7.0 (Media Cybernetics, Inc., Rockville, MD, USA) software was used to capture the images.

The organization of regeneratory connective tissue was examined using the Bonar score which evaluates cell morphology, collagen arrangement, cellularity, vascularity and ground substance in a standardized manner [14]. Assessment of Bonar score was performed by a senior pathologist blinded to the type of experimental model.

For the detection of PKH26 fluorescence, freshly cut sections from frozen tissue samples were evaluated in a fluorescence Olympus BX51 microscope (Olympus, Center Valley, PA, USA).

Uniaxial biomechanical properties

Samples for biomechanical testing were placed in separate sterile petri dishes with sterile phosphate buffered saline (PBS) until testing. Testing was performed two to four hours after sacrifice and removal of tissue strips.

We used a TA.XT plus Texture Analyser (Stable Micro Systems, Godalming, Surrey, UK) tensiometer with TA 94 Pneumatic Grips (Thwing-Albert Instrument Company, West Berlin, NJ, USA) modified by using a grip paper (3M) to secure a tight grip without squeezing the tissue. Two tissue strips (strip B and C, Figure 1) were examined. Tissue strip B was inserted at a grip-to-grip separation of 1.0 cm and thus, only ithe partial defect area was tested. The grips moved with a speed of 0.333 mm/second. Tissue strip C was inserted at a grip-to-grip separation of 3.0 cm and evaluated both the partial defect area and the surrounding normal tissue. For strip C, the grips moved with a speed of 1 mm/second. The speed was adjusted to the length of the tissue strips that were tested between the grips to ensure a constant strain-rate. Load and elongation were recorded throughout the testing until the point of failure. Biomechanical properties were analyzed with Exponent Version 6,1,3,0 software (Stable Micro Systems, Surrey, UK). Load was plotted against elongation resulting in bilinear curves with a low- and a high stiffness zone [10]. Data were reported as stiffness (N/mm) in the low- and high-stiffness zones, load at failure (N) and elongation at failure (mm).

Statistics

Data regarding Bonar score could not be evaluated for normally distribution and are presented as median (range) and analyzed using the non-parametric Kruskal-Wallis analysis of variance test. The data from the biomechanical tests were evaluated using quantile-quantile-plots and were assumed to be normally distributed. Data are presented as mean and standard deviation (SD). We tested for variance of homogeneity between groups using Levene's test. The groups were compared with one-way ANOVA and if there were significant differences between groups, post hoc multiple comparisons analysis was performed with Tukey´s correction. One-way ANOVA with Welch correction was used for outcomes with significant difference in variance. *P* values <0.05 were considered statistically significant. All statistical analyses were performed using the statistical software R (R Foundation for Statistical Computing, Vienna, Austria).

Figure 1. Definition of groups, preparation and testing of tissue samples

a) The three groups: 1) partial defect; 2) partial defect repaired with MPEG-PLGA; and 3) partial defect repaired with MPEG-PLGA and MFFs (muscle fiber fragments). b) Removed tissue was cut into four strips (A-D). c) Uniaxial biomechanical testing of repair near strips (strip B) and larger strips (strip C).

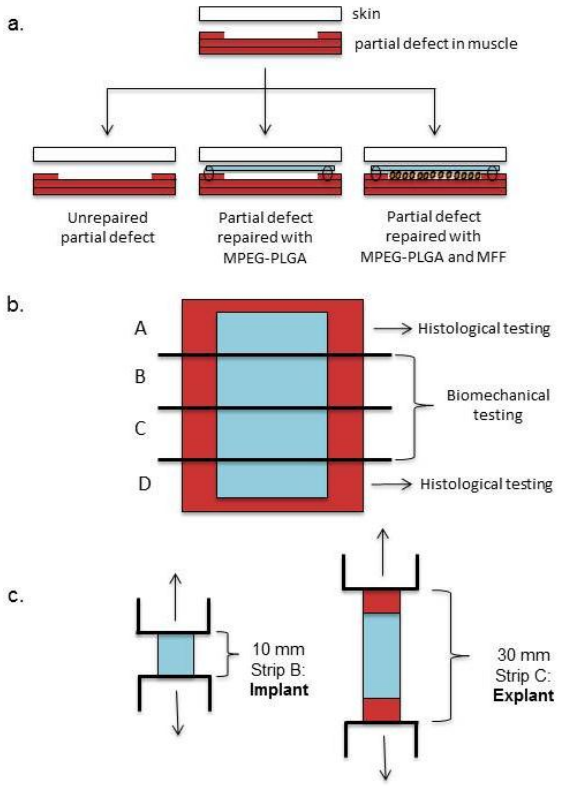

RESULTS

Surgery and postoperative period were well tolerated in all animals. No hernias, erosions or infections were detected, and after removal of the skin, no macroscopic signs of the MPEG-PLGA scaffold were visible.

Histopathology and Fluorescence

Histopathological evaluation confirmed the macroscopic impression that the MPEG-PLGA scaffold had been fully degraded in all animals (Figure 2). There were no remaining signs of a foreign body inflammatory reaction in terms of macrophages or giant cells corresponding to the scaffold area, but remnants of the Vicryl sutures used to secure the scaffold were observed in some of the animals. No significant differences in Bonar score between groups (p=0.35) were found (Table 1). Immuno-histochemical analysis revealed the presence of irregular desmin-positive muscle cells, which were positioned adjacent to the more well-defined remaining muscle layers (Figure 3a and 3b), but surgical removal of the outermost muscle layer had caused an uneven surface and did not allow us to discriminate between rugged muscle fibers and added MFFs. However, PKH26 fluorescence-positive cells were visible in all animals with MFFs (group 3) and not in the other groups that served as negative controls (Figure 3c).

Table 1. Bonar score

Semi quantitative evaluation of the connective tissue using the Bonar score.

	Group 1 Unrepaired partial defect n = 6	**Group 2 Partial defect repaired with MPEG-PLGA** n = 6	**Group 3 Partial defect repaired with MPEG-PLGA and MFFs** n = 6	***P-value****
Median (range)	5.5 (5-6)	6.0 (5-6)	6.0 (5-6)	0.35

*Kruskal-Wallis test of variance

Biomechanical properties – initial pilot study

In the initial pilot study evaluating two defect models (Table 2), we found a significant difference in load at failure (N) (p<0.001), between normal abdominal wall and abdominal wall with partial defect after removal of both one (p=0.006) or two muscle layers (p=0.001). There was no significant difference between the two partial defect models (p=0.75).

Biomechanical properties – main study

The uniaxial biomechanical results of the main study are presented in Table 3. In the smaller tissue strip B, which only included the partial defect area, we found a significant difference in load at failure between groups (ANOVA (p=0.028)). Post hoc analysis revealed a higher load at failure for partial defect + MPEG-PLGA + MFFs (group 3) compared to partial defect + MPEG-PLGA with no MFFs (group 2) (p=0.034). In the larger tissue strip C, which included the area of the partial defect as well as the surrounding normal tissue, there was no corresponding significant increase in load at failure (p=0.25). No significant differences were found between groups for the remaining biomechanical outcomes.

Table 2. Biomechanical properties: initial pilot study

Uniaxial biomechanical properties evaluating two different partial defect models and normal abdominal wall of rats.

	Normal abdominal wall n = 9	**Partial defect, removal of one muscle layer** n = 3	**Partial defect, removal of two muscle layers** n = 3	**p-value** (ANOVA)
Load at failure (N) mean (SD)	10.1 (2.5)	4.4 (1.4)	3.2 (0.6)	<0.001

DISCUSSION

This study was used to develop a model of weakened tissue in the rat abdominal wall and to evaluate the regenerative effect of a simple tissue engineering repair technique using a quickly biodegradable synthetic MPEG-PLGA scaffold seeded with autologous MFFs. By doing this study we hoped to be a step closer to the development of a stable and safe tissue engineering method for the repair of a weakened vaginal wall in POP.

Table 3. Biomechanical properties: main study
Uniaxial biomechanical properties of the smaller tissue strip B (only including tissue with partial defect) and of the larger tissue strip C (including tissue with partial defect and surrounding tissue).

	Group 1 Unrepaired partial defect n = 6	Group 2 Partial defect repaired with MPEG-PLGA n = 6	Group 3 Partial defect repaired with MPEG-PLGA and MFFs n = 6	*p-value**
Tissue strip including partial defect only				
Stiffness in low stiffness zone (N/mm)	0.09 (0.07)	0.08 (0.07)	0.15 (0.10)	0.31
Stiffness in high stiffness zone (N/mm)	1.19 (0.48)	1.10 (0.52)	1.59 (0.57)	0.27
Load at failure (N)	6.98 (1.67)	6.57 (2.07)	9.28 (1.13)	0.028**
Elongation at failure (mm)	13.41 (3.51)	13.49 (2.78)	11.54 (3.40)	0.51
Tissue strip including both partial defect and the surrounding tissue				
Stiffness in low stiffness zone (N/mm)	0.03 (0.02)	0.08 (0.07)	0.09 (0.03)	0.09
Stiffness in high stiffness zone (N/mm)	0.72 (0.68)	0.76 (0.29)	1.06 (0.30)	0.40
Load at failure (N)	7.41 (1.03)	6.77 (0.77)	8.35 (2.42)	0.25
Elongation at failure (mm)	39.60 (24.14)	21.48 (5.31)	17.88 (2.54)	0.10***

Data are presented as mean (SD).
*One-way ANOVA
**Post hoc test with Tukey correction revealed that partial defect + MPEG-PLGA + MFFs (group 3) had a significantly higher load at failure compared to compared to partial defect + MPEG-PLGA (group 2) (p=0.034), a borderline non-significant difference between the partial defect + MPEG-PLGA + MFFs (group 3) and the unrepaired partial defect group (group 1) (p=0.07), while the difference between the unrepaired partial defect group (group 1) and the partial defect + MPEG-PLGA (group 2) was clearly non-significant (p=0.91).
***ANOVA regarding elongation at failure for the larger tissue strip C was done with Welch correction.

We chose a partial defect model, which included removal of just one muscle layer, not just because it was easy to perform but also because this model proved significantly weakened when compared with normal abdominal wall. An increased load at failure was also found in the group, which had originally received MFFs added onto the scaffold, even though the scaffold was now completely degraded.
Unfortunately, the MFFs could not be convincingly differentiated from the rugged cells remaining in the abdominal muscle layer, but cells from the MFFs were identified with fluorescence labeling and confirm our previous results in two other rat abdominal wall models [8,10]. Taken together, these studies suggest that MFFs affect the regenerative repair process. They also demonstrate that the MPEG-PLGA scaffold is highly biocompatible and thus a safe carrier for the MFFs.

Figure 2. Histopathology
Histological samples from area with unrepaired partial defect alone (group 1). M marks the underlying intact muscle layers. Arrow in a) marks the transition zone between three and two muscle layers, M represents the muscle layer that was removed in the partial defect. In b) the arrows mark remnants of the removed muscle layer, leaving the surface uneven. Van Gieson Alcian blue staining, original magnification ×40 (a) and ×200 (b).*

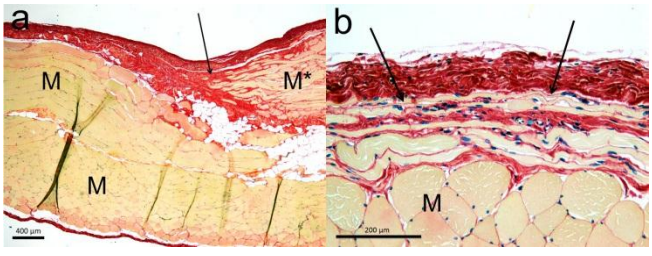

The significantly higher load at failure in the group with MFFs was only found for the tissue strip that tested the area of weakened tissue. In the tissue strip that also included the surrounding normal tissue, a non-significant difference was observed. Insufficient statistical power caused by the limited number of animals may explain this discrepancy, but also the fact that the tissue strip including normal tissue had been subjected to suturing with Vicryl which may have had a confounding effect by weakening the tissue.
We have previously detected a significantly increased stiffness in the high stiffness zone following native repair augmented with MPEG-PLGA + MFFs in a full-thickness abdominal wall defect (10). In this study, a similarly increased stiffness could not be found in the high stiffness zone, but a trend was observed in the physiologically more relevant low stiffness zone. However, since different models were used in our studies, a direct comparison was not possible.
Corona et al. have previously demonstrated that MFFs have a marked capacity for repair of volumetric muscle loss [15]. Garg et al. have also compared scaffolds made from vital and devitalized MFF muscle [16]. They found, that the devitalized MFFs ended up as a mass of fibrous tissue after eight weeks, as opposed to the vital MFFs, which had caused de novo muscle fiber regeneration. The vital MFFs used in the present study may hypothetically have served both as a scaffold and a cell provider. Cell sources from other locations could also be of clinical interest. Corona et al. seeded bone marrow-derived mesenchymal stem cells on a decellularized muscle that acted as a scaffold in a model of volumetric muscle loss in the anterior tibial muscle in rats [17]. After two months, they found that the mesenchymal stem cells had led to the formation of new muscle fibers in the area.
We successfully developed an easy-to-perform new abdominal wall model with weakened muscle tissue to evaluate the biomechanical strength of an MPEG-PLGA scaffold with MFFs but not without costs. By removing the outermost abdominal muscle

Figure 3. Desmin and fluorescence positive cells
Desmin positive cells close to the transition zone (a) and further away from the transition zone (b). Red arrows mark the desmin positive striated muscle cells; yellow arrows mark smaller desmin positive dead cells without striation. M marks the underlying intact muscle layer. Red PKH26-fluorescence positive cells in sample from group 3 are marked with white arrows (c). Original magnification: x200.

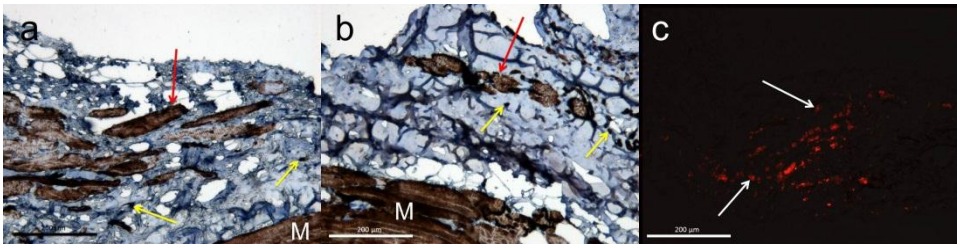

layer an uneven surface of the remaining muscle layers ensued and this complicated the histological and immune-histochemical evaluation in differentiating between 1) muscle cells or fibers separated from their muscle layer and 2) cells originating from the implanted MFFs. Consequently, and although fluorescence labeling revealed that cells originating from the MFFs did survive and were integrated in the regenerated tissue, we were unable to determine their exact phenotype. Other cell types are present within MFFs, and although in small numbers and sizes, they could be involved.

The present results only provide an eight week snapshot of the regenerative process, and the number of animals and hence statistical power was limited. Another limitation was the use of uniaxial biomechanical testing instead of multiaxial testing, which more closely mimics the actual mechanical loads put to the defective tissue in patients with POP or hernia. Further, the biomechanical testing to evaluate models in the initial pilot study was performed shortly after performing the defect and not eight weeks after surgery, although this was the follow-up time chosen for the main study. However, the initial pilot study proved that the tissue was weakened at the time of implantation.

Longer term and larger animal studies are needed in advance of clinical trials to reveal if the technique has a lasting positive effect on the strength of the repaired tissue and whether increased stiffness remains an issue. For POP repair specifically, the use of a larger animal model which allows implantation into the vaginal walls would be preferable.

In conclusion, a skeletal muscle biopsy is easy to obtain and MFFs are easily prepared. In addition, a quickly degradable and highly biocompatible scaffold like the MPEG-PLGA scaffold is advantageous and preferable from a clinical safety point of view. Consequently, this simple tissue engineering concept could translate into an attractive new treatment of POP or an adjunct to conventional POP or hernia reconstructive surgery.

FUNDING

Financial Disclaimers: The Danish National Advanced Technology Foundation and the Nordic Urogynecological Association have supported this study. Coloplast A/S provided scaffolds and facilities for biomechanical and histological testing.

Conflicts of Interest: G Lose has received compensation as a consultant for Astellas.

H Jangö, S Gräs and L Christensen have no conflicts of interest.

REFERENCES

1. *Bianco P, Robey PG. Stem cells in tissue engineering. Nature. 2001;414:118–21.*
2. *Lysaght MJ, Hazlehurst AL. Tissue Engineering: The End of the Beginning. Tissue Eng. 2004;10:309–20.*
3. *Boennelycke M, Gras S, Lose G. Tissue engineering as a potential alternative or adjunct to surgical reconstruction in treating pelvic organ prolapse. Int. Urogynecol. J. 2013;24:741–7.*
4. *Roman S, Mangera A, Osman NI, Bullock AJ, Chapple CR, MacNeil S. Developing a tissue engineered repair material for treatment of stress urinary incontinence and pelvic organ prolapse-which cell source? Neurourol. Urodyn. 2014;33:531–7.*
5. *Chen B, Dave B. Challenges and Future Prospects for Tissue Engineering in Female Pelvic Medicine and Reconstructive Surgery. Curr. Urol. Rep. 2014;15:425.*
6. *Ulrich D, Muralitharan R, Gargett CE. Toward the use of endometrial and menstrual blood mesenchymal stem cells for cell-based therapies. Expert Opin. Biol. Ther. 2013;13:1387–400.*
7. *Mauro A. Satellite cell of skeletal muscle fibers. J. Biophys. Biochem. Cytol. 1961;9:493–5.*
8. *Boennelycke M, Christensen L, Nielsen LF, Gräs S, Lose G. Fresh muscle fiber fragments on a scaffold in rats–a new concept in urogynecology? Am. J. Obstet. Gynecol. 2011;205:235.e10–235.e14.*
9. *Gräs S, Klarskov N, Lose G. Intraurethral Injection of Autologous Minced Skeletal Muscle: A Simple Surgical Treatment for Stress Urinary Incontinence. J. Urol. 2014;192:850–5.*
10. *Jangö H, Gräs S, Christensen L, Lose G. Muscle fragments on a scaffold in rats: a potential regenerative strategy in urogynecology. Int. Urogynecol. J. 2015;26:1843–51.*
11. *Chen B, Yeh J. Alterations in connective tissue metabolism in stress incontinence and prolapse. J. Urol. 2011;186:1768–72.*
12. *Feola A, Duerr R, Moalli P, Abramowitch S. Changes in the rheological behavior of the vagina in women with pelvic organ prolapse. Int. Urogynecol. J. Pelvic Floor Dysfunct. 2013;24:1221–7.*
13. *Valentin JE, Turner NJ, Gilbert TW, Badylak SF. Functional skeletal muscle formation with a biologic scaffold. Biomaterials. 2010;31:7475–84.*

14. *Fearon A, Dahlstrom JE, Twin J, Cook J, Scott A. The Bonar score revisited: Region of evaluation significantly influences the standardized assessment of tendon degeneration. J. Sci. Med. Sport. Sports Medicine Australia; 2014;17:346–50.*
15. *Corona BT, Garg K, Ward CL, McDaniel JS, Walters TJ, Rathbone CR. Autologous minced muscle grafts: a tissue engineering therapy for the volumetric loss of skeletal muscle. AJP Cell Physiol. 2013;305:C761–75.*
16. *Garg K, Ward CL, Rathbone CR, Corona BT. Transplantation of devitalized muscle scaffolds is insufficient for appreciable de novo muscle fiber regeneration after volumetric muscle loss injury. Cell Tissue Res. 2014;358:857–73.*
17. *Corona BT, Wu X, Ward CL, McDaniel JS, Rathbone CR, Walters TJ. The promotion of a functional fibrosis in skeletal muscle with volumetric muscle loss injury following the transplantation of muscle-ECM. Biomaterials. Elsevier Ltd; 2013;34:3324–35.*

Examinations of a new long-term degradable electrospun polycaprolactone scaffold in three rat abdominal wall models

Hanna JANGÖ, MD[1]; Søren GRÄS, MD[1]; Lise CHRISTENSEN, MD, DMSc[2]; Gunnar LOSE, MD, DMSc[1]

[1] Department of Obstetrics and Gynecology, Copenhagen University Hospital Herlev, Denmark
[2] Department of Pathology, Copenhagen University Hospital Herlev, Denmark

Correspondence: Hanna Jangö, Department of Obstetrics and Gynecology and Copenhagen University Hospital Herlev, Herlev Ringvej 75, DK-2730 Herlev
E-mail: hanna.jango@regionh.dk

Financial Disclaimers: The Danish National Advanced Technology Foundation and the Nordic Urogynecological Association have supported this study. Coloplast A/S provided scaffolds and facilities for biomechanical and histological testing.
Conflicts of Interest: G Lose has received compensation as a consultant for Astellas and Contura.
H Jangö, S Gräs and L Christensen have no conflicts of interest.

Alternative approaches to reinforce native tissue in reconstructive surgery for pelvic organ prolapse are warranted. Tissue-engineering combines the use of a scaffold with the regenerative potential of stem cells and is a promising new concept in urogynecology. Our objective was to evaluate whether a newly developed long-term degradable polycaprolactone scaffold could provide biomechanical reinforcement and function as a scaffold for autologous muscle fibre fragments. We performed a study with three different rat abdominal wall models where the scaffold with or without muscle fibre fragments was placed 1) subcutaneously (minimal load), 2) in a partial defect (partial load) and 3) in a full-thickness defect (heavy load). After eight weeks, no animals had developed hernia, and the scaffold provided biomechanical reinforcement, even in the models where it was subjected to heavy load. The scaffold was not yet degraded but showed increased thickness in all groups (p=0.70). Histologically, we found a massive foreign body response with numerous large giant cells intermingled with the fibres of the scaffold. Cells from added muscle fibre fragments could not be traced by PKH26-fluorescence or desmin-staining. We found no differences regarding biomechanical properties between groups. Taken together, the long-term degradable polycaprolactone scaffold provided biomechanical reinforcement by inducing a marked foreign-body response and attracting numerous inflammatory cells to form a strong neo-tissue construct. However, cells from the muscle fibre fragments did not survive in this milieu. Properties of the new neo-tissue construct must be evaluated at the time of full degradation of the scaffold before its possible clinical value in pelvic organ prolapse surgery can be evaluated.

ABBREVIATIONS
ANOVA = analysis of variances
MFFs = muscle fibre fragments
MPEG-PLGA = methoxypolyethyleneglycol-polylactic-co-glycolic acid
PCL = polycaprolactone
POP = pelvic organ prolapse
SD = standard deviation

INTRODUCTION
New alternatives to conventional implants for reconstructive pelvic organ prolapse (POP) surgery are required for tissue reinforcement since biological materials are ineffective[1], and the use of permanent synthetic meshes is associated with frequent and harmful adverse events[2]. Regenerative medicine aims at creating functional tissue with the use of stem cells. Tissue-engineering, which usually refers to the use of stem cells in combination with a degradable scaffold, is a promising adjunct to POP repair, but the optimal scaffold-material and cell-source remain to be identified[3].
We have previously implanted a methoxypolyethyleneglycol-polylactic-co-glycolic acid (MPEG-PLGA) scaffold, which is fully degraded within eight weeks, and seeded it with fresh autologous muscle fibre fragments (MFFs) in various rat abdominal wall models[4–6]. MFFs have a noticeable ability to regenerate skeletal muscle tissue[7–9] thanks to their content of muscle stem cells, also called satellite cells[10], which are capable of differentiating into new muscle fibres. In these studies, we found that cells from the MFFs survived and participated in the regenerative process, significantly affecting some of the biomechanical properties[4–6].
Because the MPEG-PLGA scaffold per se is fragile with limited strength, it cannot provide any biomechanical reinforcement, and can only be used as an adjunct to conventional native tissue POP repair by delivering stem cells. We were therefore looking for a stronger scaffold that could be useful in a wider range of surgical applications similar to the existing permanent meshes.
Polycaprolactone (PCL) is an FDA approved polymer, which provides a promising platform for the design and fabrication of stronger degradable meshes, which are capable of providing both initial strength and being scaffolds for transfer of stem and progenitor cells[11]. PCL has a long degradation time of 2-4 years[12], and this may allow native tissue cells as well as transplanted cells to

inhabit the scaffold and over time – with the degradation of the PCL fibres – generate a new and durable restoration of tissue. The aim of the present study was to evaluate whether a newly developed electrospun PCL scaffold could provide initial biomechanical tissue reinforcement on one side and functioning as a scaffold to transfer muscle stem cells in the form of MFFs on the other. As no optimal animal models for POP repair exist [13,14] and we wanted to mimic different surgical mesh application scenarios, three different rat abdominal wall models, which impose different loads to the scaffold, were used.

MATERIALS AND METHODS

A total of 36 Sprague Dawley retired female breeder rats, weighing 250-295 g (Taconic, Denmark) were used. The study was approved by the Danish Animal Experiments Inspectorate (permission no. 2012-15-2934-00242) and guidelines for care and use of laboratory animals were followed. The rats were housed at the Animal Facility at the Panum Institute, Copenhagen, Denmark.

We used three abdominal wall models (Figure 1). In the first model (model 1) the scaffold was placed subcutaneously[5], exposing it to a limited load. In the second model (model 2) we performed a partial abdominal wall defect[6], where the outermost muscle layer was removed. As previously shown this results in decreased abdominal wall strength and hence exerts extra load to the scaffold. In the third model (model 3) we performed a full thickness abdominal wall defect[15], in which all three abdominal layers were removed and replaced with a scaffold that was exposed to the full abdominal wall load.

The electrospun PCL scaffold (Coloplast, Humlebaek, Denmark) consisted of a thin layer of randomly spun fibres with a mean diameter of 1.58 µm (SD 0.96 µm). It measured 2.5 × 4.0 cm and had a thickness of approximately 50 µm. In all three models, the PCL scaffold was placed lateral to the rectus muscle, and in models 2 and 3, the defects, measuring 3.0 × 1.5 cm, were overlapped by the scaffold with 0.5 cm on each border.

In all three models, the scaffold was implanted with (n=6) and without (n=6) MFFs. The MFFs were harvested during the same surgical procedure, in model 1 from a thigh muscle punch-biopsy, and in models 2 and 3 from the removed abdominal wall. The MFFs were cut into fine fragments, labelled with PKH26-fluorescent dye (Sigma-Aldrich®, St. Louis, MO, USA) and placed evenly all over the scaffold prior to its insertion and suturing to the abdominal wall. In models 1 and 2, the MFFs were placed on the surface of the scaffold facing the existing muscle layers. In model 3, where all muscle layers had been removed, the MFFs were placed on top of the scaffold facing the skin. In all three models, the scaffold was held in place with single non-absorbable Prolene 5-0 sutures in each corner, followed by a continuous, absorbable Vicryl 4-0 suture along the borders. The skin was closed with staples (Reflex® One, REF 3036, ConMed®, Utica, NY, USA). Antibiotic prophylaxis and analgesia were administered according to veterinarian recommendations.

Rats were euthanized by cervical dislocation after eight weeks. The skin was removed and four tissue strips were marked and removed after initial measurements of the scaffold and macroscopic evaluation in situ. After removal, the implants and tissue were cut into the marked tissue strips (Figure 1) and subjected to biomechanical testing and histopathological evaluation.

Histopathological evaluation

Tissue strips A and D (Figure 1) were used for histopathological evaluation. Tissue samples were fixed in 10% buffered formalin, embedded in paraffin, cut in 5 µm sections and stained with haematoxylin-eosin (H&E) and Masson trichrome (Sigma-Aldrich, St. Louis, MO, USA). Neighboring sections were immunohistochemically analysed for desmin (Dako, Glostrup, Denmark), a cytoplasmic marker of smooth and skeletal muscle. We also performed orcein staining (Orcein Stain Kit, Artisan, Dako, Denmark) that stains elastin fibres. The slides were viewed under an Olympus BX60 Microscope (Olympus, Center Valley, PA, USA), and the images were analysed using the Image-Pro Plus 7.0 software (Media Cybernetics, Inc., Rockville, MD, USA). To estimate the number of giant cells and nuclei, we used a mask to calculate the proportion of nuclei in the sample. This was done in four separated areas, two with large giant cells and two with smaller giant cells, on photos of magnification ×200. To detect PKH26-fluorescence, tissue sections were cut from frozen samples and evaluated in a fluorescence microscope Olympus BX51 (Olympus, Center Valley, PA, USA).

Figure 1. *Overview of models without (a) and with (b) added muscle fibre fragments (MFFs), tissue explant with tissue strip marking (c) and testing of biomechanical strips B and C (d).*

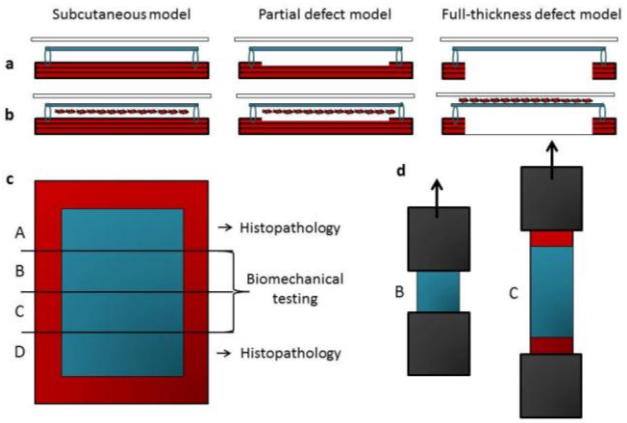

Uniaxial biomechanical testing

The fresh tissue strips B and C (Figure 1) were shortly after explantation placed in separate sterile petri dishes with sterile phosphate-buffered saline. The fresh tissue samples were then tested using a TA.XT plus Texture Analyser (Stable Micro Systems, Godalming, Surrey, UK) with TA 94 Pneumatic Grips (Thwing-Albert Instrument Company, West Berlin, NJ, USA). The clamps were modified with a grip paper (3M) to secure a tight grip while avoiding squeezing of the tissue. Strip B was tested with a grip-to-grip separation of 1.0 cm and thus only evaluating the area with scaffold and underlying tissue or defect. The larger tissue strip C was tested with a grip-to-grip separation of 3.0 cm and thereby evaluating both the area with scaffold and underlying tissue or defect and the surrounding normal tissue bordering the scaffold. To ensure constant strain-rate the grips moved with a speed of 0.333 mm/second for the smaller tissue strip B, while they moved with a speed of 1 mm/second for the larger tissue strip C. Load (N) and elongation (mm) were recorded until failure. Biomechanical properties were analysed with Exponent Version 6,1,3,0 software (Stable Micro Systems, Surrey, UK). Load was plotted against elongation resulting in bilinear curves with low- and a high stiff-

ness zones[4]. Data were reported as stiffness (N/mm) in the low- and high-stiffness zones, load at failure (N) and elongation at failure (mm).

Statistics

Uniaxial biomechanical results were presented as means ± standard deviation (SD), since data were evaluated using quantile-quantile-plots and were assumed to be normally distributed. To evaluate differences between the three groups, we performed one-way Analysis of Variances (ANOVA). Variance of homogeneity was tested between groups using Levene's test. If significant difference was found between groups using ANOVA, post hoc multiple comparisons analyses were performed with Tukey's correction. One-way ANOVA with Welch correction was used for outcomes with significant difference in variance. As there were no differences between the six groups, the results from groups with or without MFFs were pooled to evaluate the possible differences between models. Discrete data were presented as numbers (%) and groups were compared using Fisher's exact test. *P* values <0.05 were considered statistically significant. Statistical analyses were performed using the statistical software R (https://**cran**.r-**project**.org/, R Foundation for Statistical Computing, Vienna, Austria).

RESULTS

Macroscopic results

The scaffold was easy to handle, and surgery was well-tolerated in all animals. After eight weeks, we found no hernias or erosions, and the implantation-area was clearly identified in all animals (Figure 2a). In six animals, we found macroscopic signs of localized infection on the superior surface of the scaffold (facing the skin) (Table 1).

After eight weeks, the thickness of the scaffold had increased to a mean value of 1.6 mm (SD 0.4) with no differences between groups with or without MFFs (p=0.70) (Table 1). The three models were compared by pooling data from groups with or without MFFs and no differences were observed (p=0.31). The mean shrinkage of the scaffold in all animals was 11.1% (SD 9.0%) with borderline non-significant differences between groups with or without MFFs (p=0.05) (Table 1). When the three models were compared, a significant difference was observed with ANOVA (p=0.014), and post hoc tests revealed that shrinkage in model 3 was significantly lower than in model 1 (p=0.011).

Figure 2. *Macroscopic photo of the explanted neo-tissue PCL construct (a) and the corresponding histopathological tissue response showing bluish collagen deposition marked with black arrows (b) (Masson trichrome staining) and the numerous giant cells (examples marked with red arrows) located around the scattered PCL fibres (examples marked with yellow arrows) (c) (H&E staining). In (b) and (c) magnification ×200.*

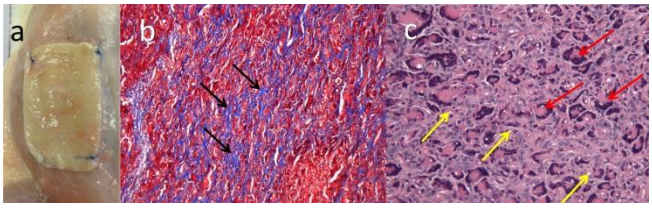

Histological findings

The increased thickness of the scaffold was caused by a marked in-growth of primarily foreign-body inflammatory cells (macrophages/giant cells) with formation of vessels and deposits of collagen (Figure 2b). The inflammatory response was dominated by numerous large giant cells located around and between the PCL fibres, forming a "neo-tissue/PCL construct" (Figure 2c). There were no differences in the number of giant cells, evaluated as percentage of nuclei between groups or models (Table 1, Figure 3). The central part of the construct was acellular or partially acellular (Figure 4) and although there were small differences between individual animals, no systematic differences between groups or models were observed. Granulation tissue in its classical definition or formation of a fibrous capsule around the implant was not found. Only in those animals that showed macroscopic signs of infection, we found abscesses with necrosis, granulocytes and hemosiderin-laden macrophages, as well as lymphocytes and plasma cells, reflecting different stages of tissue-degradation and healing (Figure 5).

No PKH26-flourescent or desmin-positive cells or fibres were observed around or inside the area of scattered PCL fibres, and the orcein staining revealed no elastin fibres in this area.

Biomechanical results

The uniaxial biomedical outcomes from the ANOVA analysis revealed no significant differences between groups with or without MFFs (Table 2). When the three models were compared (Table 3), post hoc analysis demonstrated that the neo-tissue/PCL construct in the full-thickness model 3 had reduced elongation at failure compared with model 1 in the smaller tissue strip B (p=0.008), and compared with model 2 in the larger tissue strip C (p=0.002).

Figure 3. *Calculation of percentage of nuclei (percentage of white area) (a) based on H&E stained specimens (b). Magnification ×400.*

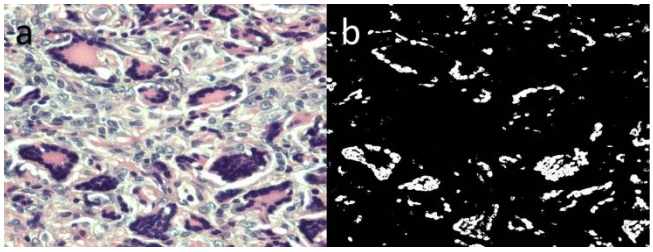

Figure 4. *Central acellular or partially acellular specimen in Masson trichrome staining (a) and H&E staining (b), magnification ×40 and ×200, respectively. In (a), the underlying muscle layer is marked with M and the superficial connective tissue/subcutaneous layer facing the skin is marked with C.*

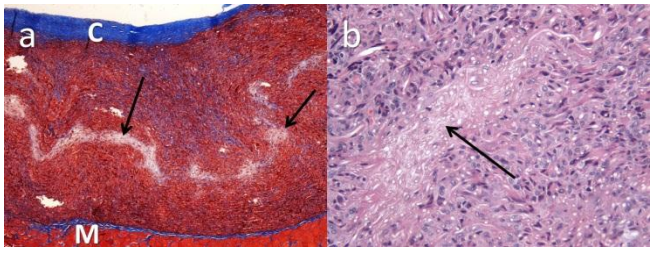

***Table 1**. Tissue properties eight weeks after implantation of electrospun PCL scaffold with or without MFFs in three rat abdominal wall models.*

	Subcutaneous model		Partial defect model		Full thickness defect model		*p-value*
	without MFFs	with MFFs	without MFFs	with MFFs	without MFFs	with MFFs	
Thickness (mm) Mean (SD)	1.42 (0.30)	1.50 (0.32)	1.63 (0.58)	1.76 (0.40)	1.47 (0.36)	1.58 (0.32)	*0.70*
Shrinkage (%) Mean (SD)	15.7 (6.6)	16.2 (5.7)	10.6 (6.8)	12.7 (7.3)	9.6 (14.3)	1.7 (4.3)	*0.05*
Abscess present Numbers (%)	2 (33%)	1 (17%)	0	1 (17%)	1 (17%)	1 (17%)	*0.98*
Nuclei (%) Mean (SD)	2.4 (0.3)	2.5 (0.4)	2.5 (0.2)	2.6 (0.4)	2.7 (0.3)	2.7 (0.5)	*0.11*
MFFs: muscle fibre fragments PCL: polycaprolactone							

DISCUSSION

There is an obvious need for tissue reinforcement in adjunct to reconstructive POP surgery. However, biological and degradable synthetic materials per se have failed to improve outcome[1,16] and polypropylene has been related to adverse and serious side effects[2]. We explored a tissue-engineering strategy that possibly could serve as an adjunct to reconstructive pelvic surgery to restore functional tissue. We used a newly developed, long-term degradable electrospun PCL scaffold and demonstrated that this scaffold was capable of providing mechanical reinforcement to a defective abdominal wall in rats. After eight weeks, there was a massive ingrowth of cells between and around the PCL fibres resulting in the formation of a neo-tissue/PCL construct, which was sufficiently strong to prevent hernia formation in a partial and even in a full thickness abdominal wall defect. In contrast to our previous findings with an MPEG-PLGA scaffold[4–6], the present study demonstrated that the PCL scaffold seemed to be unable to function as a carrier or anchor for muscle stem cells in the form of autologous MFFs. No fluorescence-labelled or desmin-positive cells or fragments were recovered in association with the neo-tissue/PCL construct, and biomechanical testing showed no differences in parameters between scaffolds with or without MFFs.

***Figure 5.** Localized infection, histologically characterized as abscess with necrosis and hemosiderin-laden macrophages, lymphocytes, plasma cells and granulocytes. In (a) and (b) magnification ×100 and ×200, respectively.*

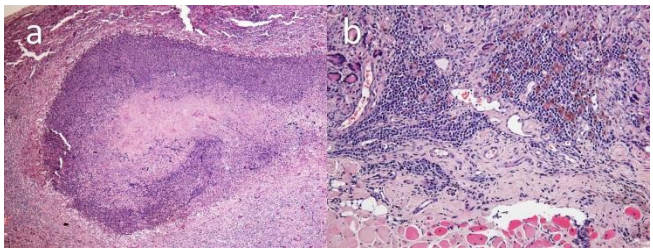

***Table 2.** Uniaxial biomechanical properties of the long-term degradable electrospun PCL scaffold with or without MFFs in three different rat abdominal wall models.*

	Subcutaneous model		Partial defect model		Full thickness defect model		*p-value*
	without MFFs (n=6)	with MFFs (n=6)	without MFFs (n=6)	with MFFs (n=6)	without MFFs (n=6)	with MFFs (n=6)	
Smaller tissue strip B							
Stiffness in the low-stiffness zone (N/mm)	0.47 (0.47)	0.37 (0.28)	0.31 (0.19)	0.38 (0.41)	0.43 (0.49)	0.22 (0.06)	*0.85*
Stiffness in the high-stiffness zone (N/mm)	2.22 (0.78)	2.14 (0.83)	2.97 (0.78)	2.51 (0.82)	2.93 (0.90)	2.96 (0.70)	*0.26*
Load (N)	13.47 (2.13)	13.12 (2.30)	12.22 (1.94)	11.90 (2.99)	12.52 (3.63)	13.12 (3.46)	*0.92*
Elongation (mm)	11.60 (2.64)	13.06 (4.71)	11.15 (3.57)	11.12 (4.87)	7.67 (1.48)	8.03 (2.86)	*0.09*
Larger tissue strip C							
Stiffness in the low-stiffness zone (N/mm)	0.06 (0.08)	0.12 (0.11)	0.07 (0.09)	0.05 (0.02)	0.04 (0.03)	0.03 (0.03)	*0.36*
Stiffness in the high-stiffness zone (N/mm)	0.51 (0.40)	0.53 (0.33)	0.41 (0.23)	0.36 (0.09)	0.55 (0.21)	0.78 (0.73)	*0.39*
Load (N)	10.32 (2.90)	11.13 (2.74)	10.98 (0.99)	10.87 (1.12)	9.72 (2.36)	8.91 (1.22)	*0.11*
Elongation (mm)	49.62 (23.95)	53.94 (29.57)	67.69 (29.69)	65.53 (18.84)	34.74 (9.60)	33.16 (17.60)	*0.05*

Data are presented as means (SD).
MFFs: muscle fibre fragments
PCL: polycaprolactone

Table 3. *Uniaxial biomechanical testing for simplified models comparing the three rat abdominal wall models, irrespective of whether MFFs were added or not.*

	Subcutaneous model (n=12)	Partial defect model (n=12)	Full-thickness defect model (n=12)	*p-value*
Smaller tissue strip B				
Stiffness in the low-stiffness zone (N/mm)	0.42 (0.37)	0.34 (0.31)	0.33 (0.35)	*0.78*
Stiffness in the high-stiffness zone (N/mm)	2.18 (0.77)	2.74 (0.80)	2.95 (0.77)	*0.06*
Load (N)	13.29 (2.12)	12.06 (2.41)	12.81 (3.40)	*0.54*
Elongation (mm)	12.33 (3.72)	11.14 (4.07)	7.85 (2.18)	*0.009*
Larger tissue strip C				
Stiffness in the low-stiffness zone (N/mm)	0.09 (0.10)	0.06 (0.06)	0.04 (0.03)	*0.16*
Stiffness in the high-stiffness zone (N/mm)	0.52 (0.35)	0.39 (0.17)	0.52 (0.35)	*0.17*
Load (N)	10.73 (2.72)	10.93 (1.01)	9.31 (1.84)	*0.05*
Elongation (mm)	51.78 (25.75)	66.61 (23.73)	33.95 (13.54)	*0.003*

Data are presented as means (SD).
MFFs: muscle fibre fragments
PCL: polycaprolactone

We used three different abdominal wall models to impose different loads to the PCL scaffold, but interestingly, the strength of the neo-tissue/PCL constructs at eight weeks was comparable among models and also comparable to the strength of normal rat abdominal wall tissue[6]. Furthermore, we found less shrinkage of the construct with no effect on the PCL/neo-tissue thickness in the full-defect model compared to the subcutaneous model. These findings indicate that the construct was able to adapt physiologically to biomechanical environmental stimuli, in contrast to the permanent meshes, which exert a fixed supraphysiological strength and form when implanted in vivo[17]. Consequently, the PCL scaffold of this study showed biomedical adaptation and may therefore serve as a more physiological alternative to permanent meshes with a potentially lower rate of complications in the treatment of both POP and hernias. The stiffness of the neo-tissue/PCL construct was also lower than the supraphysiological data reported for permanent meshes[17]; however, our results represents only a snapshot of the 2 - 4 years degradation period of the PCL scaffold, and the biomechanical properties may change over time concurrent with the degradation and eventual disappearance of the PCL fibres. In this context, the long degradation period is a major disadvantage. We would have to await the results of long-term studies in larger and longer living animals as well as human studies, before the clinical implementation of the PCL scaffold would be possible. Yet, although extrapolation of our results to the clinical situation of hernia or POP must be performed with caution, the PCL scaffold might be a long-term degradable alternative to permanent synthetic meshes in the future.
On the microscopic level, it was observed that the increased thickness of the PCL scaffold, in addition to formation of vessels and small strands of collagen fibres, was caused by a massive foreign-body response with primarily giant cells located between and around the PCL fibres. Foreign-body reactions influence the specific environment by inducing a low pH, reactive oxygen intermediates and degenerative enzymes, all of which are considered unfavourable for added cells used for tissue-engineering[18]. It is therefore possible, that the foreign-body response might have affected the local micro milieu to an extent where survival of the MFFs was impossible[18]. In vitro studies have demonstrated that PCL in itself is not toxic to cells as it supports the growth and proliferation of different cell types[12], but tissue conditions in vivo are different, and we suspect that the foreign-body reaction was too massive to allow survival of the MFFs. This notion is supported by the fact that we did not find any signs of survival of these cells in the present study, but we did in a previous study using the quickly degradable MPEG-PLGA scaffold. MPEG-PLGA was found to support transplantation of MFFs, and induced only a limited inflammatory response at three weeks, which had disappeared completely after eight weeks [4–6].
Previous clinical studies using short-term degradable biological implants to reinforce the tissue at POP surgery have failed to prove superior effect compared to native repair alone[1]. Whether the use of a long-term degradable PCL scaffold is advantageous remains to be determined. If the massive foreign-body reaction prevents ingrowth of normal native tissue cells, the neo-tissue/PCL construct may eventually end up forming undesirable scar tissue when the PCL fibres have finally been degraded[19].
Erosions caused by acute or chronic infection are a concern with the use of permanent meshes for POP repair. In our study, we found localized and small abscesses in six animals from different groups. We suspect these were caused by autobiting due to itching and irritation, a well-known phenomenon following abdominal wall surgery in rats.
There are some limitations to this study. Since a similar study has not been performed previously, we decided to use the lowest number of animals possible. Thus, we used six animals in each group, as recommended by Slack et al.[13]. However, this limited number resulted in a reduced statistical strength. Another limitation was the short-term follow-up of this study, which only provided a snap-shot of the ongoing foreign-body response, but long-term studies would have necessitated other species than rodents. We are also aware that supplemental biomechanical testing like multiaxial ball burst test and testing of active biomechanical properties would have added information to our understanding of the biomechanical properties of the neo-tissue/PCL construct[17].
Future studies will reveal the process of degradation of the electrospun PCL scaffold using several different time points including long-term studies to explore properties of the regenerated tissue when the scaffold had been fully degraded.

CONCLUSION

In conclusion, we demonstrated that implantation of a newly developed long-term degradable electrospun PCL scaffold after eight weeks induced the formation of a neo-tissue/PCL construct capable of providing initial biomechanical reinforcement to abdominal wall defects in rats. Addition of muscle stem cells in the form of MFFs to the scaffold did not influence the neo-tissue formation, and cells from the MFFs could not be traced. Because of the long degradation time of 2 - 4 years, long-term studies in larger animals are needed before the PCL scaffold can be used in the clinic as an adjunct in reconstructive surgery for POP or hernias to restore functional tissue.

REFERENCES

1. *Cox A, Herschorn S. Evaluation of current biologic meshes in pelvic organ prolapse repair. Curr Urol Rep. 2012;13(3):247–55.*
2. *U.S. Food and Drug Administration. FDA safety communication: Update on serious complications associated with transvaginal placement of surgicalmesh for pelvic organ prolapse [Internet]. 2011 [cited 2014 Apr 6]. p. 1–6. Available from: http://www.fda.gov/MedicalDevices/Safety/AlertsandNotices/ucm262435.htm*
3. *Boennelycke M, Gras S, Lose G. Tissue engineering as a potential alternative or adjunct to surgical reconstruction in treating pelvic organ prolapse. Int Urogynecol J. 2013 May 1;24(5):741–7.*
4. *Jangö H, Gräs S, Christensen L, Lose G. Muscle fragments on a scaffold in rats: a potential regenerative strategy in urogynecology. Int Urogynecol J. 2015 Dec 24;26(12):1843–51.*
5. *Boennelycke M, Christensen L, Nielsen LF, Gräs S, Lose G. Fresh muscle fiber fragments on a scaffold in rats-a new concept in urogynecology? Am J Obstet Gynecol. 2011 Sep;205(3):235.e10–4.*
6. *Jangö H, Gräs S, Christensen L, Lose G. Tissue engineering with muscle fiber fragments improves the strength of a weak abdominal wall in rats. Submitted Manuscript.*
7. *Studitsky AN. Free auto- and homografts of muscle tissue in experiments on animals. Ann N Y Acad Sci. 2006 Dec 16;120(1):789–801.*
8. *Carlson BM. The regeneration of minced muscles. Monogr Dev Biol. 1972;4:1–128.*
9. *Corona BT, Garg K, Ward CL, McDaniel JS, Walters TJ, Rathbone CR. Autologous minced muscle grafts: a tissue engineering therapy for the volumetric loss of skeletal muscle. AJP Cell Physiol. 2013 Oct 1;305(7):C761–75.*
10. *Mauro A. Satellite cell of skeletal muscle fibers. J Biophys Biochem Cytol. 1961 Feb;9:493–5.*
11. *Woodruff MA, Hutmacher DW. The return of a forgotten polymer—Polycaprolactone in the 21st century. Prog Polym Sci. 2010 Oct;35(10):1217–56.*
12. *Woodruff MA, Hutmacher DW. The return of a forgotten polymer—Polycaprolactone in the 21st century. Prog Polym Sci. 2010;35(10):1217–56.*
13. *Slack M, Ostergard D, Cervigni M, Deprest J. A standardized description of graft-containing meshes and recommended steps before the introduction of medical devices for prolapse surgery. Consensus of the 2nd IUGA Grafts Roundtable: optimizing safety and appropriateness of graft use in transvaginal pe. Int Urogynecol J. 2012 Apr;23 Suppl 1:S15–26.*
14. *Abramowitch SD, Feola A, Jallah Z, Moalli P a. Tissue mechanics, animal models, and pelvic organ prolapse: A review. Eur J Obstet Gynecol Reprod Biol. 2009;144(SUPPL 1):146–58.*
15. *Konstantinovic ML, Lagae P, Zheng F, Verbeken EK, De Ridder D, Deprest JA. Comparison of host response to polypropylene and non-cross-linked porcine small intestine serosal-derived collagen implants in a rat model. BJOG an Int J Obstet Gynaecol. 2005 Nov;112(11):1554–60.*
16. *Maher C, Baessler K, Glazener CM a, Adams EJ, Hagen S. Surgical management of pelvic organ prolapse in women. Cochrane Database Syst Rev. 2013;(4):CD004014.*
17. *Feola A, Abramowitch S, Jallah Z, Stein S, Barone W, Palcsey S, et al. Deterioration in biomechanical properties of the vagina following implantation of a high-stiffness prolapse mesh. BJOG an Int J Obstet Gynaecol. 2013 Jan;120(2):224–32.*
18. *Anderson JM, Rodriguez A, Chang DT. Foreign body reaction to biomaterials. Semin Immunol. 2008;20(2):86–100.*
19. *Major MR, Wong VW, Nelson ER, Longaker MT, Gurtner GC. The Foreign Body Response. Plast Reconstr Surg. 2015;135(5):1489–98.*